CRANFIELD UNIVERSITY

DAVID A BAILEY

INVESTIGATION OF IMPROVEMENTS IN AIRCRAFT BRAKING DESIGN

COLLEGE OF AERONAUTICS

PhD THESIS

CRANFIELD UNIVERSITY

COLLEGE OF AERONAUTICS

PhD THESIS

ACADEMIC YEAR 2004-2005

DAVID A BAILEY

Investigation of Improvements in Aircraft Braking Design

Supervisor: Dr. R I Jones

October 2004

This thesis is submitted in fulfilment of the requirements for the degree of Doctor of Philosophy

ABSTRACT

This work investigates and provides a methodology that enables better prediction of brake performance. Aircraft brake performance depends on the tribological properties of the friction couple used in the brake design. The behaviour of this couple combines both surface and bulk characteristics of the material. The increase in aircraft performance requirements has led to the development of new brake designs and new friction materials. The development of brakes for large commercial aircraft has stabilised to that of a carbon-carbon composite multi-disk brake design.

The results of this investigation established a relationship between mean μ, mass loading and the **mean friction radius** of the brake. This relationship provides a statistically good description of the results and will provide the brake performance engineer with a useful tool. In addition, the variance within the results of the 100 Normals aircraft qualification programme was also studied. In this case the relationship is not particularly good at describing the results.

A case study has been included to promote further understanding of the developed methodology and to illustrate some of the trade-offs required when designing a carbon brake.

The design of a multi-disk brake is a complex engineering task that requires many specialist engineering disciplines such as structural analysis and dynamic analysis etc. The wider context of aircraft braking is even broader and requires not only mechanical engineering skills but also electronic and software engineering. This research addresses all aspects of system integration and provides a framework of understanding on the interaction and dependencies of the various components.

ACKNOWLEDGEMENTS

I would like to express my sincere thanks to Dr. R.I. Jones for his help and supervision as well as his support for this endeavour.

I am also grateful to Dunlop Aerospace Limited for sponsoring this research and many of my colleagues there who provided information and assistance during the work. In particular, two deserve a special mention and these are Dr. Toby J. Hutton and Alun Thomas, both of whom provided me with an ear to bend as well as providing invaluable technical guidance.

Lastly, I would like to thank my family, in particularly my wife Tracey for her understanding and help. When I started this endeavour it was just the two of us and ended it with two boys at school!

TABLE OF CONTENTS

NOMENCLATURE

		SI Units	**Imperial**
A_R	Rotor Area	cm^2	in^2
A_S	Stator Area	cm^2	in^2
C_P	Specific heat capacity	kJ/kgK	ft.lbf/lbmK
CVD	Carbon Vapour Deposition		
CVI	Carbon Vapour Infiltration		
E	Kinetic energy	J	ft.lbf
DSA	Disk Swept Area	cm^2	in^2
H_{RD}	Height of rotor drive slot	cm	in
H_{SD}	Height of stator drive slot	cm	in
K_B	Brake Gain	m^3	in^3
KE_{BRAKE}	Brake energy	J	ft.lbf
KE_{TWB}	Tyre wheel & brake energy	J	ft.lbf
M	Mass	kg	lbm
M_R	Mass of rotor disk		
M_{DS}	Mass of double stator disk		
M_{HS}	Heat Sink Mass	kg	lbm
M_{BS}	Brake Structural Components Mass	kg	lbm
M_{EFFW}	Effective worn heat sink mass	kg	lbm
M_{EFFN}	Effective new heat sink mass	kg	lbm
M_{wear}	Wearable heat sink Mass	kg	lbm
N_I	Number of friction interfaces		
N_R	Number of rotors		
N_S	Number of stators		
N_{RD}	Number of rotor drive slots		
N_{SD}	Number of stators drive slots		
PAN	Polyacrylonitrile		
PCR	Mean friction radius of carbons	cm	ft
P_{ineff}	Brake ineffective pressure	bar	psi
P_{op}	Brake operating pressure	bar	psi

r_{SO}	Stator disk outer radius	cm	in
r_{SI}	Stator disk inner radius	cm	in
r_{RO}	Rotor disk outer radius	cm	in
r_{RI}	Rotor disk inner radius	cm	in
RTO	Rejected take-off		
T_B	Brake torque	Nm	ft.lbf
TPA	Total piston area	cm^2	in^2
th_{DS}	Thickness of double stator disk	cm^2	in^2
th_{PS}	Thickness of pressure stator disk	cm^2	in^2
th_{TS}	Thickness of thrust stator disk	cm^2	in^2
th_R	Thickness of rotor disk	cm^2	in^2
V	Volume	m^3	in^3
V_{BAS}	Aircraft velocity at brake application	m/s	Ft/s
W_{RD}	Width of rotor drive slot	cm	in
W_{SD}	Width of stator drive slot	cm	in
ΔT	Temperature rise	C	C
ρ	Density	kg/m^3	lb/in^3
μ	Coefficient of friction		

LIST OF FIGURES

LIST OF TABLES

Chapter 1

INTRODUCTION

The objective of this research work was to investigate and provide a scientifically based methodology to improve the prediction of the performance of carbon-carbon composite brakes. At present method the in use is based on the experience of the engineers tasked with designing the brake to meet required carbon-carbon composite brake performance targets. This process can lead to different design criteria being used depending on the experience of the Engineer and has no scientific basis. In addition, the variability in the performance of the brake is not well understood.

The field of Aircraft Braking is multi-disciplinary covering a diverse range of engineering and scientific fields. The secondary aim of the research was to provide a framework of understanding of the design of all the equipment involved in aircraft braking, specifically the brake, the wheel, the tyre and the landing gear. Importantly, the work was intended to provide an insight into the system integration aspects of aircraft braking and to clearly elucidate the inter-dependencies in order to improve the development of aircraft braking.

In Chapters 2 and 3 the approach taken has been to detail the aircraft requirements that have in particularly led to the development of aircraft brakes. Chapter 1 shows how the increase in aircraft performance, based on a number of improvements such as increase in engine thrust to weight ratio, improved aerodynamics both in reduction in drag and increase in coefficient of lift, stimulated the development of aircraft brakes. As with all developments of complex systems, it was the coming together of many technological developments that enabled the whole system to be continually advanced. The functional requirements on an aircraft brake is firstly to stop the aircraft safely during normal condition, secondly to stop the aircraft during emergency condition, thirdly to provide a park/hold brake and lastly to achieve all of the above requirements for a specified service life. The development of aircraft brakes has centered on two main features; they are the actuation method and the friction material. The actuation provides the clamping force necessary to bring the friction surfaces into contact. The friction material provides the surfaces that generate the required braking torque. The braking torque required increases with the aircraft deceleration rate that is required and the heavier the aircraft, for a given

deceleration rate, the more energy the brake has to absorb. Chapter 3 details the various designs that have been used to provide a solution to aircraft brake design.

The importance of the friction material in aircraft brakes cannot be underestimated. The characteristics of an aircraft brake friction material are discussed and in particular the requirement of a high specific heat capacity is discussed. This is important because the main development in friction materials over the last 20 years has been in the use of carbon-carbon composites in aircraft brakes. In Chapter 4 the need for a friction material that can act as a heat sink and as a structural components is discussed. These requirements have led to the development of carbon-carbon composite suitable for brake design. As stated earlier the main objective of this research is to develop to method of carbon-carbon composite brake performance prediction.

Carbon-carbon composites are not a specific material they are a family of materials that depend on the nature of the fibre and the carbon matrix. The manufacturing processes of carbon-carbon composites are discussed in order to provide the reader with an understanding of the technology and importantly to learn about the material microstructure. The microstructure and composite fabrication is believed to have a profound effect on the behaviour of the composite and ultimately on the brake performance.

The multi-disk brake is the design standard for all aircraft except small general aviation aircraft. A methodology for multi-disk brake design is detailed and the various design parameters discussed. In particular, brake parameters such as Mass Loading, Area Loading and Rate Loading are discussed and guidelines provided for typical values used. The constraints placed on the brake by the aircraft constructor and how these affect the solution is also discussed.

The wheel, tyres and landing gear are briefly discussed in order to understand the design drivers and the inter-relationship with the brake. The Brake Control System/Anti-Skid System covers many engineering disciplines within its own context and as shown can have a severe impact on the performance of the brake.

A major part of the work was to establish relationships that would enable brake performance to be better predicted. In order to achieve this a combination of establishing theoretical models and/or empirical models was needed. However, the testing of aircraft brakes is expensive and could not compete with the time demands of an aircraft development programme and hence it was obvious that a specifically tailored test programme would not be possible. However, through the development and qualification process for an aircraft programme various data are recorded. It was decided to use this data for the investigation as it provided the largest set of data to analyse. In addition, a brake is deemed successful if it meets the aircraft constructor's development and qualification requirements and therefore was the criteria by which a brake is judge to be an acceptable design.

A study was also undertaken to provide the designer with a parametric method of sizing a brake. This was performed to enable at the initial stage the designer to decide the sizing of the brake. This method would be useful for aircraft constructor and landing gear designer in the aircraft scheme design phase by enabling them to quickly size a carbon-carbon composite brake.

Chapter 2

AIRCRAFT DEVELOPMENTS

In the early days of aviation aircraft, due to their design and operation, did not require brakes. This was the result of the low landing speeds, the landing weight and the fact that most airfields were just that – fields, and hence provided ample ground drag to enable the aircraft to stop before the end of the runway.

The first aircraft were biplanes, a design which gives rise to a considerable amount of aerodynamic drag. The use of this type of wing design was necessary in order to achieve enough lift to attain flight. This was because only a low take-off speed was achievable due to the poor engine thrust that was available at that time. In addition, aircraft in this period used plate-like wings of thin cross-section, which also were highly cambered in order to produce an adequate amount of lift to be developed at low speed, hence making it possible for early aircraft to stagger into the air. All of which contributed to the fact that aircraft brakes were not necessary for early aircraft designs.

A series of figures showing the development of critical performance parameters associated with the evolution of brake design follow. Figure 1 relates average skin friction coefficient to year of service and indicates how dramatic the reduction in drag was up to about the 1950 - 1960's. This reduction in the aerodynamic drag of the aircraft, in turn reduced the total retarding force on the aircraft when landing and was a contributory factor in aircraft requiring brakes.

Figure 2 illustrates the relationship between wing load and take-off field length. Wing loading is proportional to the product of the square of the velocity, the coefficient of lift and air density. For a given coefficient of lift and density, the higher the aircraft velocity the smaller the wing can be to support the weight of the aircraft. The smaller wing provides a lower weight and less drag. Therefore, aircraft are optimised for cruising flight as they spend the greatest time in this phase, for this reason the wings are designed for high-speed operation and have a lower maximum coefficient of lift than otherwise. This results in the ratio of cruising speed to stall speed being lowered due to the lower dynamic pressure and

which then in turn leads to higher landing speeds. In addition, as the rotation speed is a factor of stall speed this also is lowered necessitating the use of high-lift devices.

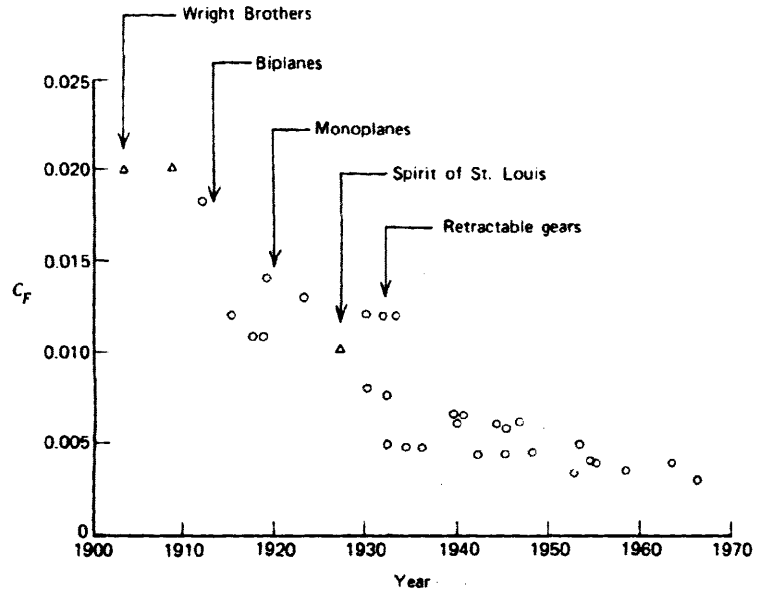

Figure 1 Reduction in Aircraft Drag (McCormick, 1995)

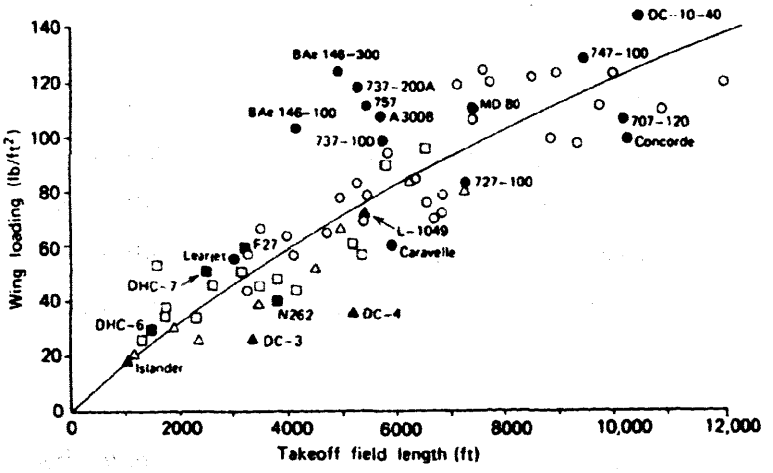

Figure 2 Wing Loading vs. Takeoff Field Length (Ashford & Wright, 1992)

This is shown in Figure 3, which relates maximum lift coefficient to year of service and importantly shows how the introduction of high-lift devices enabled aircraft to be optimised both for take-off/landing and for cruise.

Another development in aircraft design, which should be mentioned, is the replacement of the tailskid by the nose wheel. This change made high-speed landings possible while greatly reducing the drag of aircraft when running on wheels.

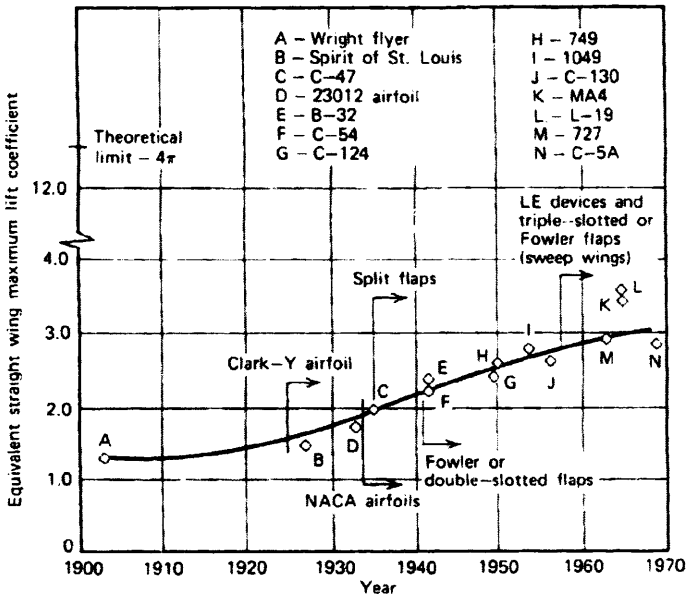

Figure 3 Progress of Maximum Lift Coefficient (McCormick, 1995)

One other important development was the introduction of the jet engine, which not only increased the take-off thrust but also reduced the aircraft drag in flight, which in turn increased the landing speed. In addition, it removed the use of the wind drag of the propeller at idling speed as an aid to braking, which was considerable and which could be enhanced by the introduction of reverse pitch. Figure 4 correlates take-off thrust ratio to that of bare engine weight and shows quite clearly the technological advances in the field of engine design.

All of the factors discussed gave rise to a steady increase in the energy requirements that the brakes had to be designed to absorb and spurred the advancements in brake design and friction material development.

The first brakes were fitted to aircraft in the 1920's and were justified at first by the fact that they enabled the stopping of aircraft in restricted spaces due to a forced landing and hence improved overall safety. However, as aircraft grew larger, landed faster and the airfield requirements on aircraft turnaround, due to the volume of traffic, became more onerous, brakes started to be required for normal operations. One other interesting point

to note is that the development of longer runways lagged behind the aircraft requirement for longer landing runs and until the infrastructure caught up this was another driver in the development of aircraft brakes. The trend in runway length against year is shown in Figure 5. As example of how far the situation had changed from the very early days, by 1937 monoplanes were landing at speeds of 100 mph on hard runways.

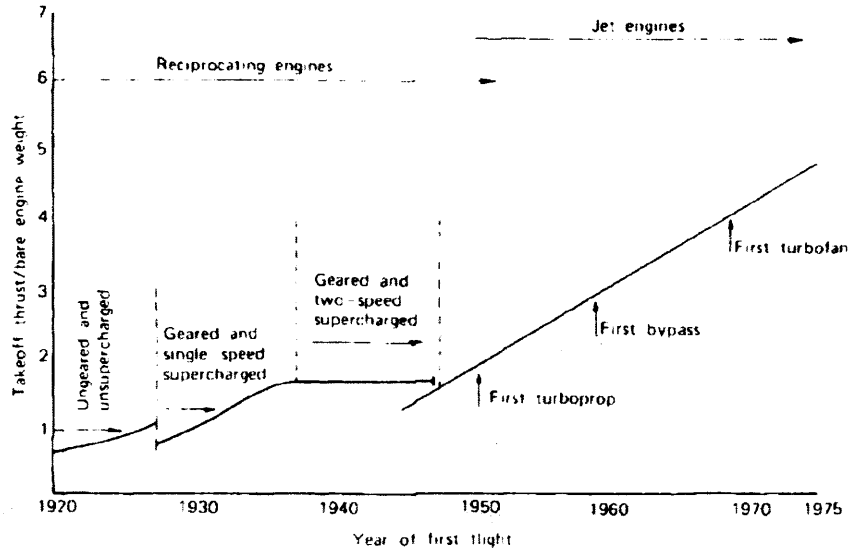

Figure 4 Progress of Takeoff Thrust/Weight Ratio (Ashford & Wright, 1992)

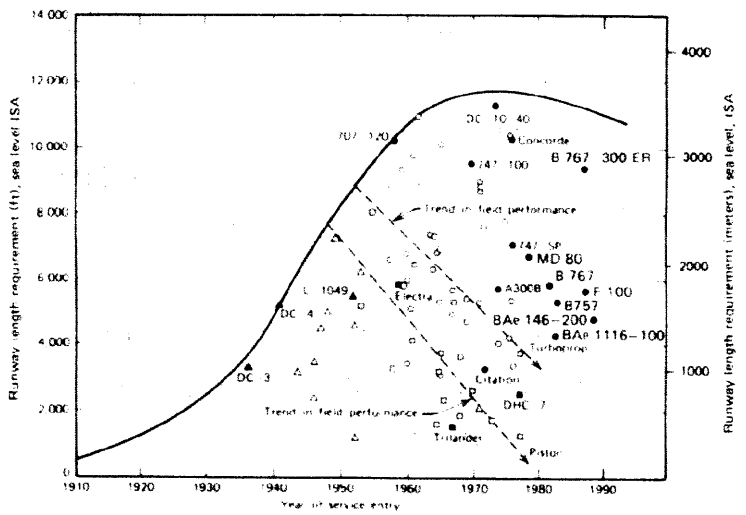

Figure 5 Increasing Runway Length Requirements (Ashford & Wright, 1992)

The evolution of brakes on aircraft followed a similar path to that of other equipment on aircraft in that the first brakes fitted were road vehicle brakes. In order to help the understanding of the evolution of aircraft brakes, it is first useful to understand the fundamental requirements of aircraft braking.

The top-level functional requirements on aircraft brakes are:

1. To absorb the necessary energy to stop the aircraft in a specified distance during normal landing conditions.
2. To absorb the necessary energy to stop the aircraft in a specified distance during a rejected take-off.
3. To provide sufficient drag to hold the aircraft stationary against a specific engine thrust.
4. To have enough wear capacity to achieve the desired service life.

As can be seen from the above, the most important function is to absorb the kinetic energy of the aircraft when necessary and via mechanical energy change it into thermal energy. This thermal energy has to be convected, conducted and radiated away from the aircraft safely.

Chapter 3

EVOLUTION OF BRAKE DESIGN

The first aircraft brakes employed where just mechanically operated road vehicle drum brakes. The basic components of a drum brake are a pair of curved shoes lined with a friction material and a drum that is secured to the hub and rotates with the wheel. When the pilot presses down the pedal a mechanical link presses the shoes against the inside face of the drum thus slowing down the wheel. A return spring is attached to both of the shoes to facilitate release. If each shoe has its own pivot point and its own actuation point, then both shoes are leading and the design is known as a two-leading shoe brake, examples of which were found on the Junkers 88 and Focke Wulfe 190. As aircraft grew larger, the force required to actuate the brakes also increased until a point was reached where the pilot's force had to be augmented or supplanted by the use of hydraulics or pneumatics.

An example of a hydraulically actuated drum brake is shown in Figure 6. In this design, there is one pivot point shown at the top of the diagram and a piston situated at the bottom of the picture. In this case, one shoe is termed the leading shoe and the other is the trailing shoe. The increase in energy required to be absorbed by the brake during the 1930's led to the development of multi-shoe brakes instead of the twin-shoe brakes, see Figure 7.

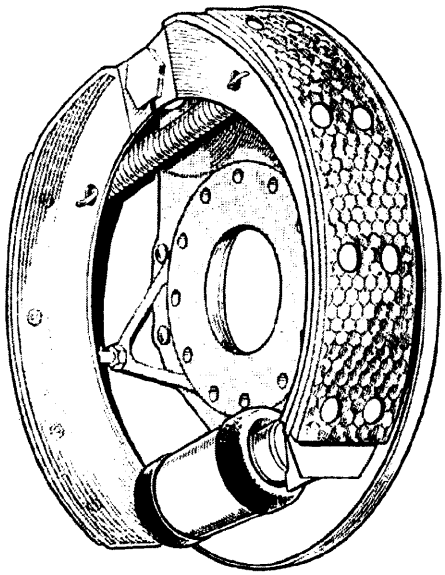

Figure 6 Twin Shoe Brake (Dunlop)

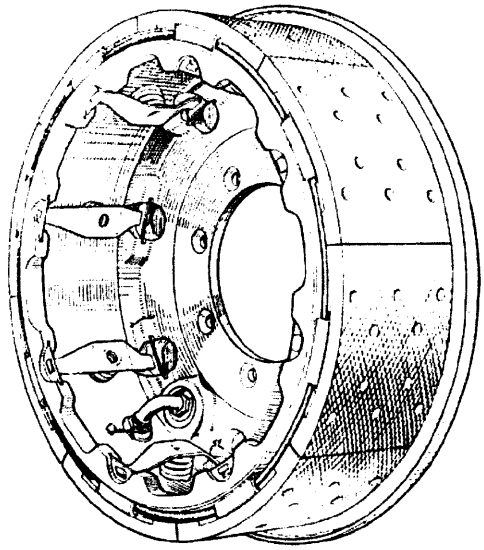

Figure 7 Multi-Shoe Brake (Dunlop)

Another type of drum brake was the bag-type drum brake. This consisted of a series of brake blocks, keyed to the back of the brake housing, which when the bag expands applies pressure to the drum. In 1933 Dunlop fitted one of the first commercial pneumatically operated aircraft brakes to the Fokker F-XXXVI monoplane, this was previously tested on an Avro Avian. The pressure was supplied by an air bottle with enough volume for several applications and the brake was applied by means of a bicycle-type lever attached to the joystick and operating a pneumatic relay. This relay was mechanically attached to the rudder and provided a differential steering capability. It was not until 1935 that Dunlop demonstrated an equivalent hydraulically actuated system. An interesting feature is that certain designs utilised two bags for added safety. An example of a bag-type drum brake is shown in Figure 8.

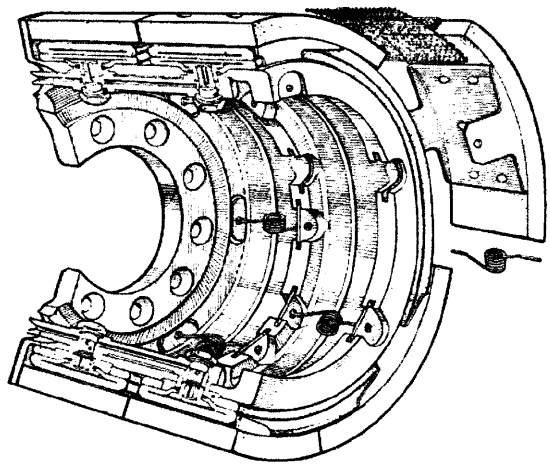

Figure 8 Bag Actuated Drum Brake or just Bag Brake (Dunlop)

Air or oil pressure is used to expand the tube or bag and the strength of the bag limits the operating pressure to around 150-200 lbf/in^2. An additional problem with this design was the considerable delay in releasing the brake due to the volume of air or oil in the bag.

In 1939, the British Air Ministry put a limit of 35 lbf/in^2 on brake pressures and banned the use of pneumatics while mandating the use of hydraulics for large aircraft. The stated explanation was that since large aircraft needed to have hydraulics available for gear retraction, flap operation and turret rotation then to have to supply a pneumatic source only for the brakes would be adding unnecessary weight. Another reason might have been the fact that the Americans were achieving better braking performances than the British and they were employing hydraulics. The fact they operated from paved runways (unlike the British) and consequently could use higher tyre pressures was not taken into account. Dunlop privately modified a prototype Handley Page Halifax and installed pneumatic brakes to demonstrate an improvement in braking over those aircraft fitted with hydraulic brakes. This work led to the Air Ministry rescinding their previous ruling. However, the fight against the use of hydraulics was ultimately lost and eventually forced their use on brakes.

Drum brakes have friction linings that are simple to replace and are generally reliable with a typical 1940's drum brake being capable of absorbing approximately 15.5 million ft.lbf. However, the main drawback is that the drum tends to expand in a direction that releases the brake. This coupled with the fact that heat distortion on cooling, limits the drum life

and requires more fluid to be fed to the brake to effect the same braking force stimulated the development of alternative brake design.

The next development in terms of brake design was the introduction of the disk brake and in 1946 the first high speed jet-propelled aircraft, a Canberra, equipped with disk brakes landed on a British runway. The main advantage of the disk brake is that the disk expands in a direction normal to that of the braking force – this does not act to reduce braking effort and reduces asymmetric stresses. Other benefits are reduced inertia achieved by lowering the effective radius of the mass and more efficient cooling due to the increased exposed surface area.

A disk brake consists of two parts: the disk itself, which is fixed to the wheel hub and was usually either steel or copper and the caliper. Two examples of which are shown in figure 9, a single piston and a three piston.

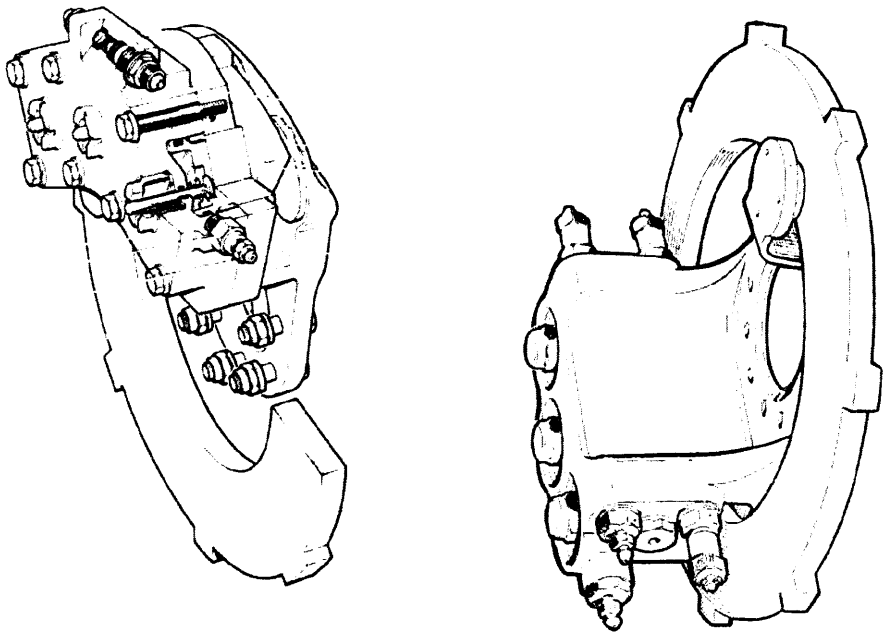

Figure 9 Examples of Caliper Brakes (Dunlop)

The next design enhancement on from the caliper brake occurred around the 1950's and was the development of the single plate (disk) brake, which is shown in figure 10. In this design a disk rotates with the wheel and when operated pads are then forced into contact thus forcing the disk (and thus the wheel) to slow down.

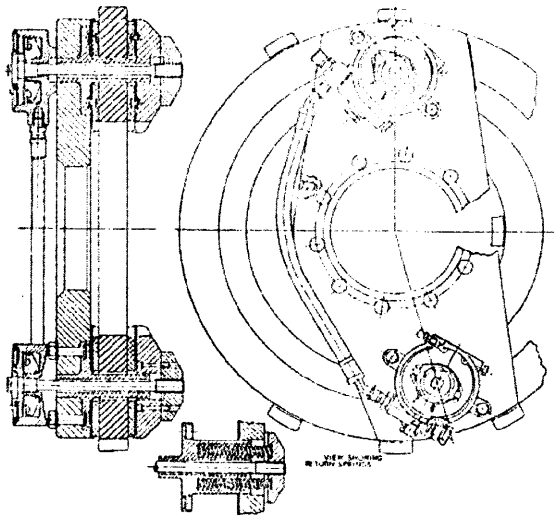

Figure 10 Plate Brake (Dunlop)

The difference between the plate-brake design and the caliper brake was that in the plate-brake the piston assembly does not span either side of the disk. Due to the large exposed disk area the brake possesses good heat dissipation properties however, the main disadvantage is the small friction area. This small area requires high pressures to obtain the desired braking torque and necessitates the use of special friction materials. By the mid to late 1950's the continuing increase in energy and drag requirements gave rise to the development and introduction of the multi-plate disk brake. This design tried to overcome the limitations of the single disk plate brake by introducing more than one plate, figure 11.

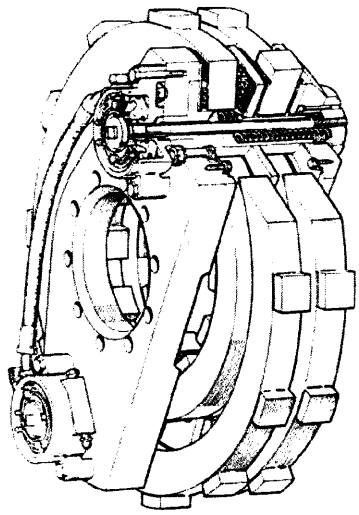

Figure 11 Multi-Plate Disk Brake (Dunlop)

However, with the never-ending requirement of being able to absorb more energy and to produce more drag the multi-disk brake was developed and first used in the late 1950's, an early Goodyear design is shown in figure 12.

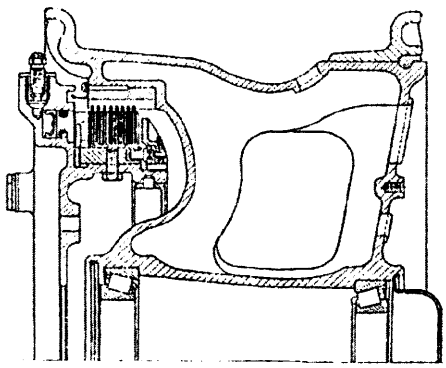

Figure 12 Early Multi-Disk Brake (Conway, 1958)

The main drive for the use of multi-disk brakes has been the desire to utilise the largest number of friction surfaces as possible, thus enabling the required torque to be developed at lower operating pressures. In all designs, the brake consists of a series of alternating fixed rotating and stationary disks known as the rotors and stators, which are brought into contact together typically by the use of hydraulic pressure. Early multi-disk brakes used thin solid disks but eventually articulated disks came into use. The articulated disk offered distortion free use, provided ventilation paths by which the lining dust is removed, as well as enhanced cooling after a stop.

A major change in brake design took place during the late 1990's with the development of electrically actuated electric brakes or as they are commonly known as electric brakes. In this type of design electric motors, gears and a screw mechanism replace hydraulic pistons.

An electric brake consists of a set of electric pistons distribute around the torque plate and each consisting of the necessary motor, gears and screw mechanism to provide end-load. A schematic of one type of electric piston is shown in Figure 13.

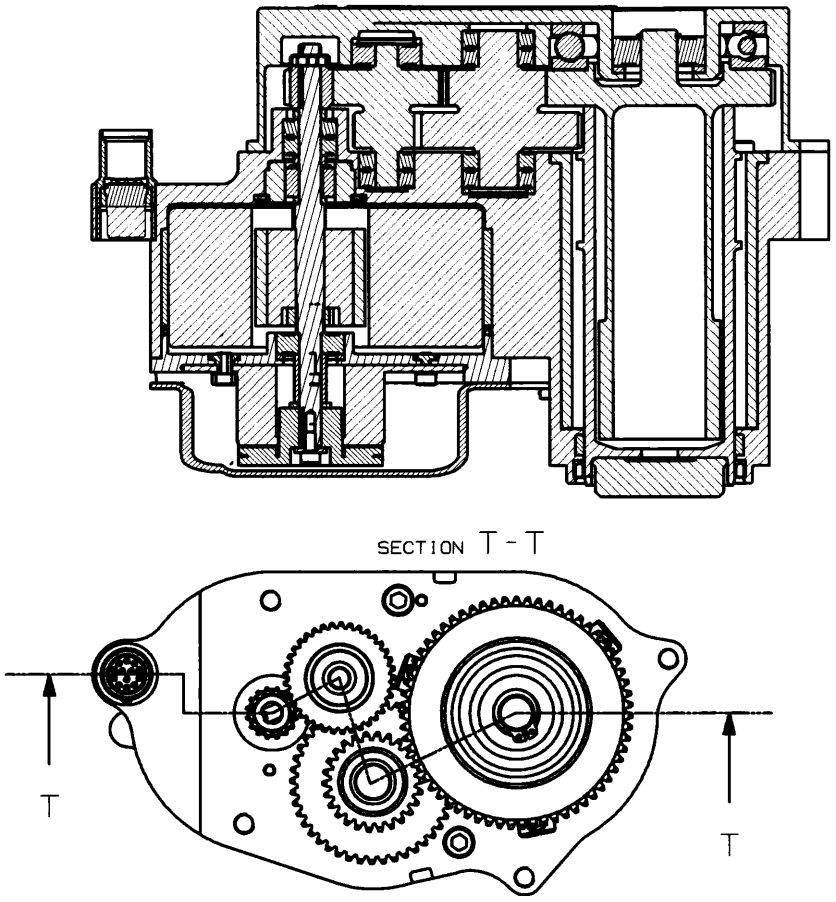

Figure 13 Electric Piston (Dunlop)

The impetus to move to electric actuation has been driven through a move at the whole aircraft level to remove hydraulics, which would ultimately lead to the development of the All Electric Aircraft. This research showed that this aircraft system architecture leads to a reduction in overall aircraft weight and that this would provide either longer range or increased payload capability.

In particular electric brakes have a number of additional benefits and these will be discussed in turn.

The introduction of electric actuation will enable load to be controlled bi-directional i.e. driven on and off. This is in comparison to the existing single acting hydraulic piston currently in use, which relies on the stiffness of the structure to provide the force to release the brakes. In an electric brake the screw is driven off by the motor and, if designed correctly, can provide a faster time to remove brake end-load. This is in turn can translate to an increase in anti-skid efficiency (see Chapter 9).

Another drawback with hydraulic systems and in particularly brakes is that it is difficult to ensure that all the air in the system is removed. If the system is not bled correctly the system can appear to the pilot as inconsistent and difficult to control. This consistency of bleeding is also very important, as pilot feel is very subjective. Electric brakes obviously do not have this effect.

Another reason for the initial research into electric brakes was the need to remove the possibility of brake fires. At the time the F16 aircraft was prone to brake fires and the removal of the hydraulic fluid would eliminate the major source of flammable liquid in that area. However, developments in hydraulic fluids and better thermal modelling have led to better thermally designed brakes thus removing this as a major driver.

As with all electric actuation systems there is as greater capability to provide increase built-in-test functionality and this in turn leads to reduced maintenance costs. The capability to accurately identify the faulty component quickly in particularly has a beneficial effect on the direct maintenance cost.

Chapter 4

FRICTION MATERIALS

Introduction

Developments in brake design were only possible due to the developments of new and better friction materials. This chapter will discuss the characteristics of a material suitable for use as an aircraft friction material and in particular discuss the development, manufacture and properties of carbon-carbon composite friction materials.

The selection of a suitable friction material for aircraft brake applications is based on the following requirements;

- High Specific Heat
- High Thermal Conductivity
- Low Linear and volumetric expansion
- High Melting Point
- Good Strength at Temperature
- High Friction Coefficient
- Consistent Friction Coefficient
- Low Wear Rate

Additional requirements that are also very important are raw material cost, manufacturing cost, mechanical robustness and chemical inertness (corrosion resistance, chemical contamination etc.). The development of friction materials has progressed steadily from using organic pads through ceramic materials to sintered iron and more recently carbon-carbon composites.

The earliest friction material used consisted of asbestos fibres woven into a synthetic organic resin, typically phenol-formaldehyde. These organic pads were used in conjunction with cast-iron or steel drum brakes. The difficulty with this material is that the resin tended to seep into the area between the drum/disk at lining temperatures above 250-300°C resulting in severely reducing the friction generated. Another important design

consideration with organic pads is that they have "poor thermal conductivity and the mass of the pads cannot be considered as part of the heat absorbing mass when making design calculations" (Roberts, 1981).

A further refinement to this friction material was the development of copper or steel in the organic resin. This type of friction material was used in early caliper brakes and performed better than the asbestos & phenol-formaldehyde combination because it did not suffer the same problems of fade, i.e. loss in performance. In addition, this material allowed brake temperatures to rise up to approach 700°C.

The next step in the evolution of friction materials was the introduction of sintered materials. Sintering is a manufacturing process by which powders are heated to form dense materials. For friction materials a metallic matrix is used in which lubricants, fillers and friction materials are mixed in powder form.

Typically pad material consists of

- A copper or iron matrix accounting for 70-80% of pad mass
- Secondary metals to the basic matrix
- Graphite, typically around 10%
- Friction Modifiers
- Refractory materials such as silica and/or silicon carbide, typically around 10%.

Sintered friction materials are still widely used due to their wear and stable friction characteristics. Another advantage is that their performance is insensitive to conditions.

Development of Carbon-Carbon Composites

The time taken to stop an aircraft is relatively small and essentially no heat transfer takes place. This requires that the heat sink must be able to absorb the energy input and importantly the rate of energy absorption. If the temperature rise due to each brake application results from

$$M\Delta H = E \tag{1}$$

Where M is mass, ΔH is the change in enthalpy and E is the kinetic energy absorbed by the brake. Separating the brake into heat sink mass and structural components mass, M_{HS} and M_{BS} respectively then

$$M_{HS}\int_{T_0}^{T_0+\Delta T} C_{pHS}\,dt + M_{BS}\int_{T_0}^{T_0+\Delta T} C_{pHS}\,dt = E \tag{2}$$

The time required for heat transfer to the structural components is long and therefore the heat sink material's change in enthalpy determines the maximum temperature reached during each application.

The specific heat C_{pHS} of a material varies with temperature, T and therefore using an average value through the brake application $\overline{C_{pHS}}$, then

$$M_{HS}\overline{C_{pHS}}\Delta T = E \tag{3}$$

Re-arranging this equation gives a ratio by which to judge the suitability of a brake heat sink material.

$$\frac{E}{M_{HS}} = \overline{C_{pHS}}\Delta T \tag{4}$$

As can be seen from this equation the main driver that determines the mass required to absorb the energy is the specific heat capacity of the material. The higher the specific heat the lower the mass needed to absorb the energy while maintaining low temperatures.

High specific heat properties are associated with elements that have a low atomic number. This is explained through quantum physics using phonon mode vibration (Nave, 2003) From the periodic table it is clear that the first few elements are gases while others such as boron and lithium are not suitable through either low strength, low melting point, low thermal conductivity etc and only Beryllium and Carbon satisfy these basic requirements.

Early development of lightweight friction materials concentrated on Beryllium and this was used on the Shuttle in the early days. However, the main disadvantage of Beryllium is the formation of the toxic Beryllium Oxide both in the manufacturing process and during operation as a friction material. This resulted in the pursuit of Carbon based friction materials as the main opportunity to achieve a lightweight heat sink material. Note that Carbon has a specific heat of nearly 2.5 times that of steel while its density is approximately 4 times lower.

The added advantage of using carbon materials was the possibility to create a friction material that also has enough structural strength to be used without the need of a carrier plate.

The breakthrough came with the development of carbon-carbon composites. The term carbon-carbon composite is used for all composites that have carbon fibre based on carbon precursors embedded into a carbon matrix. Carbon-carbon composites were initially developed for the defence and space industries in the USA. The first application on commercial aircraft was Concorde with the weight saving provided by carbon-carbon composites over steel brakes being over 600kg (Stimson and Fisher, 1980).

Manufacture of Carbon-Carbon Composites

It is important at this point to clarify what exactly is a carbon-carbon composite. The definition is that of a "carbon fibre reinforced carbon matrix consisting of carbon fibres embedded in a carbonaceous matrix" (Savage, 1993). One must also remember that carbon-carbon composites are not a single material but a whole family of materials.

The exact manufacturing process of carbon-carbon composites are kept confidential to each manufacturer. However, general principles are well known and are discussed below.

The manufacture of carbon-carbon composites consists of two main processes producing the carbon fibre and formation of the carbon matrix.

Carbon fibres can be formed from heat treated rayon, polyacrylonitrile (PAN), pitch (petroleum or coal tar). They are basically "filaments consisting of non-graphitic carbon produced by the carbonisation of synthetic or natural organic fibre or of fibres spun from organic precursors" (Savage, 1993). Rayon was the original material used to produce carbon fibre however, only PAN and pitch precursors are used in large-scale manufacturing today.

The carbon matrix acts as the binder in the composite and provides positional alignment to the fibres and fibre bundles. The carbon matrix also acts to transfer the externally applied load the individual reinforcing filaments. The importance of the carbon matrix is that the structural characteristics of the matrix have a direct and significant effect on the physical properties of the composite.

The carbon matrix can be directly formed using chemical vapour deposition (CVD) or by carbonising phenolic or pitch precursors, figure 14

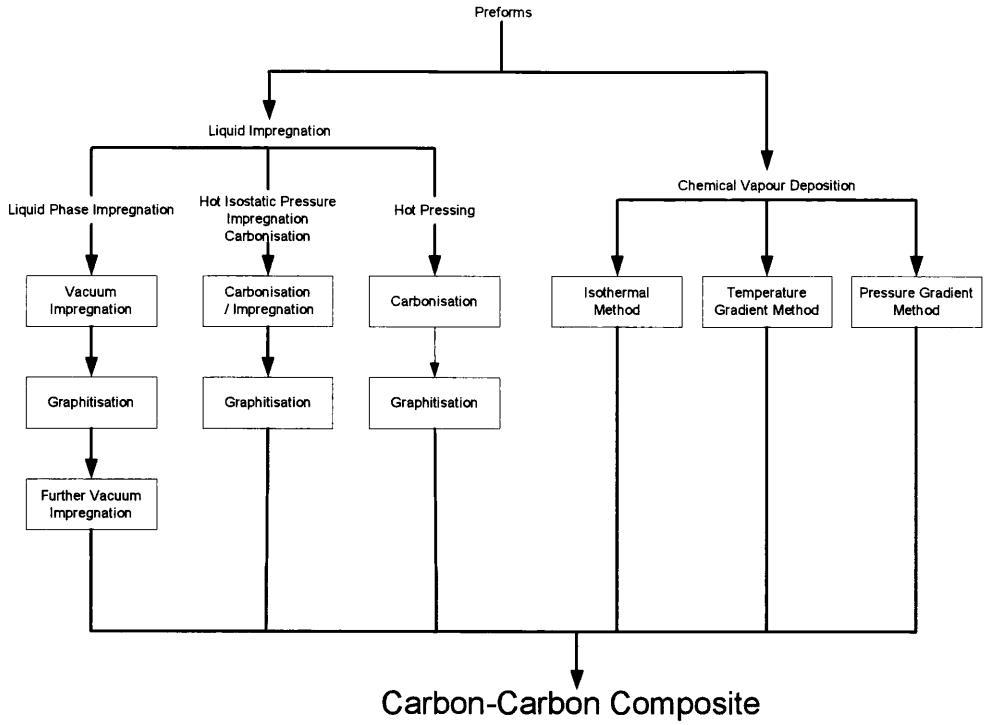

Figure 14 Carbon-Carbon Composite Manufacturing Routes (Windhorst and Blount, 1997)

Chemical Vapour Deposition

"CVD is a process in which a solid product nucleates and grows on a substrate, by decomposition or reaction of gaseous species, and involves the heating of a fibre perform in a gaseous environment so that the matrix is deposited from the gas phase" (Savage, 1993)

The CVD processes takes considerable time due to the slow rate of deposition and can take several months. There is considerable research being undertaken to deliver a carbon-carbon composite material suitable for aircraft brake applications quicker than the existing routes however, most of this is in-house to the aircraft brake manufacturers. One route is discussed on the literature is that of Luo (2002) who uses a rapid direction diffused CVD approach.

There are three main routes for CVD these are;

- Isothermal
- Thermal Gradient
- Pressure Gradient

The thermal and pressure gradient method will not be discussed here as the aircraft brake manufacturers use the isothermal route to produce disks.

Isothermal Method

The isothermal route utilises the diffusion of a hydrocarbon gas into the preform through pores and subsequent "cracking" of the gas to deposit the carbon. The chemistry and thermodynamics are complex but for the interested reader the paper by Delhaes (2002) gives a thorough treatment of the subject. In practice it is found that both gas composition and flow rate are important parameters of the process that require controlling and every aircraft brake manufacturer keeps the exact process a closely guarded secret.

In the CVD route the carbon fibres produced during the first stage are then laid-up into a disk shape with the number of layers being determined by the required disk thickness. This stack of cloth layers is then placed between graphite plates in a jig.

These preforms undergo a CVD run to "bond" the fabric layers together with carbon and at this point the density and strength of the disk is such that the jig can be removed. After the removal of the jig the carbon disks now undergo the main infiltration. Lastly the disks are heat treated to achieve the desired crystallographic structure in the carbon matrix and then machined to finished dimensions. The final product is a disk with a density around 1.8 g/cm^3, usually containing 20-25% carbon fibre by volume.

The quality of the carbon microstructure deposited is important for the mechanical and thermal properties of the composite. For CVD carbon matrices there are three main carbon microstructures (Pierson and Lieberman, 1975).

- Smooth Laminar
- Rough Laminar
- Isotropic

The behaviour of the carbon-carbon composite depends on the quality of the matrix and the associated interfacial behaviour (Delhaes, 2002). Rough laminar is the only microstructure that is able to be graphitised fully with further heat treatment and is the desired microstructure.

Figure 15 Micrograph of Rough Laminar Microstructure (Dunlop)

Most carbon-carbon composites are densified by the CVD route because the rough laminar microstructure has good thermal and mechanical properties due to the well order and highly orientated nature of the structure. A micrograph of rough laminar carbon-carbon composite is shown in figure 15.

Densification by Liquid Precursor

In this route a liquid that is either resin-based or pitch-based forms the carbon matrix. There are three methods of liquid impregnation;

- Liquid Phase Impregnation (LPI)
- Hot Isostatic Pressure Impregnation Carbonisation (HIPIC)
- Hot Pressing

In all of these methods the carbon matrix is produced in the spaces between the fibres and after heat treatment, shrinkage occurs leading to a substantial reduction in volume determined by the densities of precursor and carbon product (Rand, 1993). This may require further impregnation and in some manufacturing routes a CVD process to "top-up" the matrix is used.

General Properties of Carbon-Carbon Composites

Carbon-carbon composites exhibit high strength coupled with a low density, which in turn leads to a high strength to weight ratio. While this is not unique and many materials offer comparable properties, the ability to maintain these mechanical properties at temperatures greater than 2000°C is unique. Even above 2000°C carbon-carbon composites have useful properties until above 3000°C when sublimation takes place.

The main reason to produce rough laminar microstructures in CVD carbon matrices is that its thermal conductivity is greater than three times that of smooth laminar and isotropic microstructure. Composites produced by liquid phase impregnation often have poor thermal properties due to the isotropic nature of the carbon matrix produced.

Oxidation of Carbon-Carbon Composites

Carbon-carbon composites in common with all carbons will oxidize when exposed to high temperatures in the presence of oxygen. This process starts to be measurable in the laboratory at temperatures of about 400°C and progresses more rapidly with increased temperature.

Oxidation will result in the carbon disk mass decreasing which in turn results in reduction of the following

- Mechanical strength (5% weight loss typically gives a 25% reduction in strength)
- Heat capacity
- Friction surface area
- Refurbishment capability.

It is the reduction in strength that is the major concern and the fact that it is not always possible to judge how much mass has been lost and thus the loss in brake performance capability is not obvious.

The oxidation progresses by diffusion of oxygen molecules into the structure, which initially reacts with the carbon at the fibre-matrix bond. Subsequently the carbon fibres are also attacked and the matrix is usually the most resistant to attack in the PAN/CVD composites. Oxidation has a significant effect on the strength of structural carbon such that a small degree of oxidation results in a significant loss of strength. The rate of oxidation is exponential with temperature and follows an Arrhenius law depending on the activation energy. Another important factor in oxidation is the time of exposure. The rate of oxidation is controlled by the chemical reaction at low temperatures and at higher temperatures by the transport of the gases to and from the reaction sites. As a result of these factors the critical temperature separating the two controlling steps is not well defined. The difficulty arises due to the reaction surfaces changing with time and the fact that open pores and micro cracks are generated during the oxidation process.

At temperatures below 600°C the rate of oxidation is controlled by the reaction of oxygen with active sites on the carbon surface. The degree of graphitisation plays an important role

in that a more graphitic material has a lower number of active sites (atoms at the edge of the basal plane) available to react with oxygen. Oxidation occurs more readily at these sites because of they have a lower activation energy than other atoms contained within the graphene layers, see figure 16.

High conductivity acts to equalize temperatures within the heat sink material and this is beneficial in reducing the risk of oxidation by reducing time at temperature. As outlined above, the rate of oxidation is dependent on the activation energy and the presence of impurities, especially sodium and potassium which act as catalysts to increase this rate. Therefore to minimize oxidation it is important to have high-density (low porosity) composite material as this results in reduced surface area and less absorption of contaminants

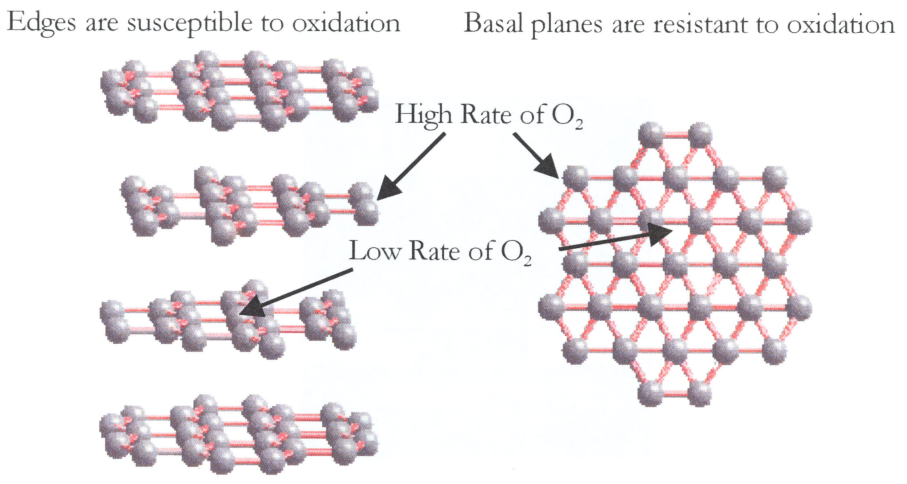

Figure 16 Schematic of Carbon Atomic Structure (Dunlop)

Oxidation of Carbon-Carbon Brake Disks

Aircraft brakes tend to exhibit two main types of oxidation,

- Thermal - repeated exposure to high temperatures
- Catalytic

Thermal Oxidation

The thermal oxidation classification is to indicate that this oxidation damage occurs through repeated extended exposure to high temperature. There is no difference in oxidation to that of catalytic oxidation however the location within the heat sink is different. Typically this type of oxidation damage occurs in the middle of the heat sink. The damage tends to be observed as de-lamination of the composite starting at the edges of the disks, this is clearly shown in figure 17.

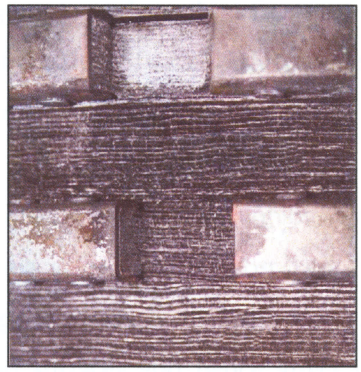

Figure 17 "Thermal" Oxidation Damage (Dunlop)

Catalytic Oxidation

Aircraft heat sink materials are exposed to high levels of contamination particularly in the form of alkali metal formates and acetates stemming from the use of aircraft and runway de-icers and aircraft cleaning agents. These fluids act as catalysts to the oxidation process and lower the temperature required to start the process (Carabineiro et al, 1999). Ironically these new de-icers were introduced to reduce the effect on the environment and ended up reducing the life of aircraft brakes. To reduce the effect on the carbon material from these agents, an anti-oxidant coating protects the non-rubbed parts of brake discs. This damage is mainly located on the exposed disks typically at the pressure stator end of the brake, figure 18 shows the typical "eaten away" affect on disks.

Figure 18 Catalytic Oxidation Damage (Dunlop)

Oxidation Protection

There are two main techniques to reduce the effects of oxidation; the first is to use inhibitors that slow the rate of reaction of carbon with oxygen and the second is to provide a barrier to prevent oxygen contact with the carbon.

Typically a phosphate binder is used to act as the inhibitor and phosphate bonding can be achieved by either phosphoric acid or an acid phosphate. It is important to note that on aircraft brakes the oxidation protection is only applied on the non-rubbing surfaces as to not interfere with the friction surfaces and hence affect brake performance. Figure 19 shows a non-oxidised microstructure and figure 20 shows the oxidation at the fibre-matrix bond.

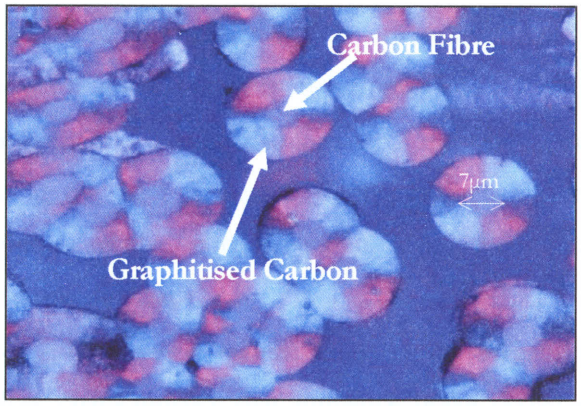

Figure 19 Non-Oxidised Carbon-Carbon Composite (Dunlop)

Proprietary glass-forming barriers are used to prevent oxygen contacting the carbon. This type of protection is required for the sustained severe environmental requirements that an aircraft brake experiences in service.

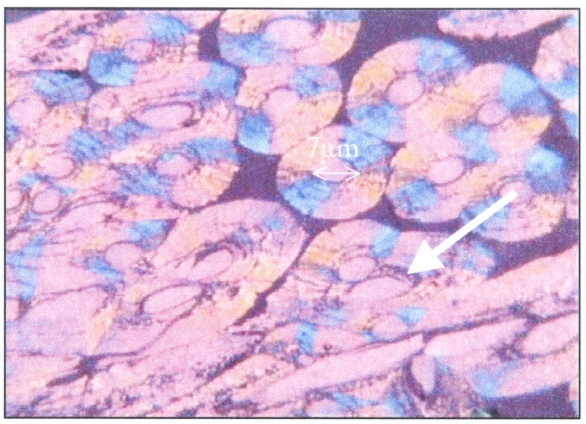

Figure 20 Breakdown of Fibre/Carbon Interface - Onset of Oxidation (Dunlop)

Brake Performance of Carbon-Carbon Composites

Taking the broad material properties discussed in the introduction and translating these into design requirements, the material must also be capable of the following;

- Torque generation – The heat sink material must be capable of generating torque to allow the aircraft to stop safely and predictably under all specified conditions. The key material property to achieve this is the friction performance of the material.
- Torque transfer – The heat sink must satisfy the structural requirement of transferring torque to wheel and tyre under all specified conditions. In order to achieve this, mechanical properties such as tensile, compressive and shear strength, as well as fracture toughness are extremely important.
- Thermal management – The heat sink material must be capable of absorbing and then dissipating the heat generated during high-energy stops The important material properties relative to this requirement are thermal conductivity, thermal diffusivity, and specific heat.
- Vibration-Free - The friction material must be dynamically stable under all load conditions. Key characteristics that influence brake dynamics are hardness and flexural modulus.

- Long-Life – Wear rate and degradation as a result of oxidation damage drives the removal of in-service heat sink material. The oxidation resistance of the material in the service environment is a critical issue in maintaining heat sink integrity throughout service life.

Friction and Wear Performance

According to Amontons' laws of friction

- The friction force is directly proportional to the applied load
- The friction force is independent of the apparent area of contact

These laws were in fact established by Leonardo da Vinci 150 years before Amonton but were subsequently lost.

Coulomb added the third law

- Dynamic friction is independent of the sliding velocity

All surfaces have a roughness and consist of peaks or junctions of contact termed asperities. The difference between the apparent area of contact and the real area of contact is due to the asperities being the only contact points between the two surfaces. As an example of this consider a 100mm by 100mm by 100mm steel cube, the apparent contact area is 10,000mm^2 however, the real contact area has been measured at only 0.03mm^2. From this it is easy to see why the apparent area of contact does not affect the friction force.

Bowen and Tabor (1954) showed that the asperities deformed plastically to give rise to adhesive wear. The friction force arises due to the asperities plastically deforming until the area of contact is enough to support the load. Once the asperities have been deformed to move the surfaces sideways requires overcoming the shear strength of these junctions or interfaces.

Archard developed this further by showing that friction can also occur if the asperities are only elastically deformed and by assuming a loading dependent asperity number distribution, equation 5

$$Q = k\frac{W}{H} \tag{5}$$

Where Q is the wear rate, W is the applied normal load, H is the hardness and k is termed the Archard wear coefficient.

In this adhesive wear mode, material can transfer between the two surfaces or stay in a transfer film. Abrasive wear can also occur between hard asperities on a surface "ploughing" into the other softer surface and once again Archard's wear equation still applies.

For carbon-carbon composites there are a number of factors that complicate the tribology. The first is that "the friction coefficient is strongly influenced by the heat transfer coefficient in the brake system as well as by the thermal conductivity of the carbon-carbon composite" [Park, Park and Kim, 1995].

Carbon-carbon composites exhibit unusual characteristics which when designing a brake must be taken into account. The most important is the fact that the static coefficient of friction is lower than that of the normal landing condition, typically between 0.1 and 0.2 while for normal dynamic conditions the value lies in the range of 0.2 to 0.4. Comparing these values to a steel brake with sintered iron friction material that can develop approximately 0.25 to 0.35 statically and around 0.18 to 0.27 dynamically, a carbon brake will require larger piston diameters to achieve the aircraft static drag requirement. This has the consequence that this higher end-load can be applied when the aircraft is moving and thus generate high dynamic or peak torques. The consequence of peak torque is that the landing gear must be design to withstand the worst-case drag imposed upon it when the brakes apply this value.

While there is a great number of published papers that try to establish a link between macro and micro-properties of the carbon-carbon composite there has not been established a definitive theory. However, general trends and mechanisms have been established. The first is that as the energy of the stop increases the coefficient of friction decreases. The second is that wear is greatest under low energy braking as in taxiing [Stanek, 1993].

Experiments have shown that during braking the coefficient of friction in a carbon-carbon composite undergoes two transitions during which its value rises [Yen, Ishihara and Yamamoto, 1997). The first occurs in the 150-200°C temperature range and is attributed to the desorption of water vapour form the solid carbon surface decreasing the lubrication effect. The second transition occurs in the range of 650-700°C and this suggests a link to oxidation.

Awashi and Woods have proposed a general wear mechanism for aircraft brakes [Awashi & Wood, 1988] and this is outlined in figure 21. The mechanism starts with abraded wear debris being deformed into a friction film that adheres to the surface. Eventually this film delaminates and is crushed and delaminated into another friction film.

The wear debris on the friction surface can be classified into two types [Murdie et al, 1991]. Type I wear debris is a particulate appearing under low energy conditions such as taxiing. The second type of debris is Type II and this forms a smooth adherent friction film under high-energy conditions such as landing. From the experimental work of Hutton [Hutton et al, 1999] Type I debris comprises a disordered carbon phase containing fibre fragments produced mainly by shear deformation of the carbon matrix. Type II wear debris is generated through the transformation of the particulate debris into a film due to the shear stresses involved and "is composed of plastically deformed and fractured components of the composite, including fibres, CVI carbon ..." [Blanco et al, 1997]. This film of amorphous carbon is responsible for the lower coefficient of friction under high-energy conditions. The formation of this film is a consequence of the higher pressure applied to the surfaces and also to the higher surface temperature generated during the higher energy stop, [Murdie & Ju, 1991].

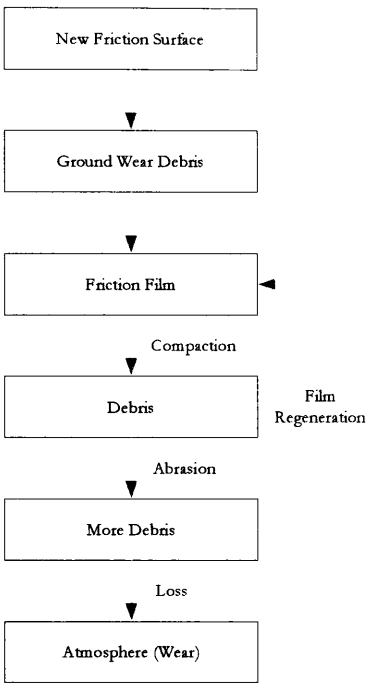

Figure 21 Wear Mechanism of a Carbon-Carbon Composite (Awashi and Woods, 1988)

This categorisation of the wear debris correlates to the transition from low wear to high as exhibited in a number of published papers. A considerable number of these papers discussed the role of oxidation in the wear of carbon-carbon composites [Chang & Rusnak, 1978; Chang, 1982]. An interesting and important recent paper [Gouider et al, 2004] has provided empirical evidence to show that the oxidation of the carbon-carbon composite is associated with a high wear rate. The method used in the experiments involved using a mass spectrometer coupled to a pin-on-disk friction test machine. This allowed the determination of the gases present initially and those generated or consumed during the stop. The experiment provided evidence that during the friction transition there is a release of carbon dioxide and oxygen consumption – corresponding to the following chemical equation.

$$C + O_2 \Rightarrow CO_2 \qquad (6)$$

This reaction also indicates that the instantaneous contact temperature is higher than the bulk temperature, which is less than 400°C. This oxidation process is shown to always

accompany the abrupt friction transition and consequently always associated with a high friction and high wear rate regime. Gouider et al also conclude that during the friction transition water is consumed.

While Yen and Ishikara have proposed that the first regime is due to the desorption of water this work by Gouider et al does not support this being the complete explanation. However, water vapour has been shown to have an effect on the friction regime of carbon-carbon composites in particular through the work of Chen et al (Chen, Chern Lin and Ju, 1996).

A number of papers discuss the various different manufacturing routes and indeed in the same routes specific process details such as heat treatment temperatures and composite construction e.g. number of PAN filaments, fibre weave etc. While all of this detail is important in understanding and being able to manufacture a better carbon-carbon composite it does not provide any help in designing a heat sink to meet the aircraft performance. It is also obvious that the nature of friction while possibly understandable will still be stochastic in nature due to the amount of variables involved.

A group of former Soviet Union researchers, led by Chichinadze, have developed a theory based on the work of Kragelsky, [Chichinadze, 2000 and 2001] aimed at providing a theoretical understanding of the friction and wear process in a carbon-carbon composite. It is based upon 6 separate but inter-related theoretical physical models of the following

- Mechanical Dynamics
- Macro-contact thermal properties
- Discrete contact parameters
- Micro-contact thermal properties
- Surface layer parameters
- Mechanics of surface layer destruction

The approach is based on the theories of external friction and fatigue wear of solids as developed by Kragelsky (1965). This assumes that the friction coefficient and the wear rate are functions of the surface temperature and temperature gradient along the normal to the friction surface. In addition, it is assumed that the temperature of the friction surface may

be determined through superposition of temperatures arising from the initial temperature of the friction couple, bulk temperature (generated through previous braking), average temperature of the contour area (defined as that formed through bulk compression of the couple) and the flash temperature of the actual contact spot. The six theoretical models are complex and require a number of parameters and their variation with temperature to be established empirically. It is the author's opinion that the main difficulty with this theory is that there are a large number of variables that the "solution" depends on and while it concentrates on the material properties there are a large number of external factors that will affect how the brake performs that have not been accounted for.

Chapter 5

MULTI-DISK BRAKE DESIGN

Introduction

It is seen from figure 22 that the brake's heat sink consists of stationary and rotating disks termed the stators and rotors respectively. The heat sink is where the kinetic energy is converted into heat and stored, as well as where the torque is generated.

The brake operates by hydraulic fluid entering the cylinder assemblies resulting in movement of the piston. This movement, through the reaction at the thrust end of the brake, results in a clamping force on the rotors and stators of the heat sink.

A multi-disk heat sink is the most efficient in terms of installation and mass due to the fact that the whole heat sink (rotating and non-rotating components absorb the heat with the consequence that compared to a caliper brake there is considerable mass reduction - this and the use of thin plates, in conjunction with their large working area, results in a surface temperature not too different to that of the bulk temperature. Another advantage of this type of brake is that the actuation needed to provide the clamping force can be fitted within the rotating envelope of the heat sink and therefore can be reacted very efficiently.

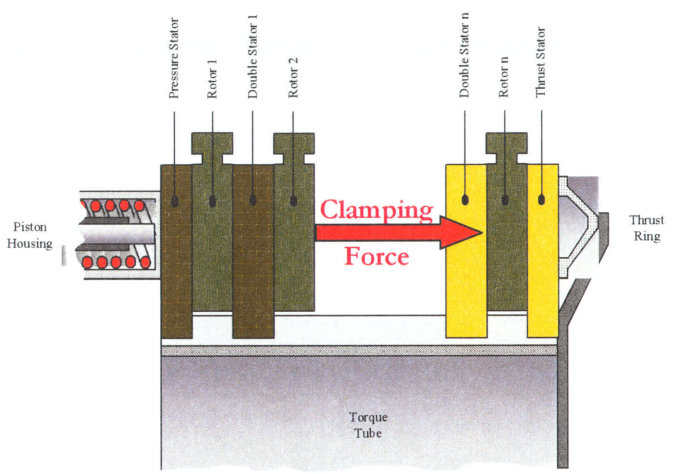

Figure 22 Illustration of Multi-Disk Heat Sink Operation (Dunlop)

Design Requirements

The design of an aircraft brake is governed by the Airworthiness regulations and for Transport Category Aircraft JAR and FAR 25. In addition, minimum standards are mandated in the Technical Standard Order C-135 and now EASA ETSO C-135. For Military Aircraft brakes are normally designed to meet the requirements of MIL-W-5013 for US aircraft and Def-Stan 00-970 for UK aircraft. However, in more and more military aircraft programmes these specifications are only used as guidelines and a Performance Based Specification is used to determine required performance. This shift in US and UK Military procurement of aircraft components is intended to remove unnecessary requirements and therefore reduce the acquisition and lifecycle cost of equipment.

In order to satisfy the Airworthiness Authorities, the aircraft constructor will specify a number of requirements that the wheel and brake should meet. These requirements can be divided into the following categories

- General Performance (stopping distance, static hold, life)
- Thermal Performance (FPNM capability, temperature limits)
- Weight Target (weight optimised solution expected)
- Structures & Safety (peak drag, structural torque)
- Controllability (torque gain, frequency response)
- Dynamic Stability (vibration)
- Product Quality {Performance Variation} (stop repeatability, effect of humidity, etc.)

An aircraft constructor will specify a number of different design cases and the performance that the brake must achieve. The design cases vary with constructor but typically these design cases are termed

- Service Landing
- Normal or Design Landing
- Overload Landing (Fuse Plug No-Melt)
- Overweight Landing
- Overspeed (or Flapless) Landing
- Maximum Rejected Take-Off (RTO) or 100% (Fully) Worn Brake RTO

For each case the constructor will specify the amount of energy to be absorbed, the deceleration required and the speed at which the brake is applied is termed the Brake Application Speed (V_{BAS}).

The Overspeed or Flapless landing case is the situation where an aircraft has taken-off and almost immediately a subsequent failure of the high-lift system occurs. In normal operation, aerodynamic drag generated through the use of surfaces account approximately a third of the kinetic energy that needs to be lost during a stop. The exact amount is proportional to the square of the velocity at which the devices are deployed – with their effectiveness decreasing at lower velocities.

The Overweight landing case is where the aircraft has taken-off but for whatever reason has to immediately land. Typically, approximately a 1% fuel burn is used to determine the landing weight

The constructor will also state the altitude and ISA temperature required for each design case based on the airports that the aircraft is aimed to operate out off. Typically the requirement will also specify the taxi sequence either in terms of distance e.g. 3 miles of roll or in a number of taxi snubs. The taxi snubs will specify the deceleration and the brake application velocity.

The Maximum Rejected Take-Off is the situation where the aircraft is accelerating during take-off and then an engine failure occurs and the take-off has to be aborted.

The typical distribution of brake energies per landing case is shown in table 1

Service Landing	Normal or Design Landing	Overload Landing	Overweight Landing	Overspeed (or Flapless) Landing	100% Worn Brake RTO
15-20%	30-50%	50-67%	100-110%	90-120%	90-100%

Table 1 Scenarios and Brake Energies

Note that the most arduous scenario will vary from aircraft configuration and operational use.

In addition there are the following static performance requirements;

- Structural Torque
- Single Engine Thrust
- Static Torque

Other tests required are;

- Yield and Overpressure
- Endurance
- Piston Retention
- Extreme Soak
- Leakage (static and dynamic)

Design Drivers/Constraints

The aircraft constructor constrains the design of the brake wheel and brake through the specification of the wheel rim diameter, axle outer diameter, axle length and the landing gear oleo position, this is shown in figure 23.

The wheel rim size is dictated by the aircraft weight and the flotation requirements of the aircraft necessary to operate out of the airports that the aircraft is being designed for.

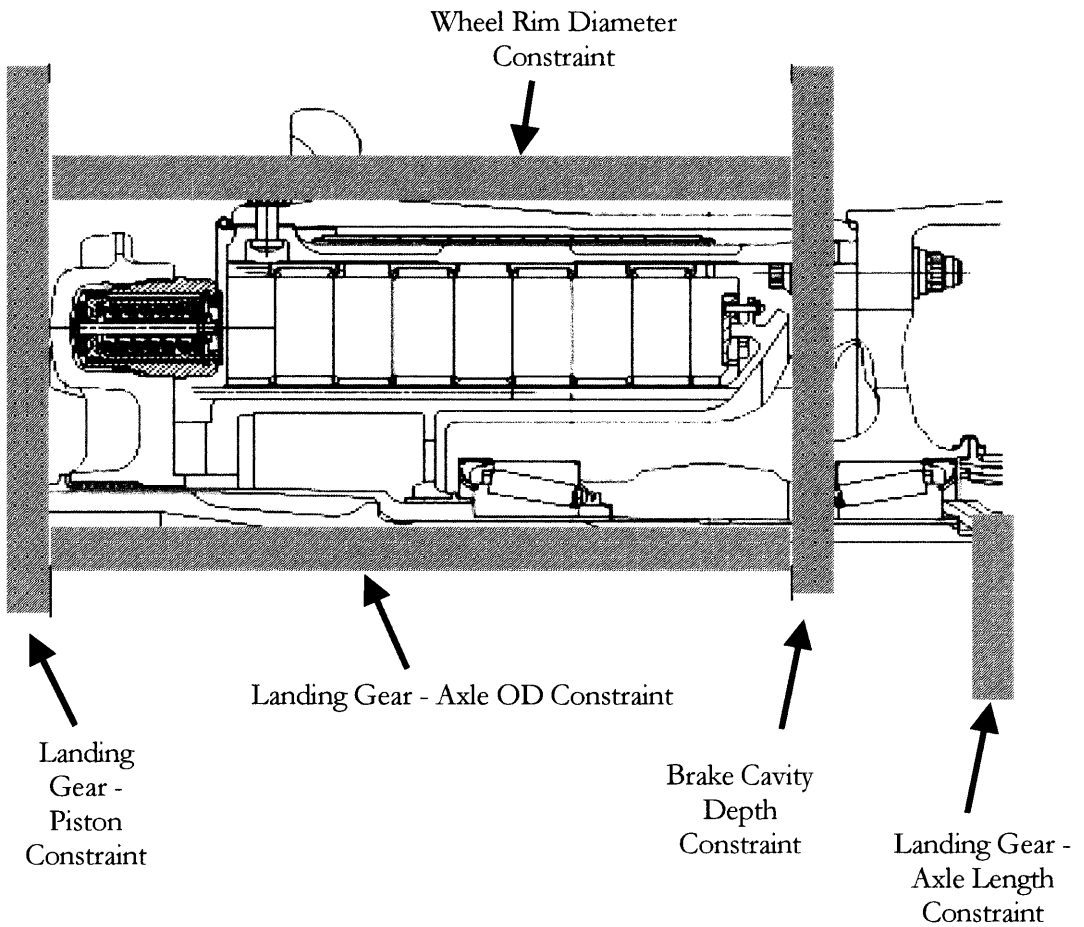

Figure 23 Aircraft Installation Constraints on Wheel & Brake Design (Dunlop)

As well as the physical envelope constraints, the design requirements outlined in the previous section affect the following components/design features; table 2 further details the effect of the various requirements. Additional insight into the design of the different features will be given in the following section.

Requirement	Heat Sink Length	Piston Area	No of Rotors	No of Drives
Static Brake Drag	✓	✓	✓	
RTO Performance (or max energy)	✓	✓	✓	
Structural Torque				✓
Torque Gain	✓	✓	✓	
Peak Torque	✓	✓	✓	
Normal Landing	✓			
Overload Landing	✓			

Table 2 Requirements and their Design Drivers

Components and Important Design Features

A modern multi-disk carbon brake is shown in figure 24 and consists of a number of components. The following section will describe the most significant components/features and it will also discuss their design drivers, the following areas are discussed;

- Piston Housing
- Cylinder & Piston Assemblies
- Torque Tube & Thrust Plate
- Heat Sink

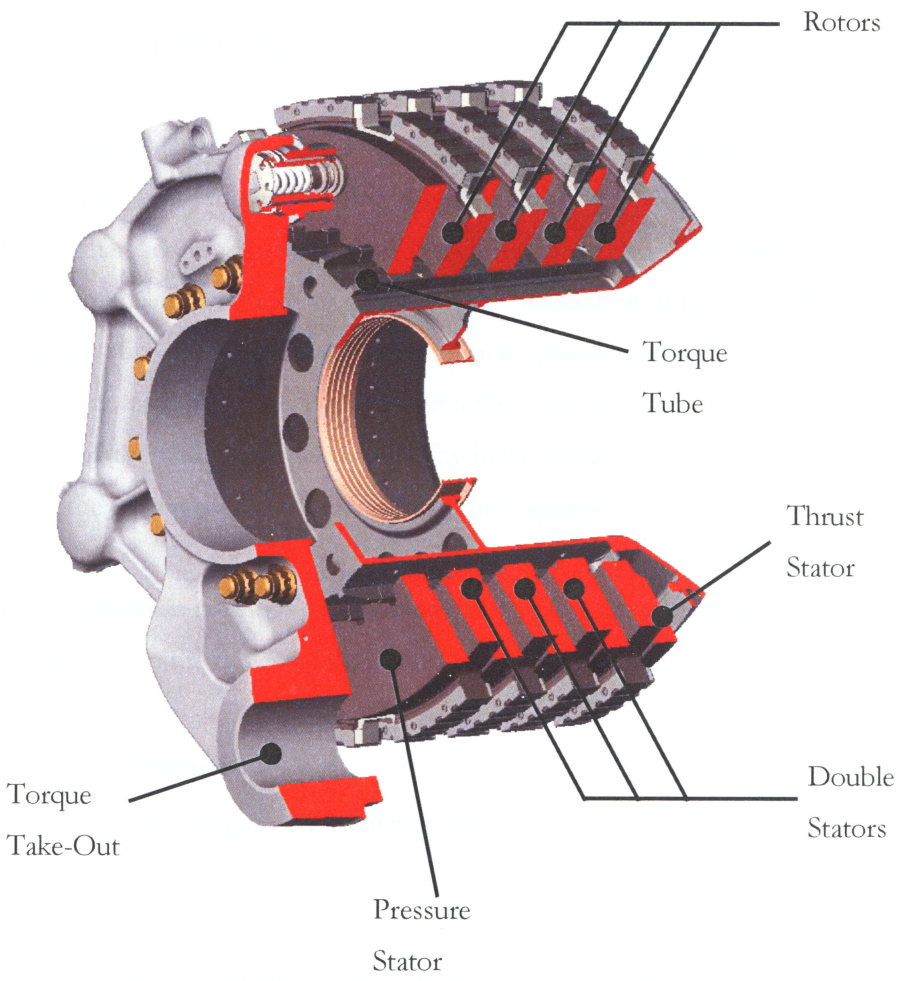

Figure 24 Multi-Disk Carbon Brake (Dunlop)

Piston Housing

Typical either forged 2000 or 7000 series aluminium alloy is selected as this will produce designs that achieve the structural, envelope and minimum weight requirements. The piston housing is a machined close-to-form die forging and is typically treated with anodising and painted for optimum corrosion protection.

The piston housing is designed to provide a lightweight, stiff and robust means of converting hydraulic pressure into axial clamping load and in the case of a torque plate transmitting brake torque to the undercarriage. Optimisation of component weight, structural strength, service life, and rapid hydraulic response is required. Rework and repair allowances are also incorporated in the design to allow continued serviceability throughout typical field service operation.

It is important to design the piston housing to have the minimum deflection possible. One way this can be achieved and still meet the minimum weight objective is through the use of radial ribs that act to stiffen up the structure. The need to minimise deflection is a reflection on the requirement to minimise the amount of fluid required to operate the brake under all conditions. The brake control system is essentially a pressure control system and as such the pilot pedal commands a set pressure, the speed of response is dependent of the volume of fluid in the hydraulic pipes and in the brake pistons/piston housing – the greater the volume the slower the response.

There are three main methods of attaching the brake to the undercarriage and the selection impacts directly on the design of the piston housing. The three configurations are,

- Flange Mounted
- Square torque lug on undercarriage leg
- Torque link and pin

A discussion of the advantages and disadvantages of the different brake attachment methods follows.

Flange Mounted

In this design the axle is heavier and has a larger diameter as compared to the other attachment designs. This is necessary to incorporate the brake-mounting flange and to withstand the brake torque. The positional tolerance of the brake attachment holes is critical and they are therefore expensive to manufacture. The bolts/studs required to attach the brake to the axle will also result in increased inventory and cost. In addition, there is an increase in turnaround time from the need for fitting and removal of the brake due to the fasteners. The brake torque tube is also heavier due to the mounting flange and again the positional tolerance of brake attachment holes is critical and expensive to manufacture. However, the brake piston housing, in this design termed the cylinder block, is lighter due to the removal of the necessity to react torque, see figure 25.

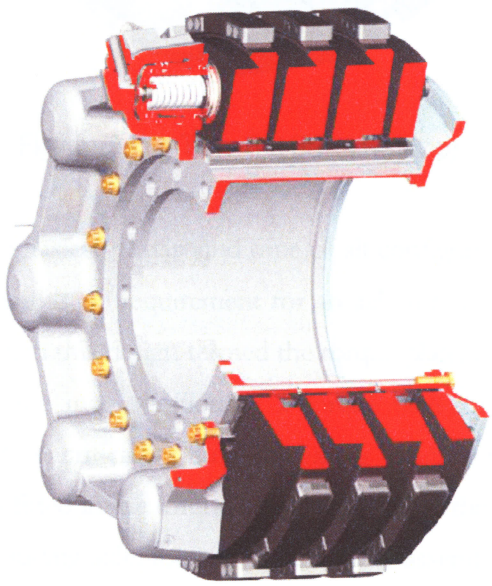

Figure 25 Flange Mounted Brake (Dunlop)

Square Torque Lug on Undercarriage Leg

The axle required for this design is light and simple to manufacture. However, the undercarriage leg requires a torque take-out lug to be provided which requires close positional tolerance and an inevitable increase in the manufacturing costs. Easily replaceable side protection plates are included on each side of the torque take-out lug on the undercarriage leg. This configuration allows for a reduction in turnaround time for fitting and removal of the brake because of the fact that due to wheel bearing pre-load the

brake is predominantly fixed to the axle, however, upon removal of the wheel, the brake remains held in place provided it is still coupled to the hydraulic brake pipes, see figure 26.

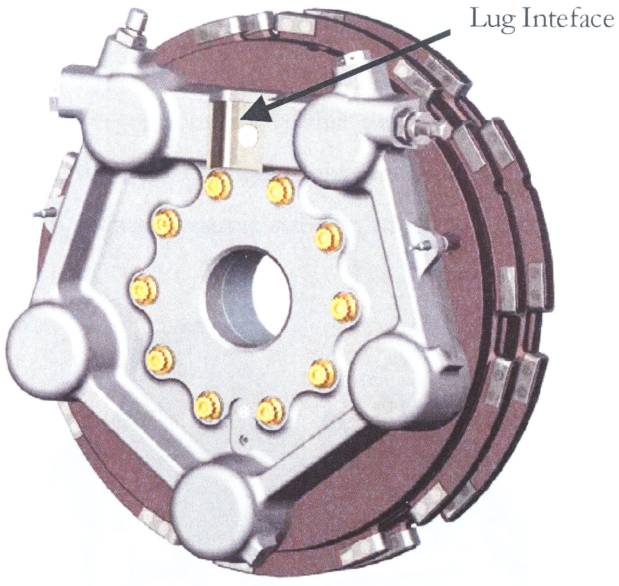

Figure 26 Lug Take-Out Brake (Dunlop)

This solution provides the fastest turnaround time of all configurations. The brake torque tube is lighter because there is no requirement for an axle mounting flange and fasteners. The brake piston housing, in this design termed the torque plate, is marginally heavier than a cylinder block due to the incorporation of a torque take-out socket. The positional tolerance of this socket is critical – thus increasing manufacturing costs. An easily replaceable steel spacer is fitted in the torque take-out socket in the torque plate. This is the lightest overall option including axle, torque lug and brake assembly and is the most easily maintained.

Torque Link and Pin

The axle is no different to that of the square lug design and is light and simple to manufacture, however a provision on the axle for a torque link is required. This extra component results in an increase in mass and cost. However, it does offer a shorter turnaround time for fitting and removal of the brake compared to the flange mounted option. The brake is located by a torque pin in the torque plate and further fixed due to wheel bearing pre-load. The brake torque tube is the same as in the square lug design however; the brake piston housing, in this design also termed the torque plate, is

substantially heavier than either of the other two options. This is due to the addition of a torque take-out lug with close positional tolerance of the torque-pin hole required – resulting in the least affordable option for the piston housing. This is the heaviest overall option including axle, torque link and brake assembly, see figure 27.

It can be seen from the three options above that the square lug torque plate design has many benefits over the other two configurations. In addition there are further benefits associated with this design such as dynamic stability, which will be discussed in Chapter 8.

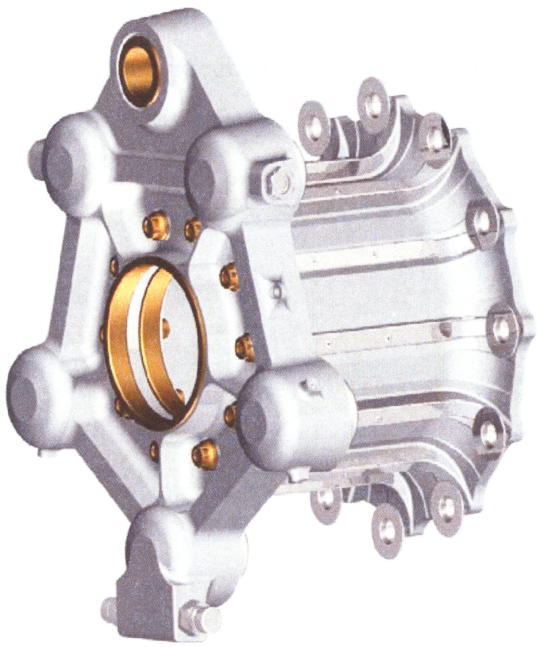

Figure 27 Torque Pin Take-Out Brake (Dunlop)

Hydraulic Circuit(s)

In order to meet the Airworthiness Regulations the constructor places a requirement that the brake must be able to operate from two independent hydraulic sources. As the brake pistons are single-acting pistons there are two design approaches that may be used to achieve this requirement. The first is to utilise a shuttle valve to switch between the two supplies. This changeover occurs when the pressure on the "Normal" circuit has fallen below a certain level and the shuttle valve then shuts that port and allows fluid from the "Alternate" system to be used - in this case the brake is termed "Single Cavity". The second solution requires the use of two separate sets of independent pistons each with

their own separate hydraulic supply. The two sets of pistons are always acting together for normal braking, and either set may be activated individually for emergency braking. A decision has to be taken as to whether the pistons are sized to produce the required end-load with only one hydraulic circuit in operation or two – in either case this configuration is termed "Dual Cavity".

Regardless of the hydraulic circuit used the construction of the housing is such that there are no natural air traps and complete bleeding can be accomplished from bleed ports.

The required shuttle valve for the Single Cavity brake is typically located at the brake. There are two configurations either integral into the piston housing – which saves weight or bolted-on which adds weight but is easier to maintain.

Piston and Cylinder Assemblies

The piston and cylinder assemblies comprise a replaceable hard-anodised aluminium alloy cylinder liner, a hollow stainless steel operating reusable piston and an automatic adjuster/retractor mechanism to ensure efficient brake release.

The cylinder liner is threaded into the hydraulic housing and sealed by a sealing ring and back-up ring recessed into the cylinder liner. The cylinder liner retains the end plate, which in turn secures a steel retraction pin on which the piston is mounted. The return pin and adjuster ball provides a retention stop to prevent piston over-travel and retain the piston in the liner.

A heat insulator of sintered stainless steel with a refractory additive is clipped into the piston head, and serves to transmit and spread the piston end load evenly to the heat sink and to minimise heat transfer from the heat sink to the hydraulic piston

The piston dome section thickness is an important dimension as it is the main driver in achieving the Airworthiness and constructor specified endurance (fatigue) requirements and burst pressure test, see figure 28.

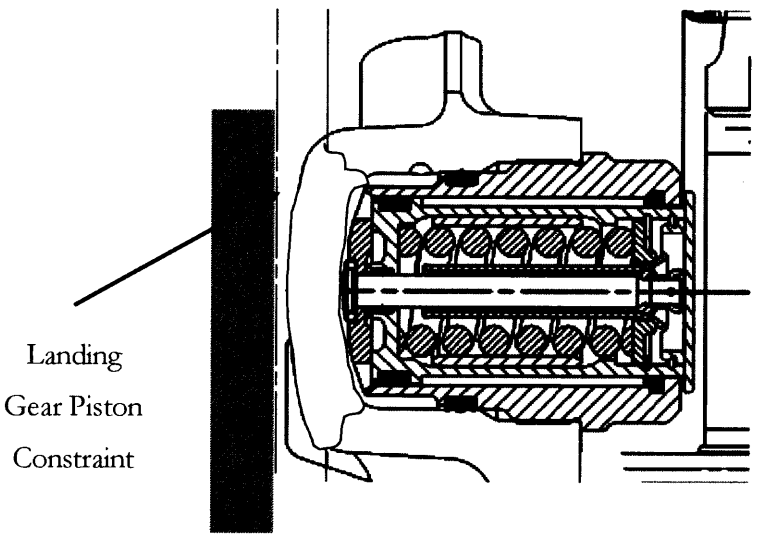

Figure 28 Landing Gear Constraints on Piston Dome Thickness (Dunlop)

Automatic Adjuster Mechanism

An automatic adjuster mechanism is located in each piston and is designed to maintain a constant running clearance and hence compensate for brake wear.

There are two configurations possible - internal or external adjusters. Internal adjusters are the more complex in that this requires that the mechanism be able to be fitted inside the cylinder assembly. They require typically a minimum piston diameter of 1¼ inches (31.75mm). The external adjuster design allows ease of maintenance and the possibility of smaller pistons to be used

There are two methods of achieving this automatic adjustment that are commonly used,

- Friction bush
- Ball & Tube

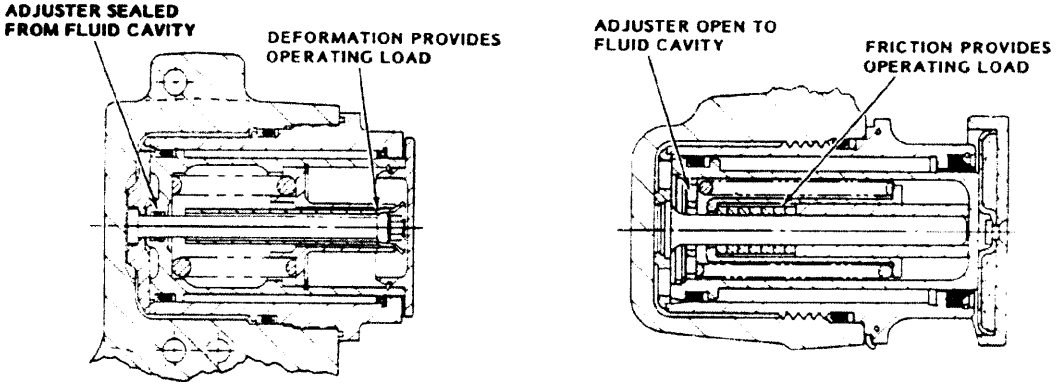

Figure 29 Ball & Tube and Friction Bush Adjuster Mechanisms (Dunlop)

The principle of the friction bush design is that during normal adjuster travel, operation is allowed through the axial movement of the pin up to the preset running clearance. Brake wear causes additional axial movement that can only occur by depending on the friction bush providing the restraining force. This design's reliance on friction can produce inconsistent results, as the friction level is dependent on the surface condition and the interference fit.

The alternative design uses plastic deformation through the expansion of a tube's diameter to generate the necessary restraining force. This enlargement is achieved by pulling a ball slightly larger than the tube's diameter through the tube. The sizing of the nut and fit determines the load necessary to deform the tube, thus providing a force for piston movement that has a narrow range. Therefore this type of mechanism provides a more consistent performance and longer life than that of the friction bush design.

At heat sink replacement the ball and tube adjuster mechanism is simply replaced by removing the retaining nut, pushing back the piston and installing a new retractor/adjuster swage and tube. The self-locking nuts are replaced and the piston is reset to its original position for the new heat pack. The friction bush is even easier and is simply pushed back by an externally applied force.

The more recent designs use efficient helical coil type springs to provide the preload. The alternative design is to use a set of disk springs however, this requires a large number of disks to achieve the stroke required and due to the fact that during normal brake operation only small movements are involved this may result in fatigue problems.

The designs discussed have only covered internal (to the piston) adjusters – there are designs that use external adjusters, a design is shown in figure 30.

The external adjuster can be either the friction bush or ball & tube type and may use either helical or disc springs. The external adjuster mechanism provides easier maintenance but results in a heavier design.

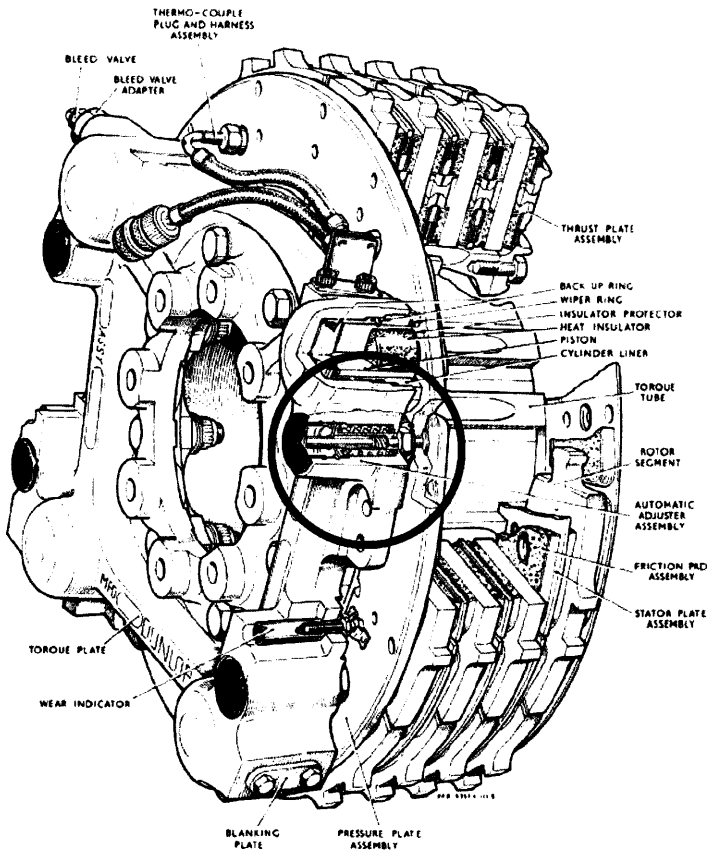

Figure 30 External Adjusters (Dunlop)

The length of heat sink necessary to achieve the specified life of the brake and brake chassis deflection determines the piston stroke required. In addition, there is a requirement for sufficient reserve stroke for brake actuation during taxi stops following an emergency landing condition. It is essential to ensure that the brake does not drag i.e. produce a residual torque when not operated, this condition is typically specified by the constructor as a residual torque level that must not be exceeded or as a probability that it does not occur. The addition of a Brake Temperature Monitoring System (BTMS) provides indication of a residual brake however; due to the measurement lag due to the thermal time constant of the heat sink it is not sufficient to rely upon this indication alone. Another requirement is that stops must be provided to prevent the over-extension of the piston, which would result in loss of hydraulic fluid and potentially leading to a fire through the fluid impinging on a hot brake.

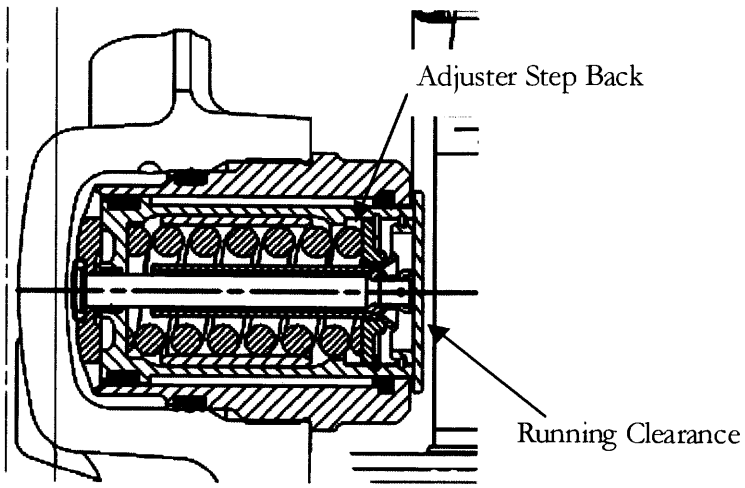

Figure 31 Adjusters Running Clearance (Dunlop)

Torque Tube

For typical applications forged heat-treated stainless steel is selected as the material to meet structural, envelope, minimum weight and high temperature resistance requirements. The steel torque tubes are forged, partially machined, heat-treated and then finish machined to provide optimum strength and surface finish. In circumstances where there is a severe mass restriction titanium alloy may have to be used. This is typically manufactured as a casting and then machined to the required finished dimensions.

A number of equally spaced torque tube tenons are machined on the exterior of the torque tube section to engage the corresponding slots in the pressure plate, stator disks and thrust plate, preventing rotation but allowing lateral movement. The exact number depends on the brake torque required and the bearing strength of the carbon used. In addition, thin section stainless steel caps are riveted to the torque tube tenons to act as a thermal barrier and sacrificial wear surface. An alternative to these caps is a complete all-in-one spline shield however, this is complex to manufacture and if damaged on one spline, would require complete replacement. Both the caps and the all-in-one shield also help to protect the carbon-carbon composite from corrosion along torque tubes tenons that may act as a "file" to enlarge the stator drive slots and potentially cause premature failure. An alternative solution is used stator drive clips and this will be discussed later in the Carbon Heat Sink section.

Depending on the propensity of the brake to vibrate a pedestal with an aluminium bronze sleeve bearing supporting the centre of the torque tube may be used, see figure 56 in Chapter 8. This feature acts to reduce some vibration modes and reacts the moment generated by the brake rod load.

The thrust section is designed to withstand brake operating end load thrust with minimal deflection. This feature can be provided as a bolt on thrust ring or as integral to the torque tube itself, see figure 32. The advantage of the bolt-on thrust ring is that it is possible to change a heat sink without removing the brake from the undercarriage and it allows heat sink volume to be maximised, the disadvantage is that the addition of the fastening bolts and extra torque tube material adds considerable mass and therefore the overall brake is heavier. Another advantage of the integral thrust ring is that it reduces the effect of creep due to bolt stretch at high temperature. Typically bolt-on thrust ring brakes are up to 10% heavier than integral thrust ring brakes.

Regardless of whether it is an integral or bolt on thrust ring there are the two different designs typically used to react the generated brake clamping force, these are cones and thrust pads. Figure 31 also shows the two different designs. The advantage of the thrust pad design is that it requires less axial length than that of the cone design, however this type of design is only possible if the carbon can withstand the torque.

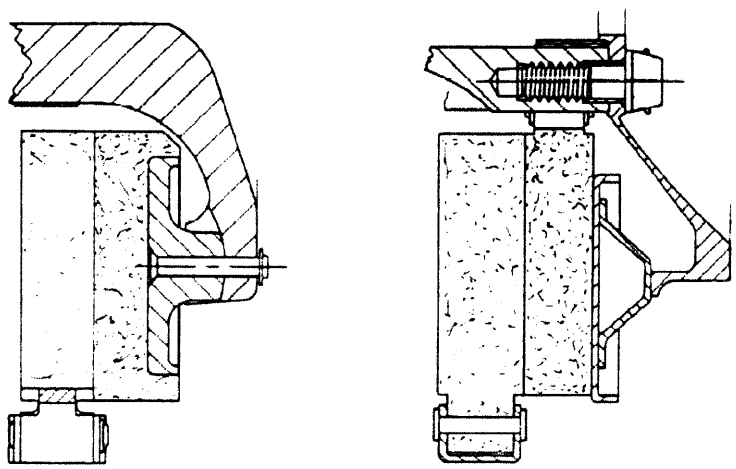

Figure 32 Integral Thrust Pad and Cone Bolt-On Thrust Plate (Dunlop)

The number of thrust pad/cones is typically twice the number of pistons; the actual number depends on envelope constraints. On both designs they are equally spaced around the thrust section to react the carbon thrust stator clamping force. A single rivet is used to attach the thrust pad/cone and this provides a limited degree of articulation and therefore self-alignment to ensure that the clamping force is evenly transmitted to the heat sink.

Wear Indicator

Normally two wear indicator pins provide visual and direct indication of the wear remaining in the heat pack.

A wear pin indicator is incorporated in the brake design to enable easy visibility and access for checking wear of the heat pack. The wear indicator is a stepped pin retained by a spring clip in a steel insert attached to the pressure stator. The pin passes through a sleeve in the torque plate, when the brake is pressurised the free end of the pin projects beyond a datum face by an amount equal to the wear remaining in the heat pack. When the end of the pin is level with the datum the heat pack should be replaced - although the capability for one RTO stop still remains. Indicator pin length is adjusted at installation and thereafter no readjustment is necessary.

Spreader Plate

A spreader plate is commonly incorporated between the pistons and the carbon heat sink in order to spread the clamping force generated by the pistons evenly across the surface of the carbon pressure stator disk. The distribution of force throughout the heat sink can be a major design problem.

BTMS Sensor Provision

The torque plate and torque tube incorporate mounting and support provisions for a Brake Temperature Monitoring System sensor. Typically, a Type-K chromel-alumel thermocouple is used to measure the heat sink temperature. The location of the sensor is designed to minimise any time lag between changes in measured temperature and actual temperature. Most designs locate the sensor in a torque tube spline thus providing support along its full length. A hole is situated in the spline just below the hottest part of the heat sink to ensure the minimum time lag.

Carbon Heat Sink

The material characteristics of carbon-carbon composite that enable it to be used in aircraft brake applications have been discussed in Chapter 4. Figure 33 indicates some of the main features of both rotor and stator disks.

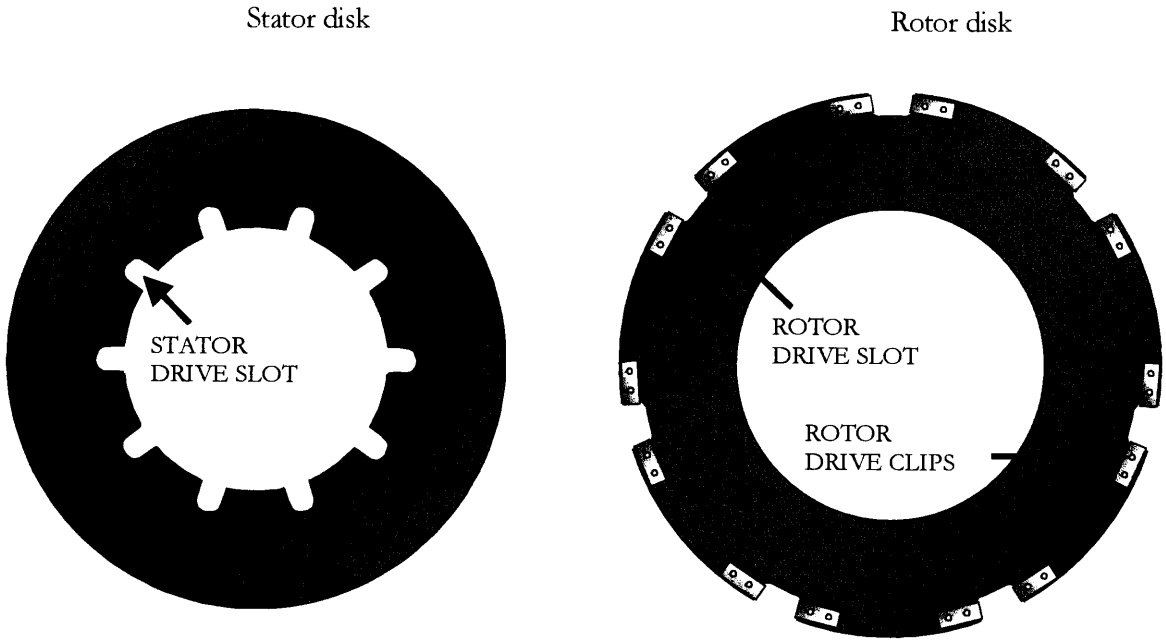

Figure 33 Illustration of a Carbon Stator and Rotor Disk

A number of equally spaced slots are machined on the inner diameter of each stator disk allowing a sliding fit over the torque tube tenons, preventing stator rotation and reacting the heat pack torque at the stator slots. Under certain applications stator clips are fitted usually as an alternative to capping torque tube tenons. One of the difficulties with this is that practical experience has shown that when a brake is exposed to de-icer and cleaning fluids (see Chapter 4 for discussion on catalytic oxidation), an amount of fluid is retained within the clip thus acting as a reservoir for the fluids and hence exacerbating the problem.

Similarly a number of slots are machined on the outer periphery of each rotor disk and are fitted with rotor clips to engage with the corresponding drive tenons in the wheel. The rotors are thereby constrained to rotate with the wheel. The rotor clips provide a durable abutment surface to assist in spreading the drive loads and to prevent damage to the carbon during wheel removal and replacement. The clips are designed for maximum bearing area and efficient load transfer through the carbon and will last the wearable life of

the heat pack. All carbon disks are provided with adequate radial clearance to counter and endure all specified wheel load conditions.

An anti-oxidation coating is applied to appropriate areas of each disk in order to reduce the effects of oxidation.

Anti-nesting grooves are used to provide a radial over-travel for the disks and prevent run-out radii being produced at the edges of the swept area that may induce vibration. The depth of these grooves usually corresponds to the nominal wear per disk face required for full life - see Chapter 8.

Drive rebates are sometimes required in order to avoid drive clash (on long-life brakes) or to enable standard clips to be used.

The section depths for the bearing, wheel bearing housing, and torque tube barrel all determine the heat pack inner diameter limit. The heat sink outer diameter is determined by the constructor specified wheel rim size and the section depths of the wheel barrel/tubewell (chosen on the basis of structural requirements) and drive bars.

Refurbishment of Carbon-Carbon Composite Heat Sinks

The purpose of refurbishment is to reduce the brake operating cost by utilising worn disks. There are the following methods in use at present

- Two-for-One
- Thick/Thin
- Graduated Heat Sink

There are a number of practical difficulties with all methods mainly due to the state of the disks after they have finished one "tour". Often disks are returned in such a condition that the expected yield is not as great as originally predicted. In this case three-for-one or even four-for-one schemes may be used.

Another difficult is that the unbalanced distribution of heat sink mass may have significant performance and life implications. For a given energy input thinner disks get hotter and this may result in reduced brake performance and/or increase in wear.

Two-for-One

The two for one is the simplest approach in which disks are inspected and machined to a given thickness and then two are joined to form a reusable disk, see figure 34. There are a number of joining methods possible either mechanically or through proprietary techniques. These reclaimed disks may be fitted to aircraft and have only the same limitations placed upon then as any new disk would. This refurbishment technique can also be applied in a three-for-one or even a four-for-one approach.

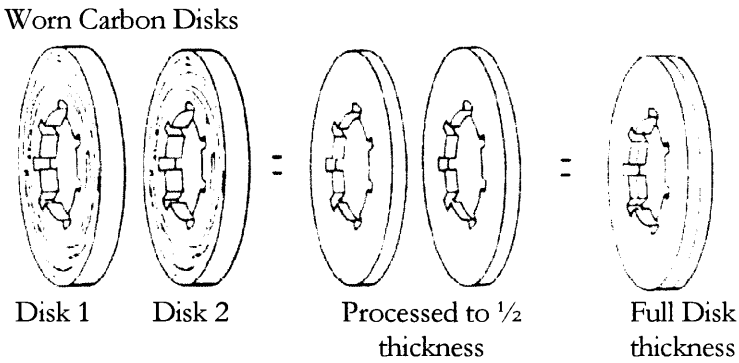

Figure 34 Two-for-One Refurbishment (Dunlop)

Thick-Thin

In this refurbishment technique initially the stators are thicker than the rotors, see figure 35. The heat sink wears down to the specified thermal mass limit at which point the stators are machined and anti-oxidant re-applied. These re-finished stators are then assembled in a heat sink with new thick rotors and are then ready for use on the aircraft. This procedure continues with maybe variations including even a re-densification if required.

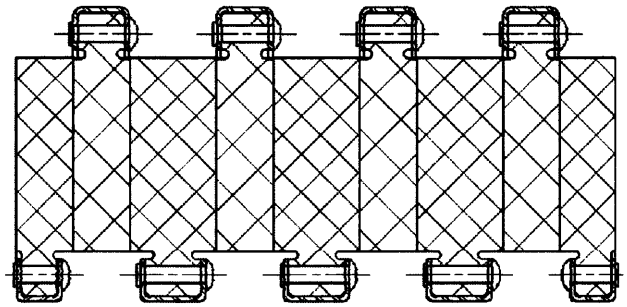

Figure 35 Thick/Thin Heat Sink Designs (Dunlop)

Graduated Heat Sink

This is a similar approach to that of the thick/thin refurbishment technique however, in this case rather than having alternate thick/thin, the mass of the heat sink is unevenly balanced throughout the heat sink - more mass is situated at the front of the heat. In figure 36, a conventional balanced heat sink is indicated alongside a graduated heat sink for comparison. In this approach when the heat sink reaches its minimum safe thermal mass the disks at the rear are removed and the front disks are shifted to the back. A new set of disks is then installed at the front and this procedure is then repeated as and when appropriate, this sequence of operations is depicted in figure 37.

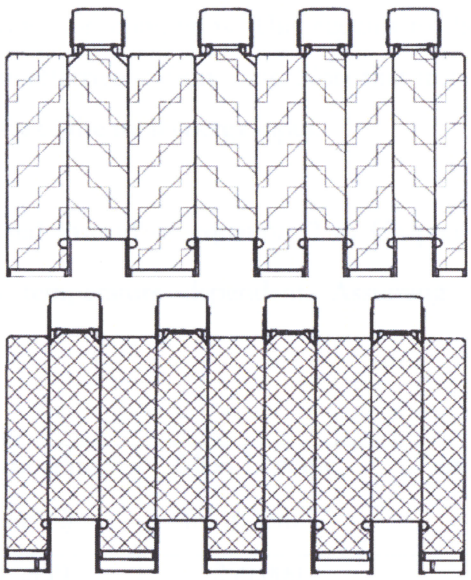

Figure 36 Graduated Heat Sink and Balance Heat Sink Comparison (Dunlop)

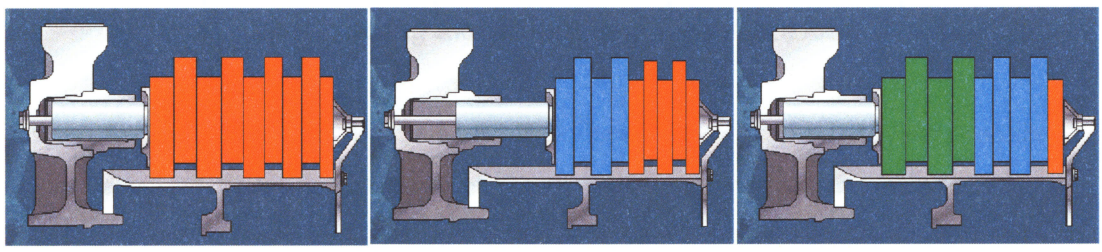

Figure 37 Graduated Heat Sink Procedure (Dunlop)

Brake Heat Sink Design Parameters

Mass or Heat Sink Loading

This is the kinetic energy absorbed by the brake's heat sink divided by the heat sink mass.

$$Mass\ Loading\ (ML) = \frac{KE_{TWB}}{M_{HP}} \quad [\text{ft.lbf/lbm}] \text{ or } [\text{J/s/kg}] \qquad (7)$$

The mass loading is a measure of the heat pack temperature rise for a specific energy input and thus provides an indication of the bulk temperature of the heat sink materials under the specified energy absorption conditions. This equates to the total energy input to the brake unit divided by the effective carbon mass. Note that from experimental evidence the tyre typically absorbs 10% of the total energy input.

The mass loading is used instead of equation 2 in Chapter 4 in order overcome the complexity that C_P is temperature dependent. Assuming $\overline{C_p}$ = 1600J/kg°C ($\overline{C_p}$ = 535ft.lbf/lbm°C)

Mass Loading (J/kg°C)	Mass Loading (ft.lbf/lbm°C)	Temperature (°C)
747,350	250,000	467
1,494,700	500,000	934
2,242,050	750,000	1,401
2,989,400	1,000,000	1,868

Table 3 Loading and Corresponding Temperature Rise

Mass loadings that can be achieved are based upon experience and require a comprehensive database of dynamometer test results for a range of heat sink sizes.

For a steel brake the heat sink mass equates to the disk and lining carrier segment mass. However, for a carbon-carbon composite heat sink the heat sink mass is the effective mass, which can be calculated from equation 8.

$$M_{EFF} = \left\{\left(\frac{N_R}{N_R\text{-}1}\right)\times\sum M_{DS}\right\}+\sum M_R \qquad (8)$$

Where N_R is the number of rotors, M_{DS} is the mass of a double stator and M_R is the mass of a rotor.

Note that this effective mass contains the mass of all the rotors and all of the double stators plus one additional double stator. The extra double stator mass is due to the fact that the pressure and thrust stators only generate torque and hence each absorb energy from one face only (all other disks within the heat pack have two rubbing faces). As a consequence the actual carbon heat sink mass will be greater than the effective.

Area Loading

This is the kinetic energy divided by the disk swept area. It is sometimes termed the Lining Loading.

$$Area\ Loading\ (AL) = \frac{KE_{TWB}}{A_{TS}}\ [\text{ft.lbf/in}^2]\text{or}[\text{J/m}^2] \qquad (9)$$

Where A_{TS} is the total swept area for carbon-carbon composite heat sinks and the total pad area per face for a padded steel brake.

$$A_{TS} = DSA\times N_R\times 4 = DSA\times N_I\times 2 \qquad (10)$$

Where DSA is the Disk Swept Area per face, N_R is the number of rotors and N_I is the number of interfaces.

Area Rate Loading

This is the average kinetic energy divided by the total swept area during the time taken to stop. It is sometimes termed the Lining Power or just Power loading.

$$Area\ Rate\ Loading\ (RL) = \frac{KE_{TWB}}{A_{TS} \times t_{stop}} \quad \left[\text{ft.lbf/in}^2\text{.s}\right] \text{or} \left[\text{J/s.m}^2\right] \tag{11}$$

Or

$$Area\ Rate\ Loading\ (RL) = \frac{AL}{t_{stop}} \tag{12}$$

Where t_{stop} is the time taken to stop the aircraft.

Brake Torque Capacity

$$T_B = \mu \times \left(P_{op} - P_{ineff}\right) \times TPA \times PCR \times N_I \tag{13}$$

T_B – Brake Torque, μ – Brake Effectiveness, P_{op} – Operating Pressure, P_{ineff} – Ineffective Pressure, TPA – Total Piston Area, PCR – Pitch Circle Radius, and N_I – Number of friction interfaces (equal to twice the number of rotors, $= 2 \times N_R$)

The ineffective pressure is that required to overcome the return spring of the automatic adjuster and the seal friction of the piston assembly. The term μ is not the material coefficient of friction as it depends on many other factors it is more appropriate to term it the brake effectiveness or efficiency.

Design Methodology

A flowchart outlining the major steps in the heat sink design process is shown in figure 38.

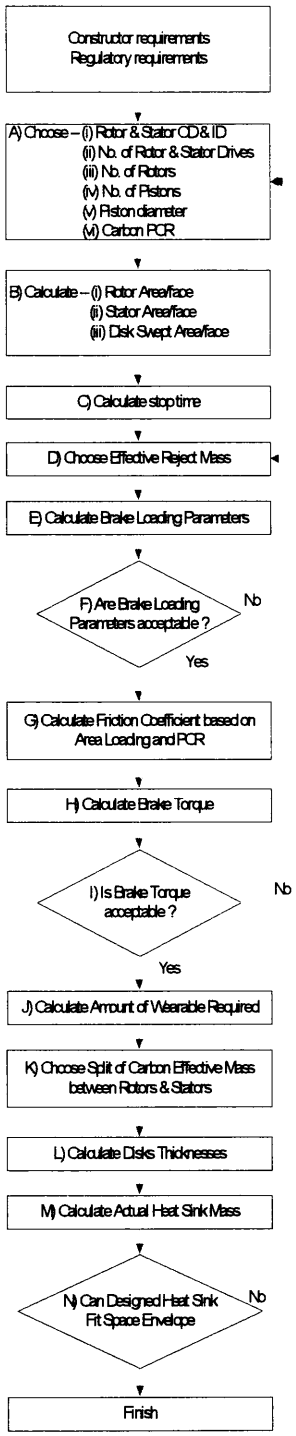

Figure 38 Design Flowchart

Stage A

Stators and rotors outer and inner diameters are chosen based upon the constraints shown in figure 23. The rotors outer diameter is constrained by the specified wheel size, which is specified by the constructor based on the flotation requirements of the aircraft. The wheel loadings will dictate a necessary barrel section thickness able to withstand the induced stress levels and the necessary drive key section thickness is designed based on the structural torque requirements.

The number of stator drives is based on the need to react the generated brake torque and the bearing strength of the carbon.

In order to allow initial parametric sizing statistical analysis was undertaken to determine relationships between the wheel rim and stator inner and outer diameters, rotors inner and outer diameters and the number of rotor drives. Another analysis investigated the relationship between axle size and stator drives. The following equations may be used to estimate the disk diameters and drives. These relationships have been established in Appendix A and are discussed there as well as information on the confidence and prediction intervals and correlation coefficients of the respective fits. The results are presented in table 4 as coefficients of the linear equation $y = Ax + B$, where x is the specified wheel rim size.

	Civil Aircraft		Military Aircraft	
	A	B	A	B (in)
Stator OD (in)	0.7091	2.286 (in)	0.7797	0.5491 (in)
Stator ID (in)	0.4170	0.391 (in)	0.5279	-1.394 (in)
No of Stator Drives	1.442 (in^{-1})	-11.25	0.9419 (in^{-1})	-3.105 (in^{-1})
Rotor OD (in)	0.7880	2.322	0.8490	0.6259 (in)
Rotor ID (in)	0.6645	-2.361	0.6954	-2.704 (in)
No of Rotor Drives	0.35 (in^{-1})	2.217	0.4706 (in^{-1})	0.706

Table 4 Parametric Estimation of Disk Dimensions

The number of pistons is chosen based on the size of the cylinder block/torque plate and how many pistons can be distributed evenly around the chosen carbon PCR. The carbon PCR is calculated using the stator outer radius and the rotor inner radius.

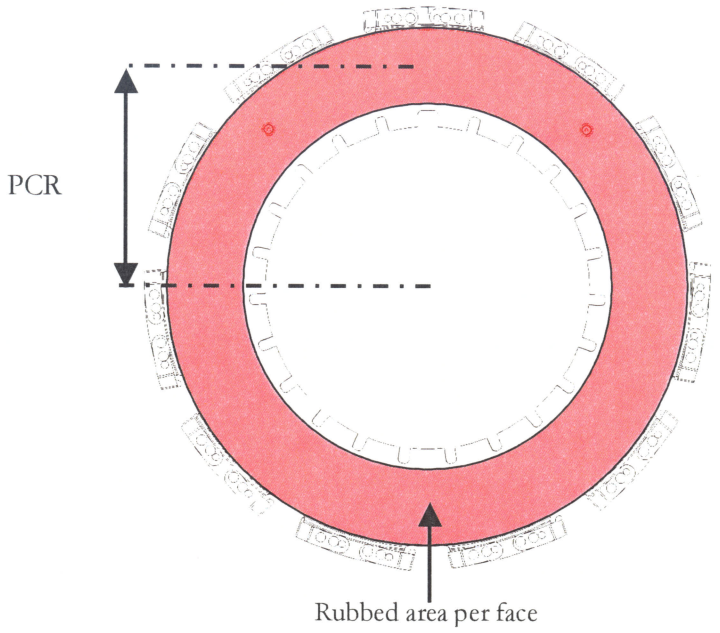

Figure 39 Friction or Rubbing Area

A number of formulae may be used, a common one is

$$PCR = \frac{2}{3}\left(\frac{r_{SO}^{\ 3} - r_{RI}^{\ 3}}{r_{SO}^{\ 2} - r_{RI}^{\ 2}}\right) \tag{14}$$

Where r_{SO} is the stator's outer radius, r_{RI} is the rotor's inner radius.

However, this is based on the assumption that the load distribution at the interface of two disks is uniform and this is generally not the case with carbon-carbon composites. A simpler geometric average is normally taken, equation 15.

$$PCR = \frac{r_{SO} + r_{RI}}{2} \tag{15}$$

The piston diameter chosen is based on the need to use an internal adjuster mechanism and to provide enough heat sink clamping force necessary to achieve the required brake torque. The minimum piston diameter that enables the use of internal adjusters has been discussed and is 1.25 inches (31.75mm). This corresponds to a minimum piston area of 1.227 in^2 (792mm^2).

The number of rotors is dictated by the need to achieve the required brake torque as well as the goal of minimising the number of friction faces. The objective of using the least number of rotors is due to the fact that wear occurs at each friction interface and that by minimising the number of friction faces the life of the brake is maximised. This also provides the added benefit of having thicker rotors that inherently are more robust.

Stage B

The rotor area is calculated as follows

$$A_R = \pi\left((r_{RO})^2 - (r_{RI})^2\right) - (W_{RD} \times H_{RD} \times N_{RD}) \quad (16)$$

Where W_{RD} is the rotor drive width, H_{RD} is the rotor drive depth and N_{RD} is the number of rotor drives, r_{RO} is the rotor's outer radius and r_{RI} is the rotor's inner radius.

The stator area is calculated in a similar manner;

$$A_S = \pi\left((r_{SO})^2 - (r_{SI})^2\right) - (W_{SD} \times H_{SD} \times N_{SD}) \quad (17)$$

Where W_{SD} is the stator drive width, H_{SD} is the stator drive depth and N_{RD} is the number of stator drives, r_{SO} is the stator's outer radius and r_{SI} is the stator's inner radius.

The Disk Swept Area or rubbing area is shown in figure 39 and is calculated as follows

$$DSA = \pi\left((r_{SO})^2 - (r_{RI})^2\right) \quad (18)$$

Stage C

From the constructor specified brake application velocity and deceleration, the stop time can be calculated as follows.

$$t_{stop} = \frac{V_{BAS}}{decel} \tag{19}$$

Where V_{BAS} is the brakes application speed and *decel* is the deceleration of the aircraft.

Stage D and Stage E

For each landing case the Mass Loading, the Area Loading and the Rate Loading are calculated. Typical values used for carbon-carbon composite brakes are shown in tables 5, 6 and 7.

	Normal	**Overweight**	**RTO/Flapless**
New [ft.lbf/lbm]	400,000	600,000	900,000
New [kJ/kg]	1200	1800	2700
Worn [ft.lbf/lbm]	500,000	700,000	1,000,000
Worn [kJ/kg]	1500	2100	3000

Table 5 Typical Mass Loading

	Normal	**Overweight**	**RTO/Flapless**
[ft.lbf/in^2]	15,000	20,000	35,000
[J/cm^2]	3150	4200	7350

Table 6 Typical Area Loading

	Normal	**Overweight**	**RTO/Flapless**
[ft.lbf/in^2.s]	600	900	1300
[J/s.cm^2]	125	190	275

Table 7 Typical Rate Loading

Stage F

There is a design iteration loop at this point until the chosen effective mass allows acceptable brake loading parameters. Normally when the RTO energy is at least twice the

normal or design case energy the heat sink mass will be dictated by the RTO requirements. Note: The worn effective mass is M_{EFFW}

Stage G

For each landing case, brake effectiveness has been in the past estimated based on the brake loading parameters. These assumptions were based on empirical evidence and experience with previous aircraft programmes. A major part of this work has been to investigate the relationships between variables and to establish mathematical formulae that allow a more accurate prediction of brake effectiveness as well as defining the confidence level of that prediction - the results of this work is presented in Chapter 6.

Stage H

The brake torque is calculated using equation 13 however for Brake Control System discussions often the alternative form shown in equation 20 is used.

$$T_B = K_B \times \left(P_{op} - P_{ineff}\right) \tag{20}$$

In this expression K_B is termed the brake gain and is given by

$$K_B = \mu \times TPA \times N_R \times 2 \times PCR \tag{21}$$

As can be seen from the expression the torque generated can be increased by

- Applying more end-load
- Moving the position that the end-load is applied radially outwards
- Increasing the number of friction faces

An increase in end load can be achieved by either a higher operating pressure or by increasing the piston area. However, this may affect the sensitivity of the brake control system.

Stage I

This stage of initial design determines the amount of wearable material required to achieve the brake life require. Typical carbon-carbon wear rates vary from 0.00006in/landing/face

(2μm/landing/face) to 0.00008in/landing/face (2.032μm /landing/face) depending on exact construction of the composite. In addition, environmental conditions also affect the wear of a brake significantly (see Chapter 4 - Catalytic Oxidation section).

The amount of wear mass required is calculated as follows,

$$M_{wear} = LPO \times I \times 4 \times N_R \times DSA \times \rho \tag{22}$$

Where the LPO is the life per overhaul required, I is the wear rate specified as worn translational (linear) length per application per face and ρ is the density of the carbon. The factor 4 arises from the fact that at every friction interface there are two surfaces and the wear rate is measured per wear face.

The required effective new mass is calculated as follows,

$$M_{EFFN} = M_{EFFW} + M_{wear} \tag{23}$$

Stage J

This stage of the design process allocates the mass between the rotors and stators. This allocation process is dependent on the refurbishment scheme chosen; see section on the Refurbishment of Carbon-Carbon Composite Heat Sinks for details. However, the simplest allocation is a 50:50 split between rotors and stators.

Stage L

A rotor disk mass is calculated as follows,

$$M_R = \frac{(0.5 \times M_{EFFN})}{N_R} \tag{24}$$

The thickness of a rotor is then determined from equation 25

$$th_R = \frac{M_R}{\rho \times A_R} \tag{25}$$

A similar set of calculations is conducted to determine the double stator thickness.

$$M_{DS} = \frac{(0.5 \times M_{EFF})}{N_R} \tag{26}$$

$$th_{DS} = \frac{M_{DS}}{\rho \times A_S} \tag{27}$$

The thickness of the pressure stator and thrust stator are establishes as a proportion of the double stator thickness. Typically, the following relationships are used.

$$th_{PS} = 0.5 \times th_{DS} \tag{28}$$

$$th_{TS} = 0.5 \times th_{DS} \tag{29}$$

Stage M and N

The actual carbon heat sink mass and length is now calculated. The designer then has to install this heat sink configuration into the rest of the brake structure. If this is not achievable the process is repeated and compromise is made until the design meets the performance and installation requirements specified by the constructor.

Chapter 6

AIRCRAFT WHEELS

Introduction

The lightest aircraft wheel for a particular rim size is typically designed using a split hub construction. The two half hubs are joined by a number of circumferentially equally spaced bolts. The bolts are placed as close as possible to the rim in order to reduce the bending stresses and hence minimise the bolt size. As the brake length increases, the required wheel cavity must also increase and this in turn results in the joint or split line moving over until this design is no longer structurally practical. In this situation a loose flange or lock-ring wheel design is required. The loose flange design (also known as a bowl wheel) consists of a single diaphragm that is significantly offset from the tyre centre. As the wheel's loads are now transmitted through one offset diaphragm, greater bending stresses result and a heavier design is required. The two alternative designs are shown in figure 40.

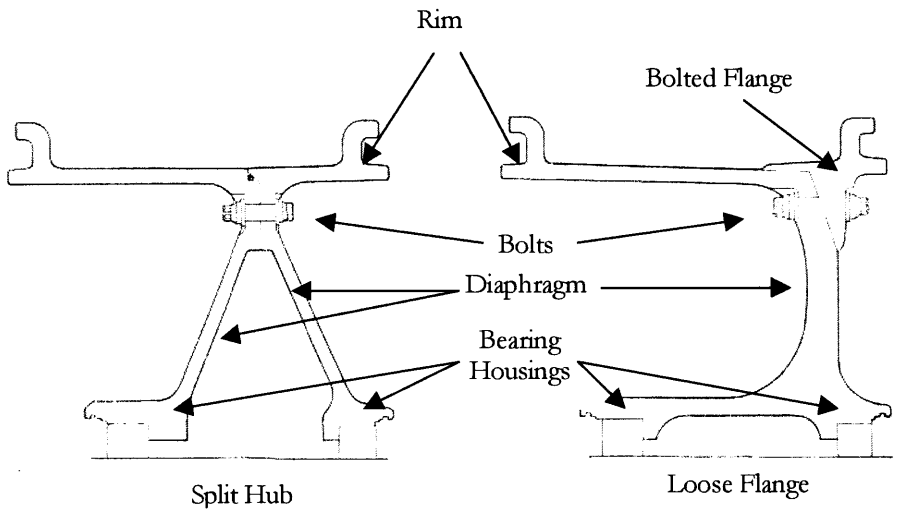

Figure 40 Alternative Wheel Designs (Dunlop)

Design Requirements

An aircraft wheel is governed by Airworthiness Regulation and for Transport Category aircraft, JAR and FAR 25. In addition, minimum standards are mandated in the Technical Standard Order C-135 and now EASA ETSO C-135. For Military Aircraft Mil-W-5013 covers the design of aircraft wheels for the US military and Def-Stan-970 for the UK military.

The specified requirements are again typically the TSO requirements plus additional aircraft constructor requirements. The following is a typical list of requirements that an aircraft wheel would have to demonstrate that it satisfies.

- Structural Strength
    - Radial Loading – MSL
    - Radial Loading - Limit Case
    - Radial Loading - Yield Case
    - Radial Loading - Ultimate Case
- Combined Radial and Side Loading - Yield Case
- Combined Radial and Side Loading - Ultimate Case
- Tyre Pressure
- Service Life Requirement
- Radial Loading (Straight Roll)
- Combined Radial and Side Loading (Yawed Roll typically at least at $\pm 15°$ and $\pm 30°$)
- Roll on Rim
- Overpressure
- Pressure Retention (Diffusion)

The roll on rim requirement requires that the wheel without a tyre be capable of rolling on its rims for at least 15,000ft without fragmenting. At present this requirement is only for main wheels but this may be extended to nose wheels at a later time.

Component and Important Design Features

Aircraft wheels are typically manufactured from forged 2000 and 7000 series aluminium alloys to meet the structural, envelope and minimum weight requirements. Typically, wheel halves are machined from close-to-form die forgings, treated to achieve maximum strength and corrosion resistance using optimised temper, shot peen procedures and surface protection treatments.

Flanges

The critical flange and bead seat areas of the wheel are designed to withstand all the imposed load requirements as specified above. A compound bead seat radius is used to increase the section moment of inertia and to reduce stress concentration factors, thus optimising the design by reducing weight and stress while increasing roll life.

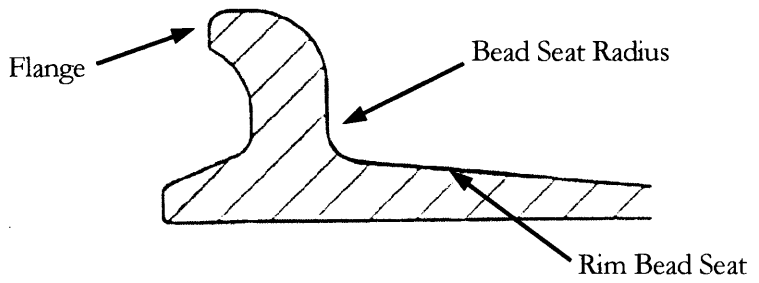

Figure 41 Flange and Rim Detail (Dunlop)

The design is influenced by whether the tyre is a radial ply or bias ply tyre. A bias tyre exerts its force axially outwards towards the wheel flange – this induces stress concentrations in the flange area but also creates a moment about the bead seat radius. On the other hand a radial tyre imposes its force radially inward on to the rim bead seat and hence substantially lower stresses are present in the bead seat radius. For further information regarding tyres refer to Chapter 7.

Spokes/Windows

Ventilation holes are equally spaced around the diaphragm area of the wheel to assist the natural cooling of the brake. Hole size and diaphragm strength are optimised to provide minimum mass and maximum ventilation.

Bearing System

The wheel halves are centrally bored and counter-bored to accommodate tapered roller bearings and are packed with grease on assembly. Timken are the only suppliers of aircraft tapered roller bearings in the Western world. The bearings used are Timken Code 629 bearings, which are selected to accept the specified wheel loads and while achieving reliability and long life.

Sufficient material is provided at the bearing housing areas to ensure bearing cup security under all load conditions, to allow bearing repair bushings if necessary, and to enhance wheel life.

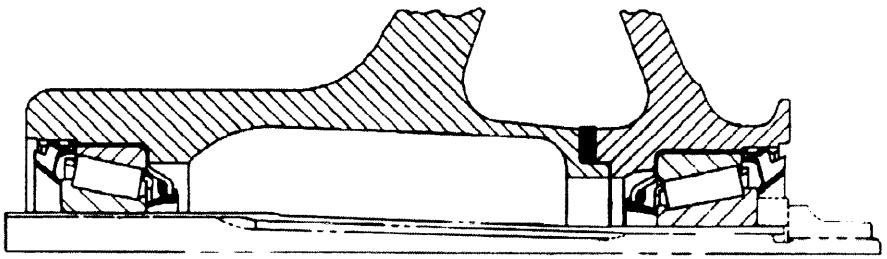

Figure 42 Typical Wheel Bearing System (Dunlop)

The bearings are statically sized by calculating radial loads using static equilibrium and include the effects of axle angles and tyre radial/side deflections. Bearing thrust loads and equivalent radial loads are then determined using equations 30 and 31.

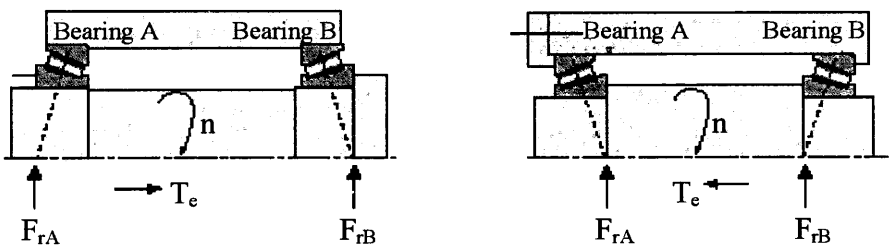

Figure 43 Roller Bearing Loading (Timken)

$$P_A = 0.4F_{rA} + K_A\left(\frac{0.47F_{rB}}{K_B} + T_e\right) \qquad (30)$$

$$P_B = 0.4F_{rB} + K_B\left(\frac{0.47F_{rA}}{K_A} - T_e\right) \tag{31}$$

Where P_A and P_B are the dynamic equivalent loads that give the same life as the combined (axial and thrust) loads applied, T_e is the external thrust and K_A and K_B are factors dependent on the bearing chosen

The fatigue analysis is based on the Timken Company's recommend methodology and the L_{10} life is calculated as follows.

$$L_{10} = \left(\frac{C_{90}}{P}\right)^{3.33} \times 90 \times 10^6 \text{ revolutions} \tag{32}$$

Where L_{10} is the life expectancy associated with 90% reliability, C_{90} is the basic dynamic radial load rating of the bearing and P is the dynamic equivalent radial load.

Now this can be modified for aircraft use with L in miles.

$$L = 8925 \times R \times a_1 a_2 a_3 a_4 \left(\frac{C_{90}}{P}\right)^{3.33} \tag{33}$$

Where R is the tyre rolling radius in inches and factors $a_1 \ldots a_4$ are various factors depending on reliability, material, environmental and useful life.

Grease dams are fitted at the bearing inner faces and grease retainers at the bearing outer faces in order to ensure the bearing grease is retained inside the bearing and foreign materials and water are excluded. The grease retainers are manufactured from synthetic rubber with metal stiffening inserts and are held by steel circlips in grooves in the wheel hubs. The inner grease dams are manufactured from nylon. The grease retainers are secured to ensure that they will not rotate and damage wheel hubs. These types of positive-action retainer, dam and groove combinations are standard practice. The designs prevent displacement of the retainers and dams during wheel assembly onto the axle sleeve, resulting in timesaving in maintenance, and gives assurance of a perfect fit.

Tie Bolts/Nuts

Wheel halves are clamped together by a number of aircraft standard high tensile steel tie bolts with washers and self-locking nuts. Tie bolt retainer devices are not necessary due to the self-locking. Tie bolt configuration (size, number, pre-torque, etc.) is the result of careful structural analysis, based on the wheel's maximum loads, in order to satisfy burst pressure and wheel life requirements.

Careful consideration is given at the design stage to eliminate fretting between the wheel halves, between wheel and mounting surfaces and between wheel and tie bolts. The tie bolts have been selected in order to achieve infinite life and are normally replaced as a result of thread damage.

Heat Shield

Main wheels are equipped with heat shields to protect the wheel and tyre from radiated and convected heat transfer from the brake. Each heat shield is of a double layer, heat reflective construction with low conduction fibre filler.

The heat shield can be either of the segmented type or a full annulus, see figure 44 and figure 45. If through normal use the brake runs hot it is recommended that a full annulus be used however, this design suffers from being difficult to maintain when compared to the segmented heat shield.

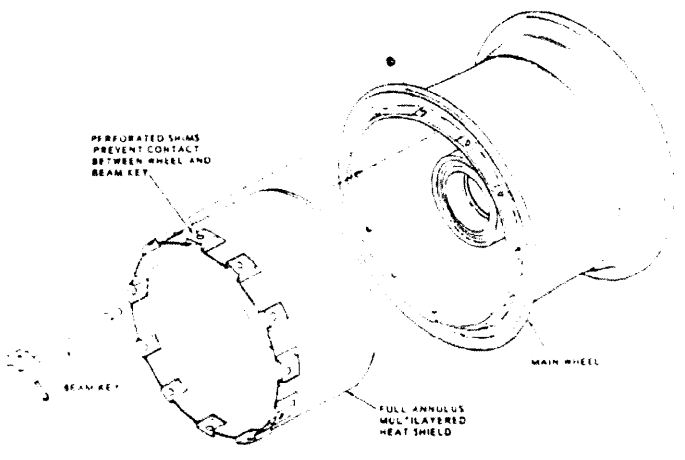

Figure 44 Full Annulus Wheel Heat Shield (Dunlop)

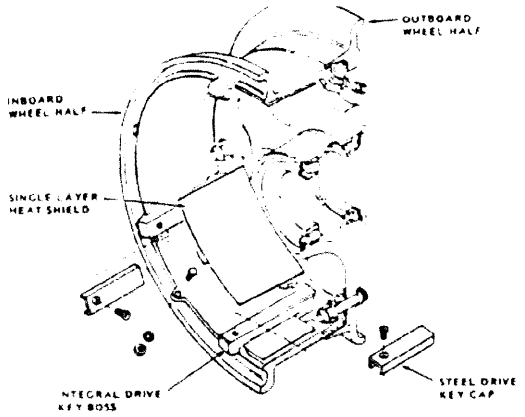

Figure 45 Segmented Wheel Heat Shields (Dunlop)

Fuse Plugs

Typically three thermo-sensitive pressure release plugs (thermal fuse plugs), are located around the barrel of the wheel. The plugs ensure tyre deflation before excessive heat, in the event of an RTO or other severe braking application, results in temperatures that exceed the limits of the wheel material, degrades the axle, brake housing or wheel and tire to an unsafe level.

Each fuse plug is a one-piece assembly comprising a light alloy body with fusible insert of eutectic material and a light alloy piston. The piston ensures that in operation the insert is ejected cleanly and is not subject to re-freezing in the bore. The fuse plugs are located and sealed in threaded holes to retain tyre pressure until the fusible insert melts and is cleanly ejected by tyre pressure. The minimum throat diameter of the plug is 0.25 inches, ensuring rapid tyre deflation.

To replace the fuse plugs the wheel must be removed from the aircraft. Wheel integrity can therefore be verified before use. An added safety feature of the design ensures tyre pressure will be released if the removal of the plug is attempted with the tyre inflated. The fuse setting of the plugs is determined by a computer based thermal model of the tyre/wheel/brake assembly and then substantiated by data obtained during qualification testing. The location and orientation of the installed plugs ensures that the expelled insert, piston, inflation medium and any other debris are directed within the wheel assembly to avoid injury to nearby personnel. The fuse plug typically has a tolerance of ± 3°C about the nominal setting.

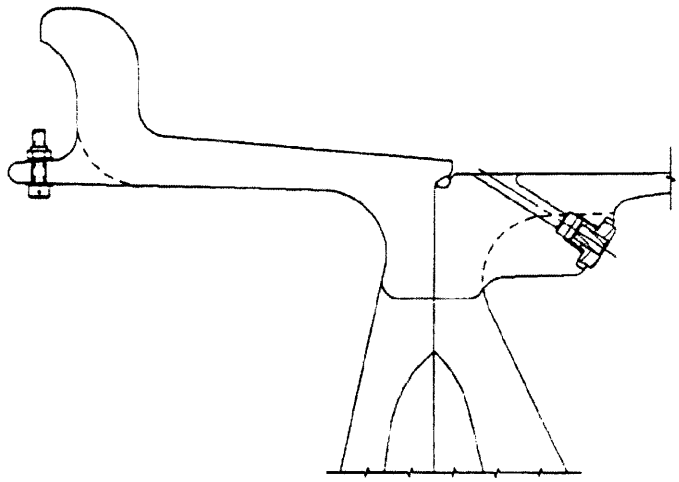

Figure 46 Fuse Plug Installation (Dunlop)

Inflation Valve

A standard Tire and Rim Association tyre inflation valve is incorporated in the bowl wheel, and connects to the tyre well by means of a radial drilling. The valve is easily removable with the wheel and tyre fully assembled, with no special tools.

Overpressure Valve

The wheel is equipped with a 'rupturing disc' inflation pressure release valve that prevents over-pressurisation of the wheel and tyre assembly. The inflation pressure release valve is located and sealed in a threaded port in the wheel and connects to the tyre well by means of a radial drilling. The valve is a tamper-resistant welded unit, which is disposed after activation. The valve incorporates a metal diaphragm that fractures when inflation pressures reach 600 +50/-25 psig at room temperature. This type of device has been found to be more reliable than spring- loaded types, which are easily affected by contamination.

Seal

A rubber 'O' ring seal is located between the mating faces of the wheel and flange to render the assembly airtight for use with tubeless tires. The 'O' ring groove is sloped to limit stress concentrations. For loose flange wheels the flange-mating force is reacted on diametrically across the lock ring - contacting the bowl wheel lock ring groove and the flange retaining ring recess.

Rotor Drive Bars

The inner periphery of the wheel incorporates a number of equally spaced integral brake rotor drive tenons, machined to accommodate a hardened steel drive cap. Two socket head screws are inserted into the drive tenon to secure each drive cap, see figure 47. If any drive cap surface is damaged, only that particular drive cap needs to be replaced, resulting in low maintenance and replacement cost. As the drive tenons are part of the wheel structure, this contributes to the circumferential stiffness of the wheel, and brake torque is transmitted directly to the wheel. This lightweight type of drive arrangement has been successfully incorporated in many existing wheel designs, and has proven extremely reliable in service.

An alternative design is to use a beam key, in which the drive is provided by beams fastened into the wheel, see figure 48. The advantage of this is that it improves thermal management as it minimises the conducted heat into the wheel. In addition, it provides a readily available method of attaching a full annulus heat shield and improves maintainability over the integral design.

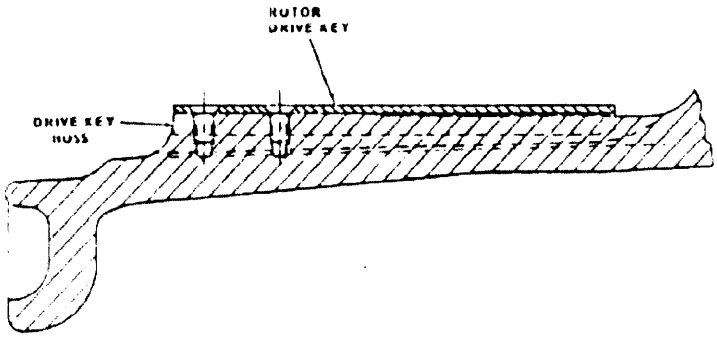

Figure 47 Integral Drive Bar (Dunlop)

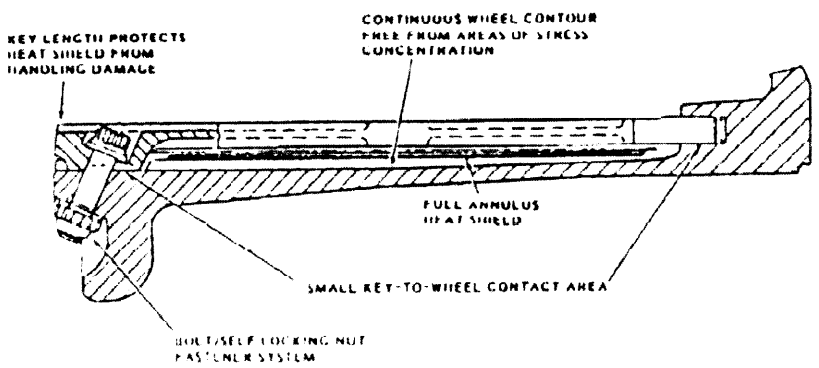

Figure 48 Beam Key Drive Bar (Dunlop)

Chapter 7

TYRES

Introduction

A tyre, once attached to the wheel and inflated, becomes a flexible toroidal shaped pressure vessel. The tyre deflects with the applied load until the contact area and pressure exerted by the tread in contact with the ground equals the imposed load. Aircraft tyres are designed to operate intermittently due to the requirement to limit heat build-up, which arises through the heavy loads, high speeds and large deflections demanded of the tyre. The taxi speed, taxi distance and inflation pressure also significantly affects the tyre's internal temperature and high taxi speeds and incorrect inflation will reduce tyre life substantially.

Wheels are inflated with nitrogen gas for two reasons, firstly to reduce the likelihood of an explosion due to a chemical reaction between atmospheric oxygen and the volatile gases from the inner tyre liner and secondly by using dry nitrogen it reduces oxidation damage to the interior of the tyre due to the moisture in atmospheric oxygen.

Design Requirements

The tyre has three main functions

- Carry the load
- Generate lateral forces
- Transmit the braking force to the ground

The minimum Airworthiness Regulation qualification test required is specified in TSO C62 for Commercial Aircraft and for Military Aircraft Mil-T-5041 specifies the tests required. In addition tyres conform to the Tire and Rim Association standards regarding rim dimensions. The tyre inflation pressure required is determined by the aircraft constructor in conjunction with the number and spacing of tyres so as to achieve the flotation requirements (bearing capacity) of the airport (airfield) from which the aircraft is designed to operate.

Tyre catalogues provide information on existing tyres and detail the following;

- Ply Rating
- Load Rating
- Maximum Speed
- Inflation Pressure
- Static Loaded Radius (at rated load and at bottoming load)
- Physical dimensions

The term ply rating is used to identify the maximum rated static load capability and corresponding inflation pressure applicable to specific operational requirements. The ply rating is an indication of tyre strength and does not specify the actual number of carcass plies within that tyre. The following identification methods are used:

- A e.g. 44"
- B-C e.g. 8.50-10
- A x B e.g. 49x17
- A x B-C e.g. 49x19.0-20

Note: See figure 49 for reference.

The latter marking applies to all recent tyre size introductions. For radial ply tyres the "-" is replaced by an "R" e.g. 46x17R20. Certain types of tyre will have the letter "H" as a prefix to designate that it is designed for a higher percent deflection.

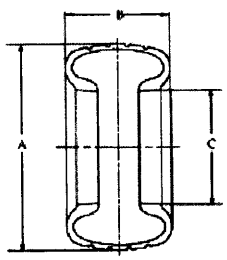

Figure 49 Tyre Sizing (Dunlop)

Bias Tyre Construction

The bias tyre is constructed using many layers of textile plies laid across each other alternatively at angles of 30-40° measured at the crown. As shown in figure 50, a large number of bead wires are required to hold this large number of plies. Additional plies may be added to improve the thermal capacity of the tyre however; this obviously increases the mass of the tyre.

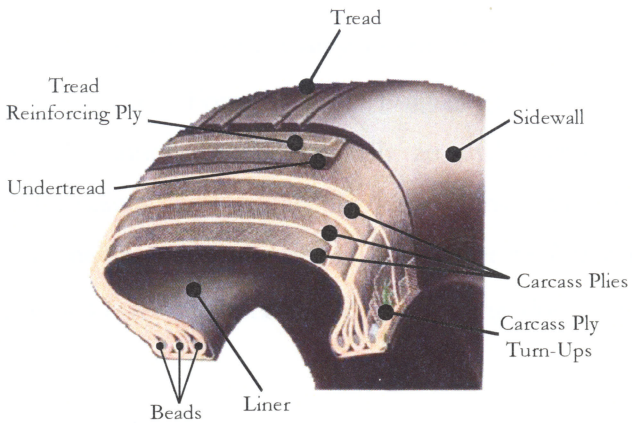

Figure 50 Bias Tyre Construction (Michelin)

Radial Tyre Construction

The radial tyre is constructed by layering carcass plies at an angle approximately 90° to the centreline. Radial tyres compared to bias tyres have fewer plies of higher denier textile cords and therefore occupy less volume and are lighter. In addition, only one bead wire bundle is used per side in contrast to that of the bias tyre that uses 1 to 3 per side, see figure 51.

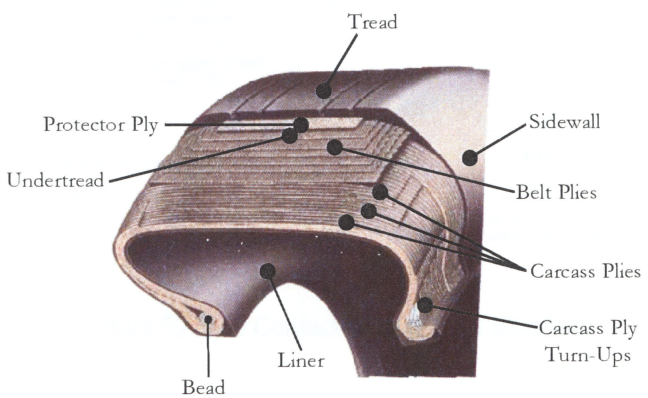

Figure 51 Radial Tyre Construction (Michelin)

The advantages of a radial tyre over the bias tyre are as follows (Olds, 1987).

- Weight Savings - Radial tyres are typically 30-40% lighter than the equivalent bias tyre due to the fact that the casing and the belt can be optimised separately.
- Increased Overload Capacity – The radial tyre generates less heat than a bias and is able to sustain an overload condition, such as a tyre failure during an RTO, longer than the bias tyre.
- Tread Life – Due to the fact that the casing and the belt can be optimised separately.
- Improved Cut Resistance – Foreign Object Damage (FOD) affects safety and airline economics, as you cannot retread. Typically an civil aircraft tyre last somewhere between 300-500 landings while military aircraft are considerably lower (the F16 Block-40 aircraft was at one time only achieving 6 landings per tyre!) (Lay et al, 1995)
- Cooler Running – Lower temperatures during taxiing due to the reduced interply friction.

The durability of tyres has been a concern for a long time irrespective of the tyre construction and is dependent on the factors described above with the most important factor being tread wear. Aircraft tyres due to their high deflection (from high loads) and high-speed exhibit more rapid wear than automotive tyres. It has been shown (Schallamach and Turner, 1960) that the tread wear is a function of the frictional energy dissipated in the slip zone of the contact area.

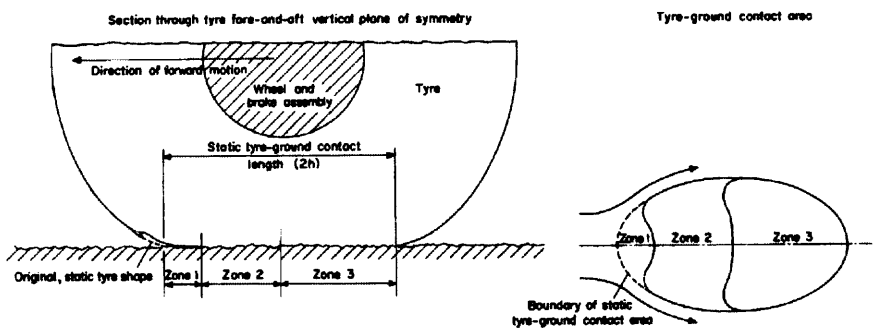

Figure 52 Tyre Contact Area (ESDU Modified)

For a description of the tyre-ground interface refer to the section on anti-skid later. Importantly the level of friction determines the amount of slip that can affect the wear rate.

In addition, tyre temperature has a great influence as it can affect tread rubber abrasion resistance, hysteresis and stiffness which all effect the wear resistance. Surface temperature has another affect in that if the temperature rises to that of the decomposition of rubber, ablation can occur.

Experience shows that while spin-up appears to cause large amount of tyre wear due to the associated "puff of smoke" it only accounts for 2% of tyre wear while most of the wear (80%) occurs during braking.

A number of studies have investigated the relationship between wear and friction energy (Lay et al, 1995 and Yager, 1995). However, all have failed to find a clear relationship between the two – recent studies have concentrated on the power loading (kW/cm^2) and results have indicated that the wear rate is approximately proportional to the cube of the power loading (Alsobrook, 1995).

Chapter 8

LANDING GEAR

Introduction

The Landing Gear functions include the following;

- Provide safe carriage of the aircraft during ground manoeuvring (i.e. taxiing, take-off and landing)
- Absorb vertical energy
- Provide means of wheel braking

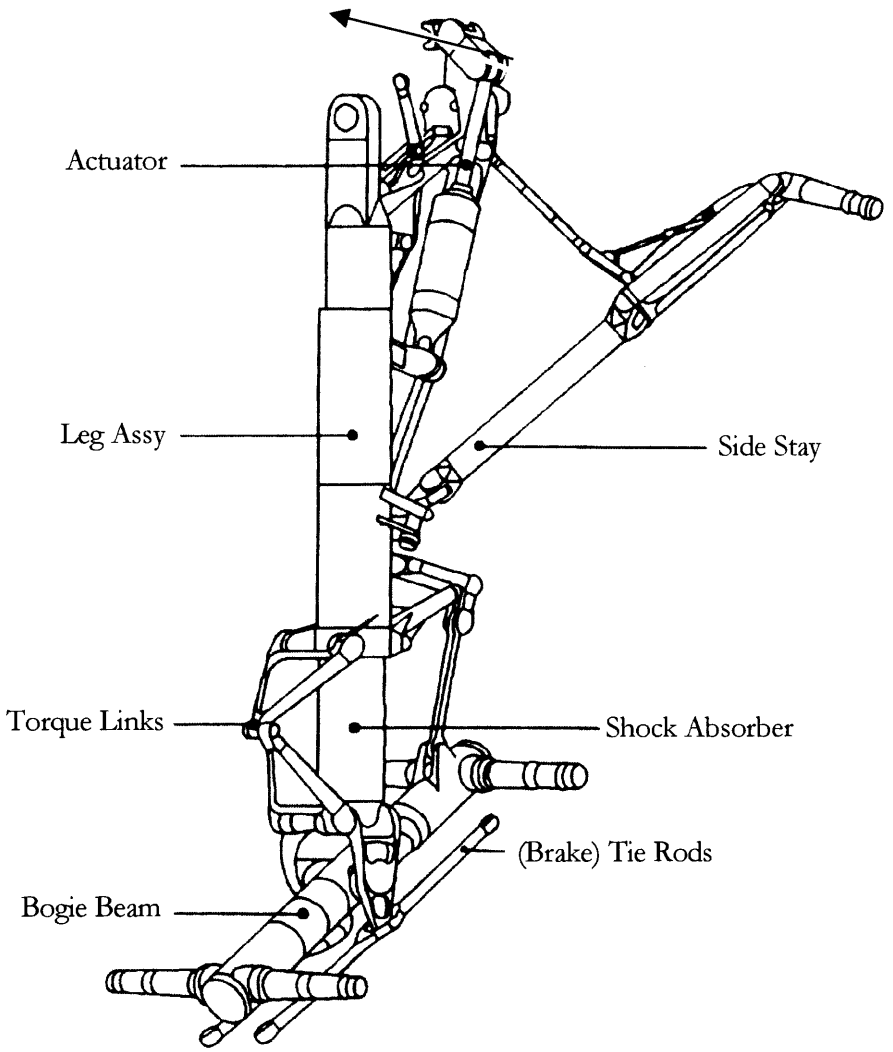

Figure 53 Main Landing Gear (Dunlop)

Typically, landing gear components are made from steel forgings and in particular ultra-high tensile, 300M steel is used extensively in larger aircraft. Major research activities are proceeding to investigate carbon fibre type gears but the most promising material at the present time is that of Titanium Metal Matrix Composite (TiMMC). This material meets the strength requirements while remaining lighter than steel. The downside to this material is the cost of titanium and the cost of fabrication.

Design Requirements

The design requirements for landing gear are again specified for Commercial Aircraft in JAR and FAR 25 and for the Military in the US, MIL-L-87139 and in the UK Def-Stan-00-970.

In general the shock absorber must be capable of absorbing the maximum energy at the design vertical velocity without exceeding the design reaction into the airframe (Jenkins, 1989).

For aircraft brakes the most important aspects of landing gear design is to ensure the compatibility of the whole system – in particular dynamic stability.

Dynamic Stability

The landing gear system including the wheels, brakes, brake control system and the landing gear itself, when operated on an aircraft may undergo various different modes of vibration sometimes with catastrophic consequences. There are six main types of vibration (Liu et al, 1996);

- Gear Walk
- Gear Shimmy
- Brake Whirl
- Brake Squeal
- Brake Chatter
- Rotor Cycloidal Motion

Gear Walk

The tyre-runway interface friction loads deflect the landing gear leading to the gear walk phenomenon. The vibration is typically in the frequency range of 5-20Hz and involves fore and aft motion of the landing gear. It can lead to passenger discomfort and may interfere with the anti-skid with the control trying to compensate for what it thinks are induced skids. If the amplitude becomes high enough it may also cause catastrophic failure of the landing gear.

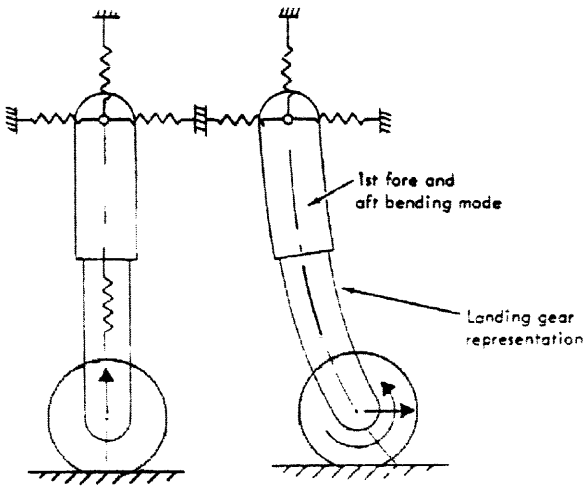

Figure 54 Gear Walk (Dunlop)

This type of motion can severely affect the operation of the anti-skid system inducing artificial skids and reducing braking efficiency.

Gear Shimmy

This mode involves torsional and lateral motion of the wheel and the landing gear. It is a low frequency mode typically between 10-50Hz and because of the high energies involved is very destructive and can damage the landing gear and its attaching structure.

Brake Chatter

This vibration mode is characterised by the torsion oscillations of the wheel and rotating parts of the brake about the axle. Chatter is mainly controlled by the elasticity of the tyre in the frequency range of 10-100Hz.

Brake Whirl

This is an out of plane "wobble" involving the brake disks, torque tube and piston housing. The frequency of this mode of vibration is typically between 100Hz and 300Hz. Often whirl mode is in the same frequency region as squeal and often coupling between the two modes is observed. The whirl mode is typically excited during high-speed landings and maybe induced by the runway surface, see figure 55 for a computer simulated brake whirl mode.

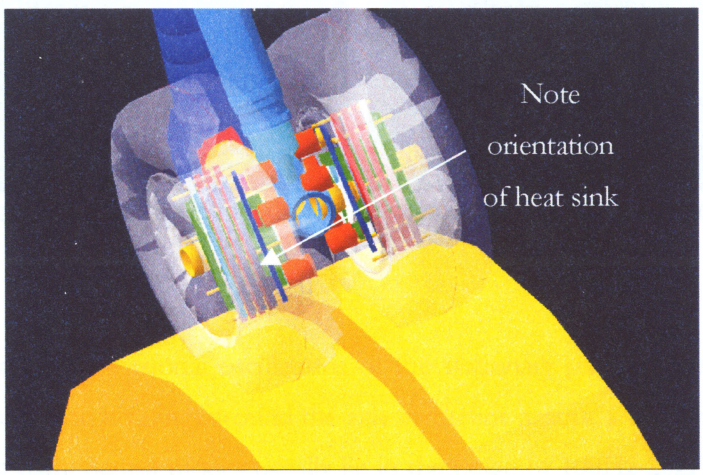

Figure 55 Computer Simulated Brake Whirl on Dynamometer (Dunlop)

A pedestal support may be incorporated to react the twisting moment applied by the offset torque take-out rod and reduce the wheel and brake misalignment under aircraft load, see figure 56. Wheel and brake misalignment can excite whirl vibration due to the heat pack out-of-balance forces caused by lateral frictional forces on the rotor drive keys, as the wheel rotates. The additional radial stiffness with the introduction of the pedestal also reduces the amplitude of whirl vibration.

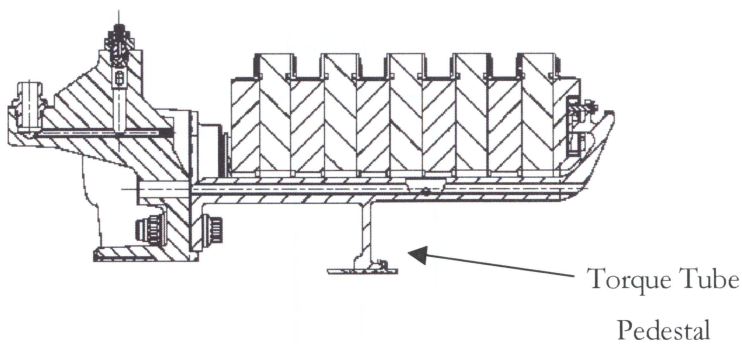

Figure 56 Torque Tube Pedestal (Dunlop)

Another solution to this mode of vibration is to introduce orifices into the piston housing passageways. These orifices effectively act to stiffen the piston and prevent fluid being "pumped" around the piston housing and driving the vibration mode. Figure 57 illustrates the effect of adding orifices to reduce vibration.

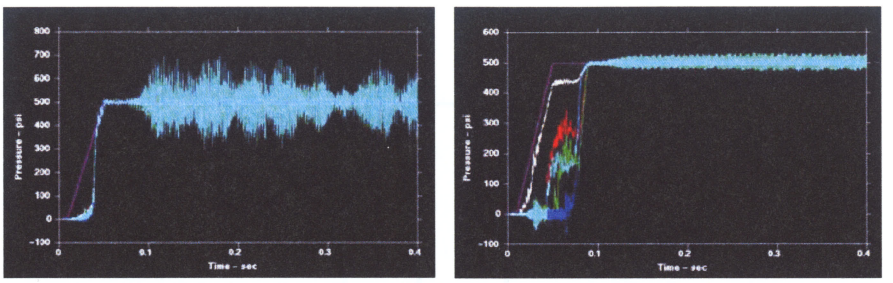

Figure 57 Before and After the Introduction of Orifices, note: different y-axis scales (Dunlop)

Brake Squeal

Brake squeal is due to torsional oscillations of the stationary parts of the brake (stators, torque tube and piston housing) around the axle centreline against a torsional spring of the torque take-out path. Squeal modes usually lie in the range of 100Hz-20kHz, however the primary modes of concern lie below 400Hz. Squeal is generated by the characteristics of the brake friction material and by modal coupling between axial and tangential degrees of freedom of the brake. It mainly occurs during landing stops and can produce very large loads on the landing gear and the brake, which sometimes can lead to brake failure.

Rotor Cycloidal Motion

This is the radial and rotational motion of the heat sink coupled with a "panting" oscillation. It occurs when wear lip formations have occurred, see figure 58.

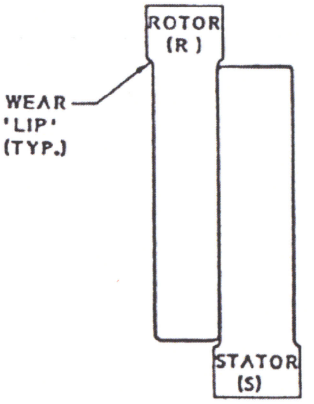

Figure 58 Wear Lip Formation (Dunlop)

This epicycloidal motion of the heat sink can be highly destructive with the motion resulting in impact loads between the rotor drive inserts and the wheel keys. The solution is relatively straightforward with it being prevented by adding grooves on the stators at the rotor inner diameter and on the rotors at the stator outer diameter – thus effectively preventing the formation of the lip, see figure 59.

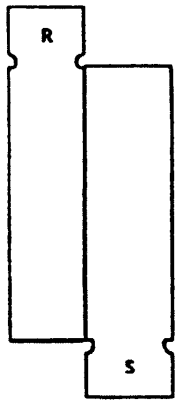

Figure 59 Grooved Rotor and Stator (Dunlop)

Chapter 9

BRAKE CONTROL AND ANTISKID SYSTEM

Brake Control System

A brake control system is a collection of components that when functioning provide the necessary power to the brakes in order to actuate them. Early brake control systems were manual in operation with mechanical linkages/cables connecting directly to the brake. This meant that the pilot had to provide the necessary force to actuate the brakes and hold them in place whilst braking. This was feasible for twin shoe drum brakes but as soon as the need to move to multi-shoe drum brakes the complexity of providing a mechanical input was too great. More importantly, "the limiting size for direct operation of brakes is reached in aeroplanes of about 15,000 lb. gross weight" (Adams, 1943). Pilot operation of the brakes was either by hand via the use of a lever or by moving the upper part of the rudder pedals, the so-called toe- or brake-pedals. An example of a Bendix mechanically actuated brake system is shown in Figure 60

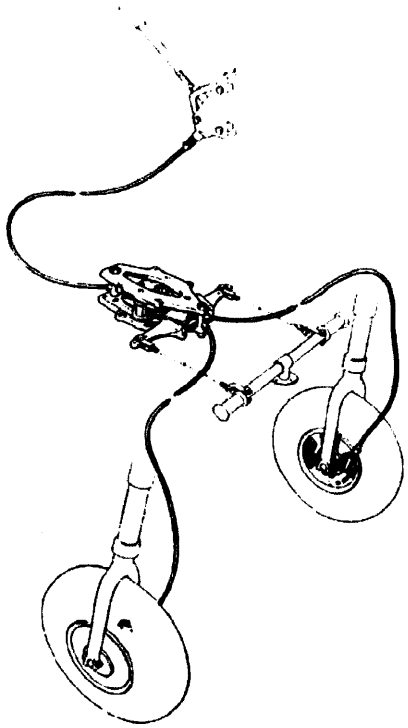

Figure 60 Mechanically Actuated Brake System (Adams)

Note: In this case the pilot operated the brake by a hand lever.

However, as aircraft grew in weight the pilot could no longer provide the force necessary to operate the brakes and so assistance was required. As discussed earlier there were two competing methods used to provide the assistance required:

- Pneumatic
- Hydraulic

In the 1940's, due to the difficulty in providing high-pressure hydraulic seals, pneumatics where the main method used to provide mechanical advantage in brake control systems. An anecdotal discussion on the move to hydraulics from pneumatics was given in Chapter 3. An early Dunlop pneumatic brake system is shown in figure 61.

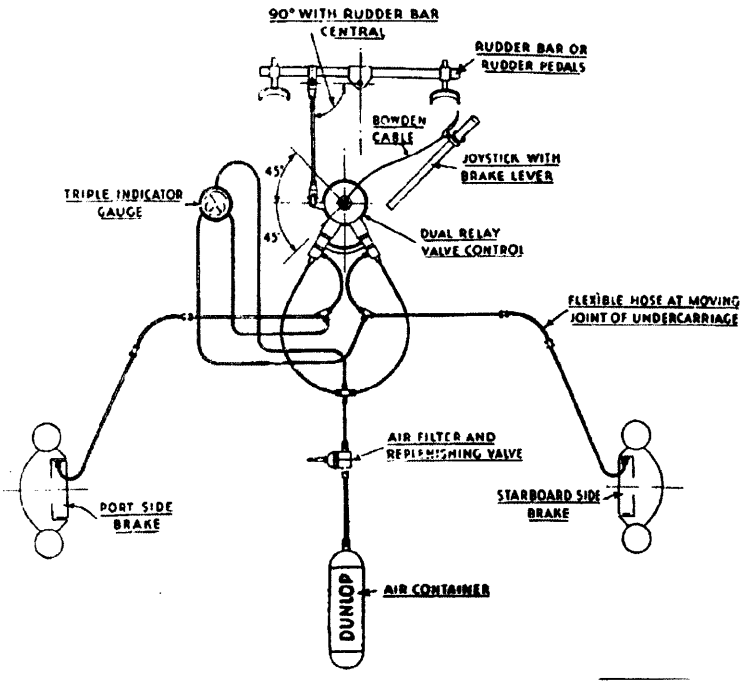

Figure 61 Pneumatic Brake Control System (Dunlop)

In this design, the pilot controlled the braking force by the use of a hand lever. Various designs of hand levers being possible, motorcycle lever type, ratchet & pawl, thumb lever or spade-grip. The system shown in figure 61 provided a significant additional function – one of differential braking. Differential braking provides the pilot with the ability to steer the aircraft when on the ground. The system achieved this function by providing a valve, the "relay valve" that allowed operation from the pilot's control and from the rudder bar.

It is fair to say that the change in flying control actuators from operating on pneumatics to hydraulics (due to stiffness requirements) and hence the subsequent availability of high-pressure hydraulic systems on board the aircraft, led to the demise of pneumatically operated brakes. It took a decade or two for the use of pneumatics to completely die out for instance, the Fokker F-27 was designed in 1953 using pneumatics for brake control, landing gear retraction and nosewheel steering. This system used high pressure (2000 psi min.) pneumatics while early systems typically used 200 psi pressure.

For hydraulic brakes, the pilot operates the toe-pedals and in the early years, this in turn connected either directly or via linkages to a master cylinder. The pilot, by pressing down on the pedal, creates a pressure within the master cylinder (sometimes termed a foot-motor), which in turn is transmitted to the slave cylinder at the brake. The slave cylinder or brake piston forces the shoes against the drum for a drum brake or the disk(s) together in disk brakes. Alternatively, the brake piston can operate a cam, which moves the shoes or clamps the disks.

In this type of system, which only provides hydraulic fluid to the brake system, the brake system is termed an independent system. On smaller aircraft, an independent sealed hydraulic system could be used to actuate the brakes and this design is still found on general aviation type aircraft today. However, on larger aircraft there is a need to provide substantially more fluid than the sealed system reservoir can supply. In addition, to prevent "dragging brakes" due to thermal expansion it is necessary to vent the system. A dragging brake is one that has residual brake torque when there is no commanded pilot signal, which if undetected can cause brake fire and lead to catastrophic consequences. There are many designs of vented master cylinders, one is shown in figure 62.

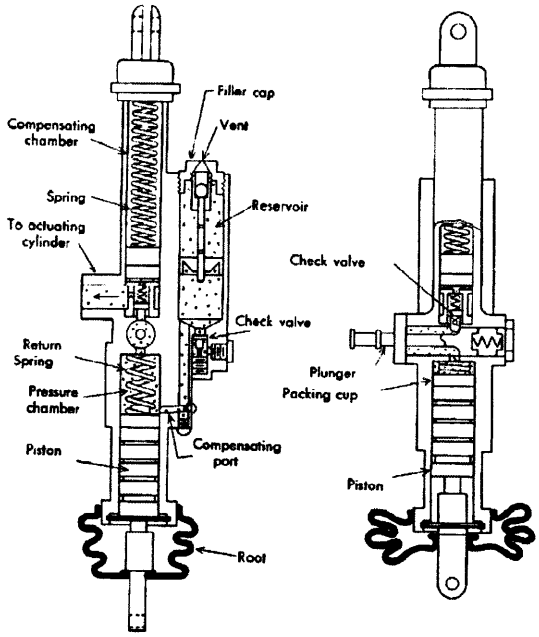

Figure 62 Vented Master Cylinder

As the size of aircraft grew so did the force necessary to actuate the brakes. There arrived a time when the pilot, even with the use of a master cylinder, could not provide enough force to actuate the brakes. This led to the development of the power-boosted master cylinder. The solution used the aircraft's hydraulics to aid the pedals in applying force to the master cylinder; this is termed a boosted master cylinder design and is still classed as an independent brake hydraulic system.

With the advent of large commercial transport aircraft and consequently a large number of wheel & brake assemblies, a substantial volume of oil is needed to operate the brakes. This large volume cannot be catered for by the use of an independent brake system and so the aircraft's hydraulic system has to be used. Two schematics depicting this type of system are shown in figure 63. The control device in this type of system is termed the power brake valve or brake-metering valve. Pilot input to the brake-metering valve is either through hydraulic means, via a master cylinder located at the pilot pedals or mechanically via a cable linkage. Smaller regional aircraft favour a master cylinder system whereas larger commercial aircraft use a cable system, (Plant, 1994). This approach, where the pilot does not control the brake directly, is termed a non-manual braking system. This type of system is also known as a Conventional System to differentiate between it and a Brake-By-Wire (BBW)

System. In addition to the metering valves there are a great number of other components shown in both schematics, the majority are required to meet the redundancy requirements laid out in the legislative requirements. The civil legislative requirements (Transport Category Aircraft) for brake control systems are laid out in FAR/JAR 25.735 while the US Military is covered by MIL-B-8075 and in the UK by Def-Stan 00-970.

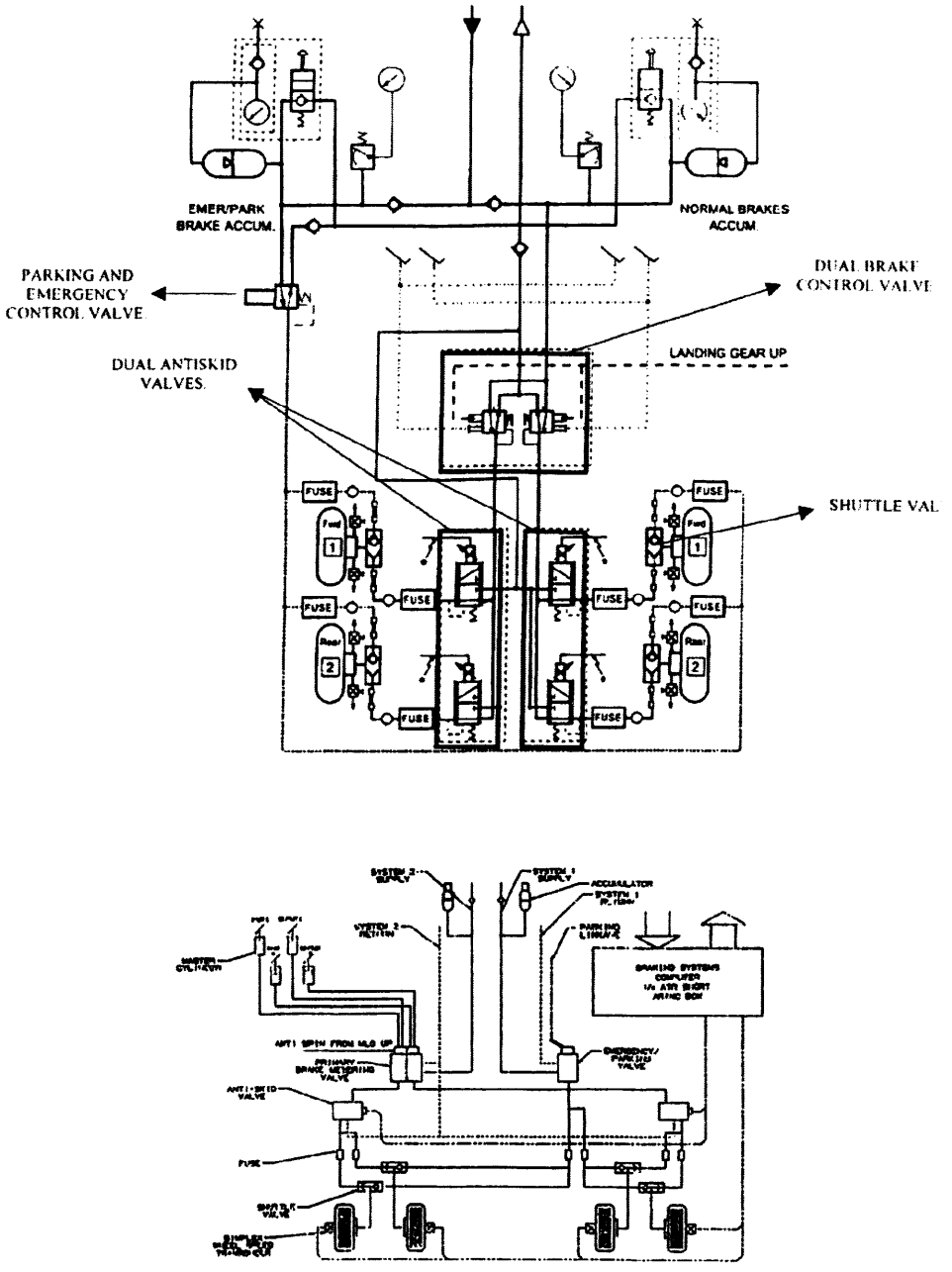

Figure 63 Two Examples of a Brake Control System (Dunlop)

Antiskid

With the introduction of power-assisted brakes, the pilot lost the 'feel' associated with manual braking. In particular, if the pilot applied the brakes excessively or too soon after landing, the likely outcome was to lock-up the wheel and burst a tyre. This was especially the case for inexperienced pilots, however even experienced pilots would occasionally burst tyres. A particular problem was on aircraft carriers where tyre skids leading to blowouts, which resulted in dangerous loss of control and importantly often caused irreparable damage to the wheels. This was the case for the US Navy in the Pacific during World War II, which had enough tyres burst and subsequent wheel damage to cause supply problems [Johnson, 1996]. In 1946, spurred on by the needs of the US Military, Boeing started to design and develop the first anti-skid system for the B-47, which ultimately led to commercial production in 1948.

Tyre-Ground Interface

When a rolling wheel has a braking torque applied, the mean circumferential speed of the tyre is less than the forward speed [ESDU 71025]. This effect is known as wheel slip or more commonly just slip and is defined as:

$$s = \frac{v - r\omega}{v} \tag{34}$$

Where s is wheel slip, v is the wheel's forward speed, ω is the wheel's angular velocity and r is the rolling radius of the tyre.

Note: (1) This definition is for an un-yawed tyre perpendicular to the surface.

(2) The rolling radius is not the same as the deflected radius.

The friction generated at the interface between the tyre and the runway generates the drag force required to stop the aircraft. This tyre-ground friction is created by forcing the wheel to slip. A typical plot of ground μ against slip is shown in figure 64.

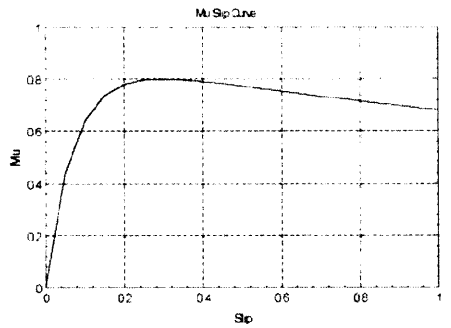

Figure 64 A Typical μ-slip Curve (Dunlop)

The shape of this curve varies with ground conditions, with wet and icy runways reducing the amount of friction available, see figure 65.

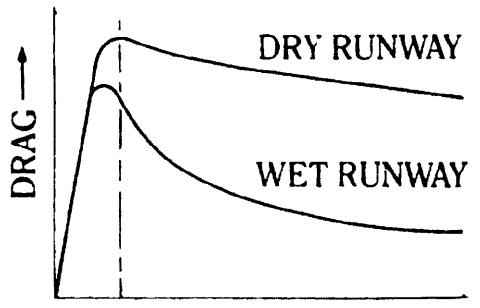

Figure 65 Typical Wet and Dry μ-slip Curves (Dunlop)

In addition, the μ-slip curve is dependent on the forward velocity of the aircraft, this is shown in figure 66.

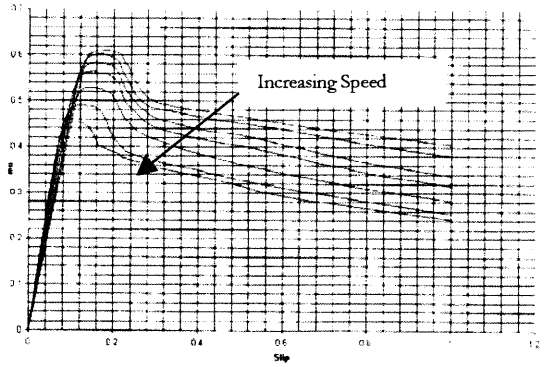

Figure 66 Variation in μ-slip Curve with Velocity (Dunlop)

In order to understand how antiskid systems operate it is necessary to understand the physics of the tyre-ground interface. When a tyre is brought into rolling contact with the ground, it deforms even when it is free rolling and there is no braking action. When braking, tread elements can only pass through the tyre-ground contact area by deflecting and deforming, this is shown in figure 67.

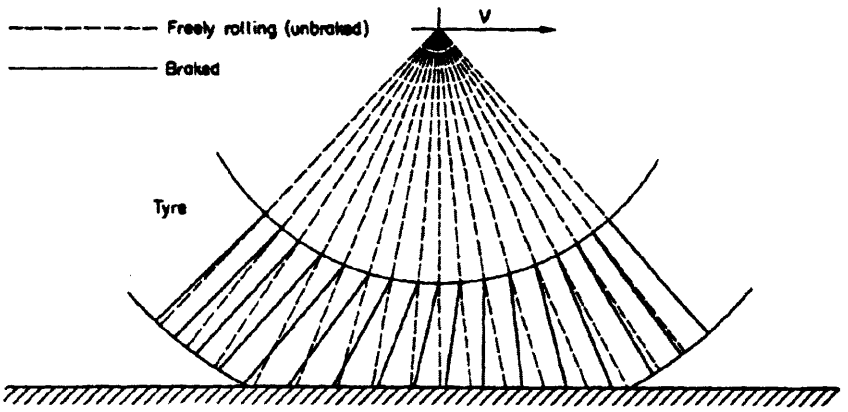

Figure 67 Tyre Tread Elements in Contact with Ground (ESDU)

This diagram shows the "passage of a single tread element through the tyre-ground contact area" (ESDU 71025). Now, as a tread passes through the contact area it undergoes more and more deflection until it reaches a point towards the rear where the distortion is too great to be maintained by the frictional drag force and sliding begins. Note that the distortion is a function of the shear force and the normal force. It is generally agreed that at low slip values the mechanism of friction is mainly due to the elastic deformation of the tyre. As braking torque increases, the tyre spring can no longer be compressed and therefore sliding starts to occur throughout the contact area, this corresponds to the peak coefficient of friction value. Now, as a tread element begins to slide, the temperature rises which reduces the local coefficient of friction, which then tends to increase sliding and hence slip. This explains the negative slope of the curve past the peak and hence the rapid onset of lock-up, particularly on high friction surfaces.

When braking occurs at low slip values most of the energy is being dissipated in the brake, however, as the slip increases energy starts being dissipated in the tyre until lock-up occurs when all the majority of the energy is being dissipated in the tyre. Hence, anti-skid can also be regarded as controlling the power transfer into the brakes under achievable runway conditions.

In addition, a tyre can only sustain a fixed amount of friction force. This force is divided between that required to slow the aircraft and that which is required to react the lateral forces on the tyre. The relationship between the two forces is shown in figure 68, (Longyear and Hirzel, 1979).

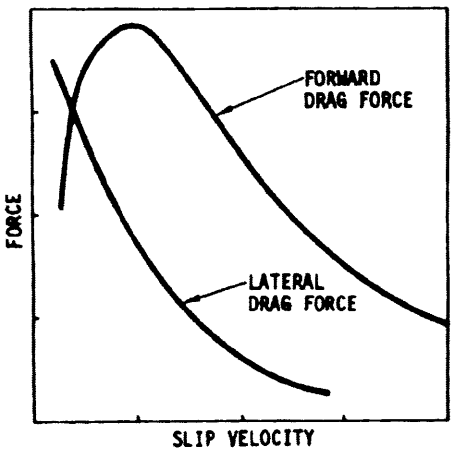

Figure 68 Lateral & Longitudinal Drag Force versus Slip Velocity (Longyear and Hirzel, 1979)

This clearly shows the trade-off between maximum drag and adequate directional control. The objective of the antiskid system is therefore not only to achieve the maximum retardation force possible under all conditions but to also provide this with minimum loss of directional control.

Antiskid Developments

As stated, the first antiskid systems were just that, systems that were designed to prevent wheel lock-up and hence preserve tyres. During operational use of antiskid, it became apparent that the system not only prevented flat-spotting and burst tyres but also reduced the stopping distance of the aircraft. This can be explained by the fact that if an aircraft could use the maximum coefficient of friction available it would stop in the shortest distance possible. Therefore, by operating at a higher coefficient of friction by using a "tyre-saver" system which is designed to prevent movement past the peak of the μ-slip curve, the aircraft will stop in a shorter distance than if it did not have an antiskid system.

Antiskid systems can be divided in to four classifications based on the stage of development (and complexity).

- On/Off Rate Control (or Bang-Bang Control)
- Rate Modulating Control
- Slip Control
- Stochastic Control/Fuzzy Logic/Neural Networks

A diagram indicating when the different types of system were introduced is shown in figure 69.

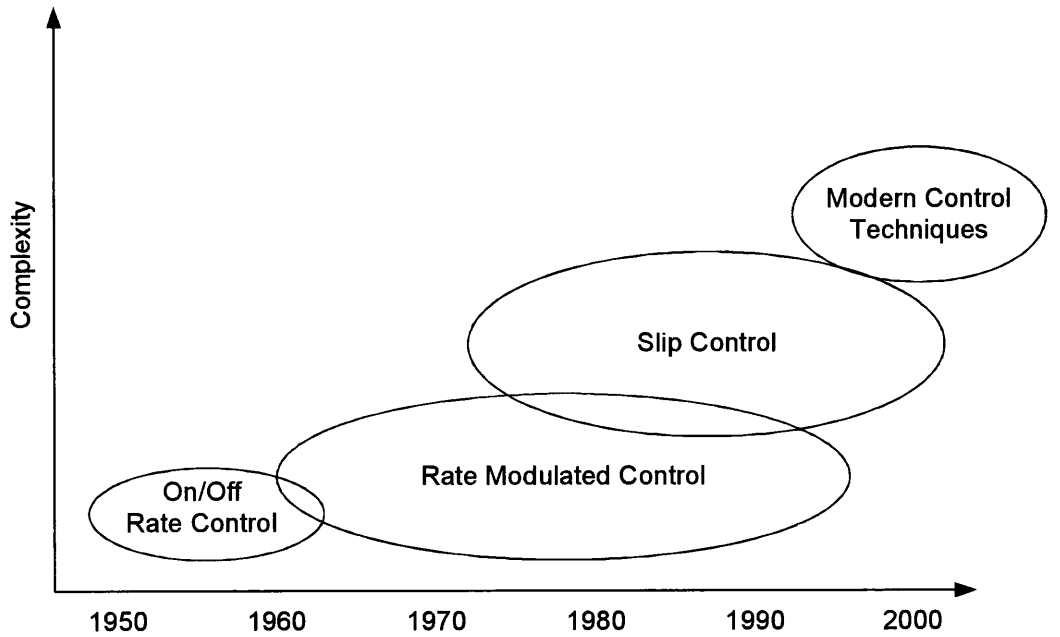

Figure 69 Antiskid Technological Developments

In the early period there were many proprietary designs such as Boeing's Hytrol system (later on Hydro-Aire's), Westinghouse with the Decelostat, Goodyear, Messier's Ministop and Dunlop's Maxaret. However, all the designs except the Goodyear system had a similar principle, this was to rotate a flywheel with the wheel. When the wheel was decelerated beyond a set limit, the flywheel over-ran and caused brake release. Interestingly once again, this technology was imported from other industrial sectors, this time taking ideas from Mining and the Railways.

Dunlop introduced the Maxaret system in 1951, an illustration of which is shown in figure 70. The Maxaret unit consists of a hydraulic valve, controlled by a flywheel that is driven by the casing of the unit. In the Mark I version the casing is in turn driven by the friction between the wheel rim and the rubber rimmed pulley wheel. In order to explain the operation of the Maxaret a sketch of the rotating components are shown in figure 71.

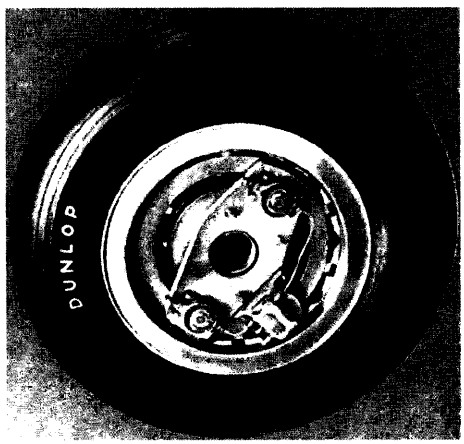

Figure 70 Rim Mounted Maxaret (Dunlop)

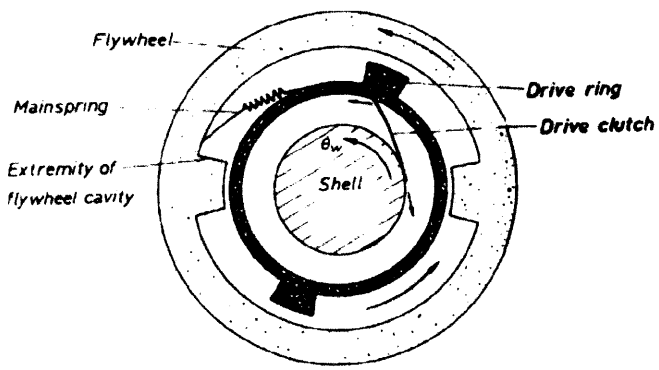

Figure 71 Maxaret Schematic (Dunlop)

The shell is connected to the wheel and therefore rotates with it and is also attached to the drive ring via a clutch. The flywheel, which has a much greater inertia than the shell and the drive ring, is attached to the drive ring by the main spring. The lugs on the flywheel and the drive ring provide a limit to the angular displacement of the two components. The drive clutch is designed to slip at a relatively low torque in the forward direction. When the wheel is travelling at constant speed the main spring exerts a restraining force that maintains contact between the drive ring lug and the flywheel lug. If a wheel skid starts, when the

deceleration exceeds a threshold, which is determined by the drive clutch and the main spring torques, the drive ring decelerates causing relative displacement between the flywheel and the drive ring. This angular displacement forces a set of balls to ride up a cam and this in turn operates a hydraulic valve, which releases brake pressure thus allowing the wheel to spin up to aircraft velocity again. An orifice that is chosen for each particular aircraft governs the rate of re-application. As described the settings of the main spring and the drive clutch are used to regulate the rate of deceleration and threshold at which the movement and thus valve operation occurs.

Later versions of the Maxaret (Mk. 2 onwards) mounted the unit in the axle and by Mk. 4 the unit was driven via a self-aligning drive from the hub, see figure 72. This version still utilised the flywheel as a rate detecting mechanism as in all previous versions.

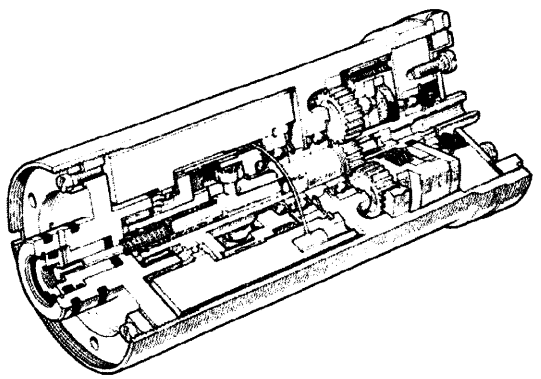

Figure 72 Maxaret Mark 4 Version (Dunlop)

A further development saw the introduction of the Maxaret Mk. 5, which removed the mechanical valve actuation and used electrical contacts to switch an electro-hydraulic valve in order to release brake pressure – this was the so-called "Electric Maxaret". Finally the Mk. 6 version moved away from the mechanical concept and utilised a variable reluctance type wheel speed transducer, which was then processed electronically.

All of these systems "provide a method of measuring rate of change of wheel speed, comparing this to a pre-set reference rate for a pre-determined time and, if it exceeds the reference rate for a pre-determined time, commanding a signal to the brake control solenoid valve causing brake pressure to be relieved completely" (Lester, 1973). As described above, the fixed standard rate was provided mechanically (excluding Goodyear's design) but all later systems adopted the electric fixed rate standard and consequent

processing of the signal. This type of system has the disadvantage that for long periods of time brake pressure is released even if there is available friction below the skid level available. This ultimately leads to relatively poor stopping efficiency. A block diagram outlining the functionality of this type of system is shown in figure 73.

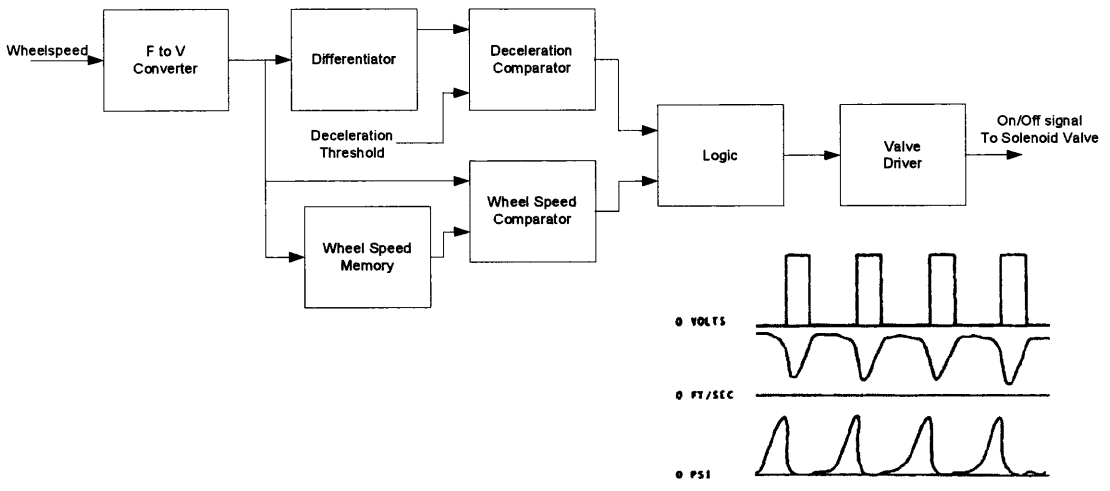

Figure 73 On/Off Anti-Skid Control System Block Diagram

This was state-of-the-art up until the early 1960's when as aircraft continued to grow in size, the need to land consistently in all weathers became more important. This requirement led to the development of the second generation of antiskid systems. These systems modulate the release and re-application of brake pressure rather than it being full on or full off, see figure 74 (Hirzel, 1972). The term modulated in this context refers to the manner in which the brake pressure is controlled proportionally and was made possible by development of the electro-hydraulic servo-valve. This type of system is still based on the rate of deceleration of the wheel with the rate of change of wheel speed being compared electrically to a fixed rate threshold. There are a number of different variants in particular; one design uses two different rates of re-application - initially using a high re-application rate and then as the brake pressure rises to that close to where the skid was induced, reduces the rate and the pressure ramps in at a lower rate. An important further development was the use of a variable rate threshold. The fixed rate threshold systems performance is determined by the threshold chosen (commonly the average aircraft deceleration required). Typically the threshold is set based on that achievable on a dry runway. However, under wet conditions this threshold would be too high with the

deceleration achievable being quite low. Thus, fixed rate threshold systems are less efficient than variable threshold systems under all runway conditions.

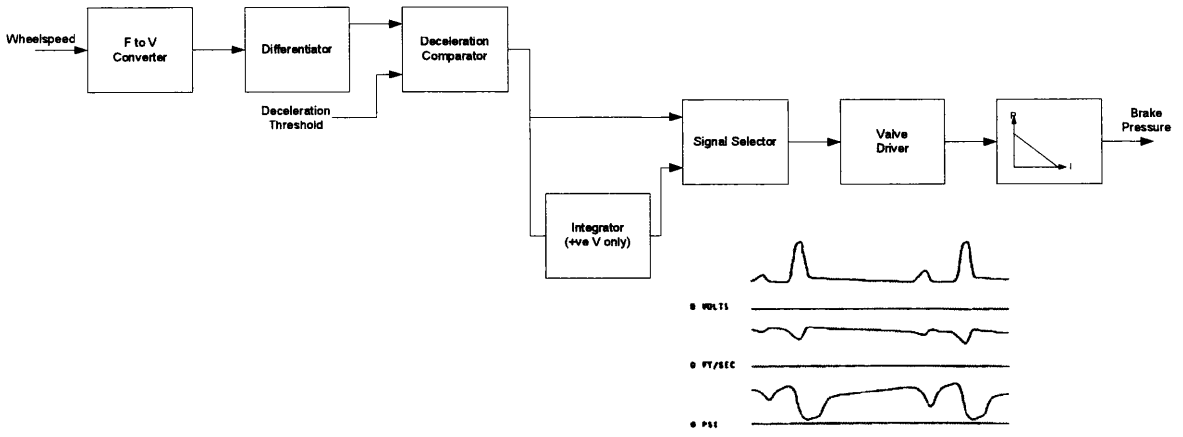

Figure 74 Modulated Antiskid Control System Block Diagram

Another technique used to improve antiskid efficiency was that of 'Pressure Bias Modulation (PBM)', and was first introduced by Hydro-Aire. PBM provides a signal proportional to the time integral of the rate signal, which in effect produces a mean pressure bias to the valve preventing the valve being commanded to zero pressure every time the rate signal goes to zero. By reducing the need to re-apply pressure after a skid occurred this enables the overall efficiency to be improved, see figure 75.

The next stage of antiskid development occurred in the mid-1960's when wet runway requirements imposed by the legislative authorities demanded more from the antiskid system than the existing systems could deliver. In order to improve the antiskid efficiency the new systems were not rate-controlled based but slip-controlled.

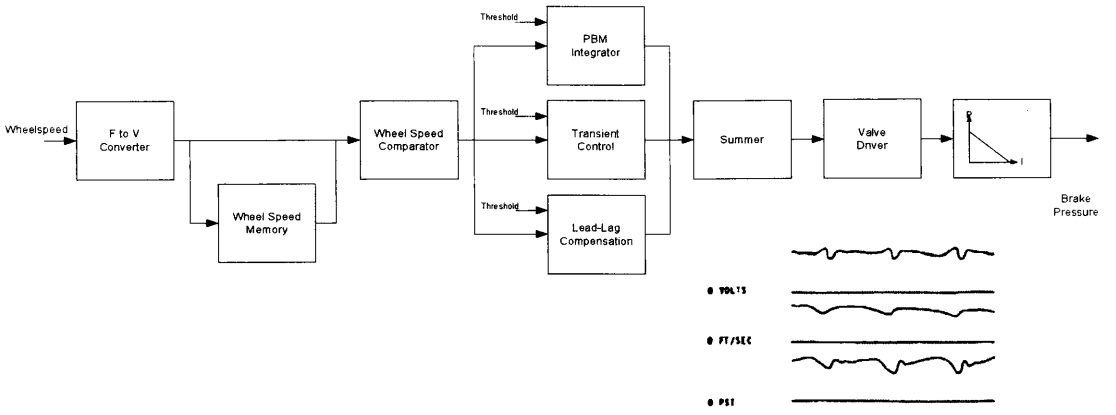

Figure 75 Slip Velocity Anti-Skid Control System Block Diagram

It is clear from examination of the μ-slip curve shown in figure 64 that there is a single value of slip that corresponds to the maximum μ available. This peak value usually occurs between slip ratios of 0.1 to 0.3. The most basic slip system controls the slip ratio to a fixed value – and consequently ignores the fact that the peak of the μ-slip varies due to runway conditions, aircraft velocity, etc., see figure 76. "To a large extent the constant slip ratio system is analogous to the fixed rate threshold modulated system..." (Lester, 1973). The deficiencies of the fixed slip ratio system are overcome by the more complex variable slip ratio systems in which the demanded slip is scheduled against aircraft velocity.

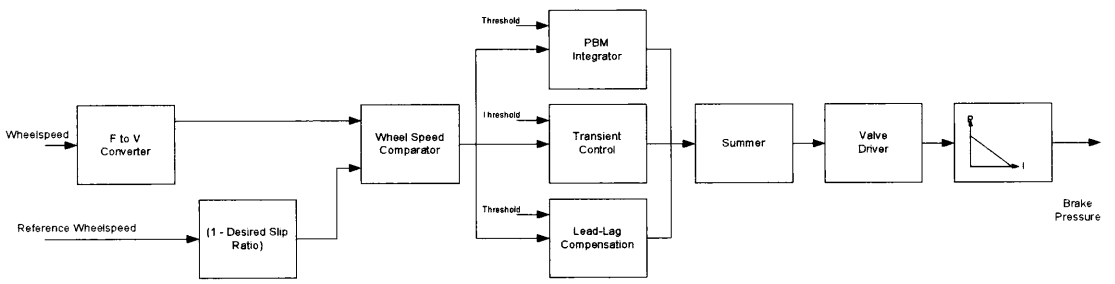

Figure 76 Slip Ratio Anti-Skid Control System Block Diagram

The main drawback of a slip-controlled system is the need to calculate slip. This reference velocity corresponds to that of the aircraft forward velocity. There are three ways of obtaining this; the first is to use an un-braked wheel – typically a nosewheel (this is the S.P.A.D. method in use on Concorde by Messier-Bugatti, the second is to use the aircraft's inertial navigation system or some other aircraft system which provides aircraft velocity

and thirdly, the more common approach, deriving an estimate of the aircraft's velocity from the initial velocity of the braked wheel itself before braking is applied and then assuming a set deceleration rate (normally chosen to be slightly greater than the maximum deceleration that the aircraft can achieve).

There are a number of difficulties with using a nosewheel consist of "not touched down or ... is worn or has a low pressure and so has a reduced radius...locked due to defective bearing" (Rudd, 1999). Alternatives include GPS, Doppler Radar or the aircraft's Inertial Navigation System. All of these are either prone to error, not reliable enough or too expensive.

Obtaining the reference velocity from the brake wheel is achieved by determining the free rolling velocity shortly after spin-up, thereafter a preset rundown rate is applied to this initial value to estimate the aircraft's velocity. This deceleration rate is chosen to be greater than that achievable by the aircraft and by doing so, the system is made to adapt. The very fact that the deceleration rate is greater than that achievable by the aircraft forces the system to traverse past the peak of the μ-slip curve causing a skid. Thus, the system is always trying to induce a skid and then to correct it – this is the only way in which the system can determine if it is at the peak of the μ-slip curve (re. observability). However, all these excursions past the peak reduce the efficiency of the system.

A recent series of patents (Rudd, 1999; Zierolf, 1999a; Zierolf, 1999b) by Goodrich have outlined new strategies that use Modern Control Theory, see figure 77. The most interesting variant uses the assumption that "since the μ-slip curve depends on so many variables (e.g. ... tire tread groove pattern, tire tread compound, temperature, tyre pressure, running surface material and finish, etc.), the μ-slip curve begins to resemble a random variable." (Rudd, 1999).

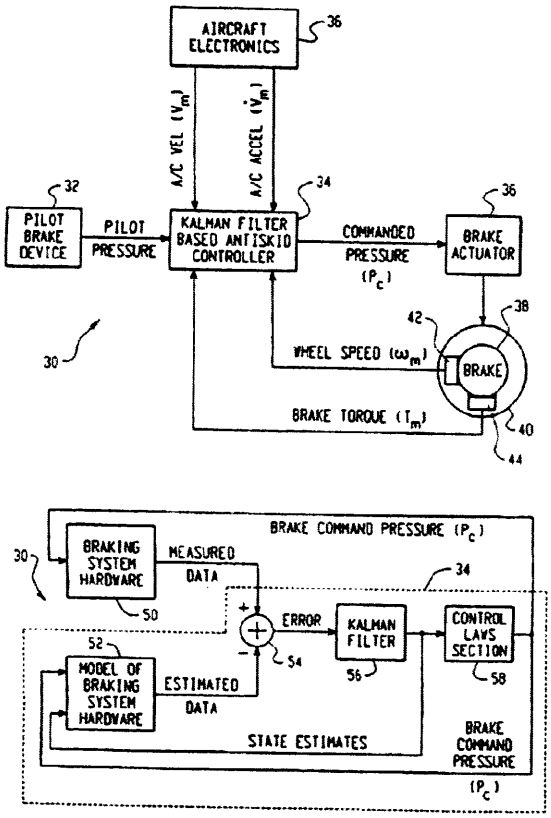

Figure 77 Modern Control Theory Antiskid Control System Block Diagram (Rudd and Zieroff)

Based on stochastic control theory it uses a Kalman Filter as a state estimator, to estimate the amount of friction available and then uses this information to control the braking effort. The patent claims that it differs from conventional antiskid systems by minimising the excursion past the peak of the μ-slip curve. It discusses the need for observability and states "any antiskid algorithm has to have the pressure applied to the brake arbitrarily perturbed to generate observable information". This is true and as stated is accomplished in a conventional slip based system by choosing a deceleration value greater than the aircraft can achieve. The detection of a skid in this new approach is based on wheel speed deviation of estimates from actual, slip error and a threshold on deceleration.

Another relatively recent development (Ewers et al, 1996) couples variable slip control system with fuzzy logic, this is shown in figure 78. In this system the conventional fixed slip control system of the A320, which has a desired slip ratio of 13%, is augmented by a fuzzy supervisor, which provides a change to the desired slip ratio based on runway

conditions. The paper states, "the simulation results show that the overall performance of the original system could be improved significantly, notably on runway surfaces with changing optimum slip" (Ewers et al, 1996). This type of system provides a credible alternative to the modern stochastic control theory type of controller utilising the best of classical control for robustness while providing adaptation using fuzzy logic.

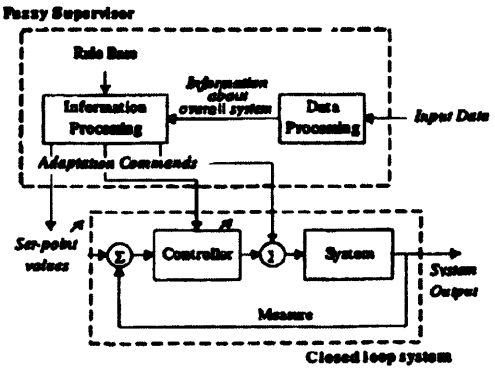

Figure 78 Fuzzy Logic Antiskid Control System Block Diagram (Ewers et al)

Another type of control that has also recently been applied to that of antiskid control is that of Extremum-Seeking Control (Tunay, 1999). Extremum-seeking control tries to optimise the output of the uncertain system in real-time and became popular in the 1950's and 1960's. Tunay applied the concept of Extremum-seeking control to remain at the peak of the μ-slip curve. The process involves superimposing a sine wave on top of the control signal and from the phase shift of this signal estimating the local slope of the friction curve. The simulation results from this work gave encouraging improvements over traditional antiskid control systems. However, one must be cautious firstly due to the number of simplifications used in all of these theoretical investigations but also due to the complexity of these algorithms and the subsequent difficulty in applying these in real-time on an aircraft with 100+ passengers on board!

Chapter 10

BRAKE PERFORMANCE INVESTIGATION

As discussed in Chapters 4 and 5, the performance of an aircraft brake depends on many variables, some intrinsic to the design and others depending on the environment. The aim of this chapter is to try to present a framework of understanding and also some quantitative relationships that can be used the by Brake Performance Engineer to help in the design of aircraft brakes.

Brake testing is undertaken on a roadwheel dynamometer, see figure 79, and due to the cost and time involved most of the development work is undertaken on the back of aircraft development programmes. This research used the results from many different aircraft development programmes to try to establish guidelines and tools to predict the performance of aircraft brakes. In particular the following have been investigated;

- Variation within the 100 Normals Qualification Tests (including any bedding in effects)
- Size of variance within the 100 Normals of the different aircraft programmes and what parameters, if any, determine or can be used to predict this variation.
- The parameters that may be used to predict the stop's mean μ under the various different stop conditions.

The Minitab statistical package was used to analyse and plot all data.

In order to protect commercial confidential and proprietary information aircraft programmes will be referred to Aircraft Programme #1 etc. A total of eight aircraft programmes were used in this investigation, two were Military and the rest were Civil. The Civil consisted of two Commercial aircraft and the rest were Regional and Business class aircraft.

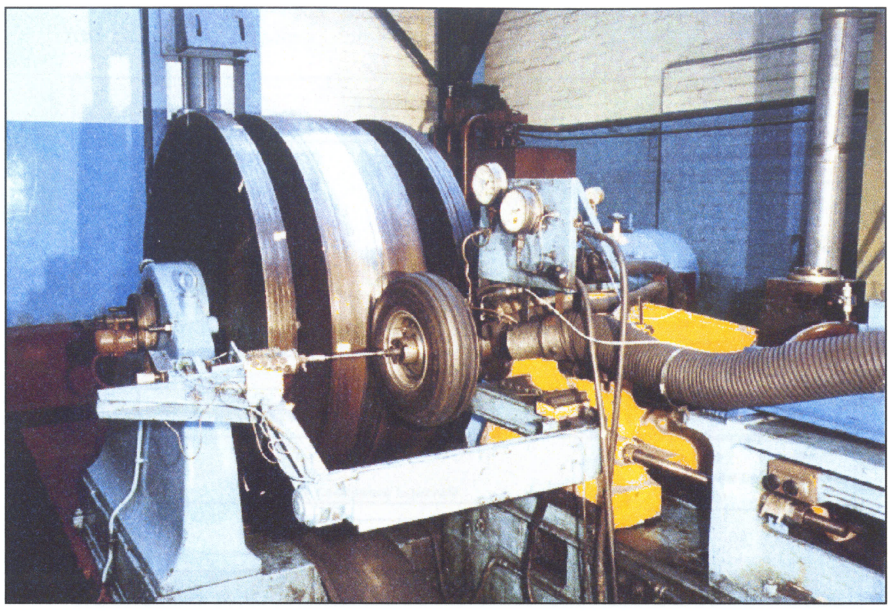

Figure 79 Aircraft Brake Testing on a Roadwheel Dynamometer

Bedding-In Effect

It is clearly evident from figure 80 that the mean μ of the stop decreases initially until it reaches a stable range of values.

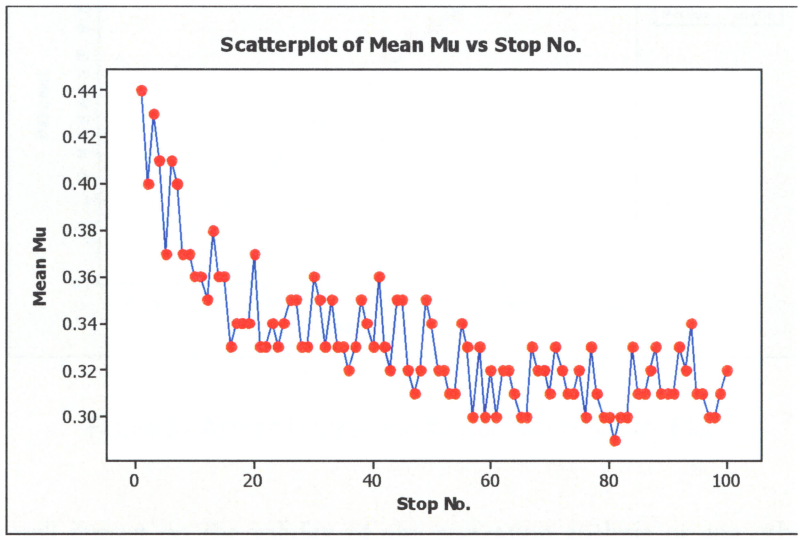

Figure 80 Aircraft Programme #1 Bedding in Effect

This bedding-in effect clearly has an effect on the normality of the data as is shown in figures 81 and 82.

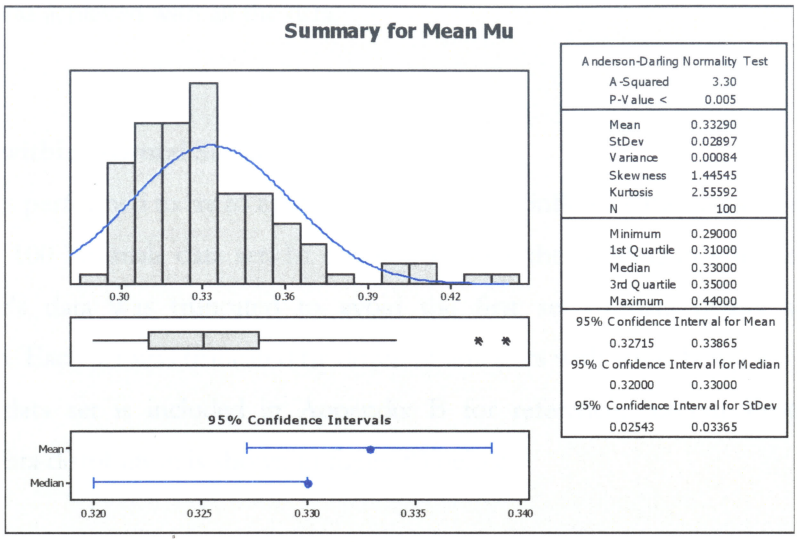

Figure 81 Aircraft Programme #1 Effect of Bedding-in on Distribution

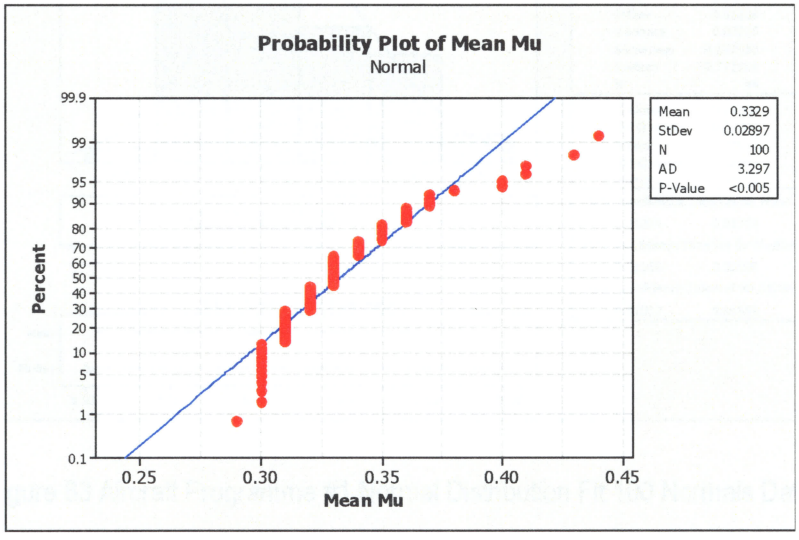

Figure 82 Aircraft Programme #1 Normal Probability Plot

This effect will impact on the validity of any regression analysis or any other statistical analysis that requires normality as a pre-requisite. Figure 82 (normality plot) also highlights another problem with the original data set used – that is of data discretisation. The stop's mean μ calculated has been artificially truncated to 2 decimal places and this has resulted in the data not being distributed along the 45°normality-line in discrete values. In order to

remove this problem a large amount of data had to be re-worked to remove any traces of discretisation. It was found that by calculating to one additional decimal place that normality was achieved with all the data.

Variation within Normal Stops

A study was performed to try to establish which factors influence the variance of the mean μ with the 100 Normals data set. In order to remove the bedding-in effect each aircraft programme's data was truncated to avoid the first set of data points skewing the distribution. Each set was truncated by different amounts with some being left untouched. The total data set is included in Appendix B for reference; Aircraft Programme #1 truncated data distribution is shown in figure 83 below.

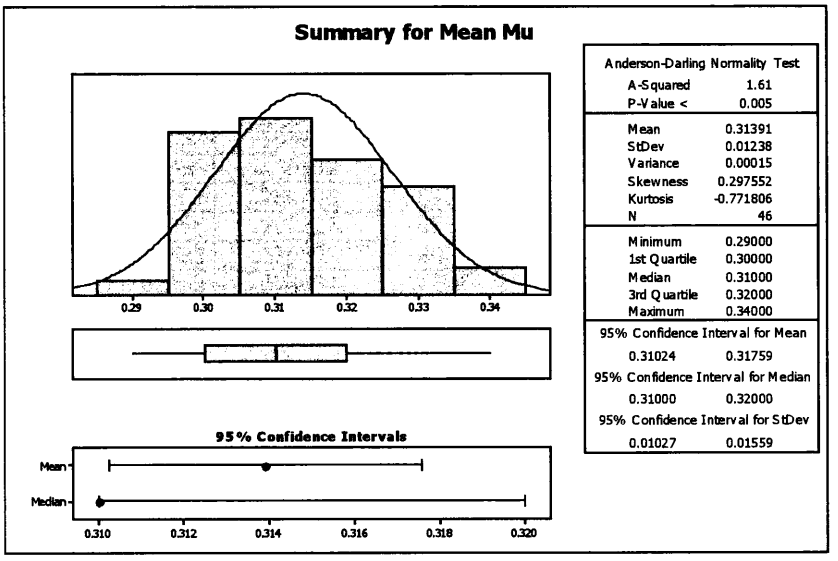

Figure 83 Aircraft Programme #1 Normal Distribution Fit 100 Normals Data

The following factors were investigated to determine if individually or in combination they would affect the variance of the mean μ.

- Mass Loading
- Area Loading
- Rate Loading
- No. of Interfaces
- Total Piston Area
- PCR

The Minitab "Best Subset" command was used to establish the best combination of variables to predict the variance, the data used is summarised in table 9.

Aircraft	Mean Mu	StdDev	ML	AL	RL	Interfaces	TPA	PCR
#1	0.31391	0.01238	353864	10053	495	6	6.056	8.836
#2	0.34565	0.01298	284933	8858	798	4	5.101	6.77
#3	0.39145	0.02183	383867	10534	570	6	5.529	8.836
#4	0.41288	0.04355	430589	15858	820	10	7.978	23.278
#5	0.41288	0.04355	289706	8954	609	4	4.797	6.765
#6	0.39624	0.04355	292327	9767	496	8	6.25	12.37
#7	0.4509	0.03623	370861	8076	512	8	6.08	13.806
#8	0.39145	0.02183	324664	7607	586	4	4.676	10.37

Table 9 Mean μ - 100 Normals Variance

Note: ML = Mass Loading, AL=Area Loading, RL = Rate Loading, TPA = Total Piston Area and PCR = Mean friction radius of carbon

The output from Minitab is shown below;

Vars	R-Sq	R-Sq(adj)	Mallows C-p	S	M L	A L	R L	Interfaces	TPA	PCR
1	29.7	18.0	-0.8	0.012440				X		
1	28.9	17.0	-0.8	0.012516						X
2	46.3	24.8	0.4	0.011913	X					X
2	42.8	19.9	0.6	0.012298	X			X		
3	52.7	17.3	2.1	0.012496	X		X			X
3	51.1	14.4	2.2	0.012709		X		X	X	
4	68.1	25.6	3.4	0.011847	X	X		X	X	
4	59.9	6.5	3.8	0.013286	X			X	X	X
5	76.5	17.8	5.1	0.012459	X	X		X	X	X
5	68.5	0.0	5.4	0.014431	X	X	X	X	X	
6	78.0	0.0	7.0	0.017050	X	X	X	X	X	X

It is obvious from the R-Sq value that the fit is not particularly good however; the information provides an interesting insight into where the variability is introduced. Not surprisingly the number of interfaces plays a significant role i.e. for an increase in the number of rotors there is an increase in the standard deviation (and hence variance). The R-Sq (adjusted) number indicates the fact that by adding more and more variables the fit tends to get better and so while it is indicator the Mallows C-p value which takes into account the R-Sq (adj) and the number of variables is a better criteria. In this particular analysis the Mass Loading and the PCR are the factors that best describe the data. This is also not surprising, as we will show that the mean μ is dependent on the mass loading. It is understandable that the PCR is a factor as it has a large effect on the torque of the brake and this relates directly to the μ. The regression equation is

$$\sigma^2 = 0.05577 - 0.00000016ML + 0.002508PCR \qquad (35)$$

Great care must be taken when applying this equation in particular due to the small sample size that it originated from. The analysis while not providing an accurate method of predicting variance does help to establish which factors influence mean μ variance.

Mean Mu Prediction

Data from all 8 Aircraft Programmes were studied to determine the factors that influence the mean μ. Firstly the relationship between energy and mean μ was explored, this is shown in figure 84. This graph clearly shows that the more energy required to be absorbed by the brake then the lower the mean μ will be. This phenomenon has been reported once in the literature (Stanek, 1993) but no quantitative evidence was given.

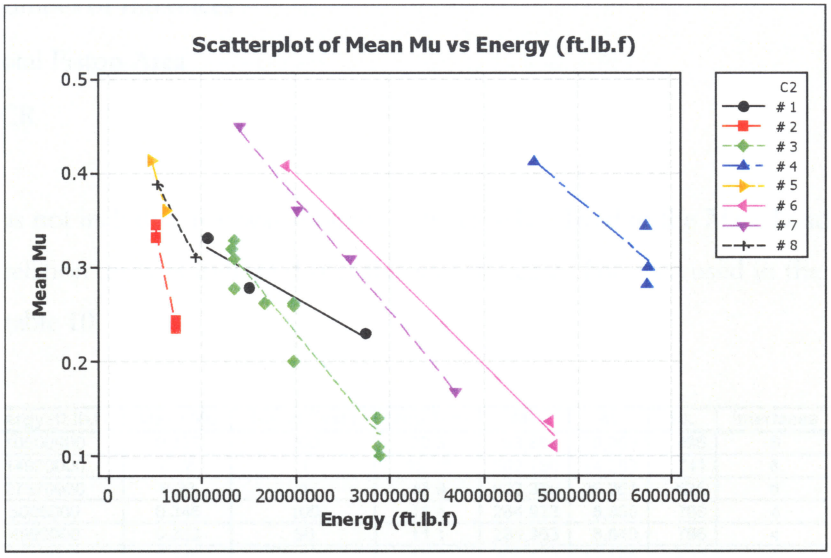

Figure 84 Energy versus Mean μ

While this plot indicates the relationship it is still not apparent as to what factors are responsible for the different slopes and for the absolute values. It is also interesting to note that Stanek (1993) implies a piecewise linear relationship with the mean μ while the data above does not. This is probably due to the data used being complete sequences i.e. landings and taxi snubs. Further work is required to determine if this piecewise linear relationship is more accurate than the one presented here.

The factors chosen as possible influences on the mean μ of the stop were the same as those used in investigating the mean μ variance within the 100 Normals. The factors are repeated here for convenience;

- Mass Loading
- Area Loading
- Rate Loading
- Number of Interfaces
- Total Piston Area
- PCR

Energy was not included as it was thought to be closely related to the Mass Loading and in fact a correlation analysis indicated that this was the case. The data used in the analysis is shown in table 10.

Aircraft	Energy (ft.lb.f)	Mean Mu	No. of Tests	Stop Time	ML	AL	RL	Interfaces	TPA	PCR
# 1	10500900	0.333	100	20.3	353,864	10,053	495	6	6.056	8.836
# 1	14920000	0.28	1	19.28	502,780	14,283	741	6	6.056	8.836
# 1	27370000	0.23	1	41.9	922,325	26,201	625	6	6.056	8.836
# 2	5000000	0.346	100	11.1	284,933	8,858	798	4	5.101	6.77
# 2	4990000	0.333	50	11.1	284,363	8,840	796	4	5.101	6.77
# 2	7110000	0.245	1	18.2	405,174	12,596	692	4	5.101	6.77
# 2	7120000	0.235	1	18.1	405,744	12,614	697	4	5.101	6.77
# 3	13420000	0.33	100	18.47	383,867	10,534	570	6	5.529	8.836
# 3	19690000	0.26	5	22.2	563,215	15,456	696	6	5.529	8.836
# 3	28780000	0.1	1	27.36	823,227	22,591	826	6	5.529	8.836
# 3	13420000	0.31	100	18.38	383,867	10,534	573	6	5.529	8.836
# 3	19690000	0.263	4	22	563,215	15,456	703	6	5.529	8.836
# 3	28640000	0.11	1	27.18	819,222	22,481	827	6	5.529	8.836
# 3	13420000	0.278	40	18.49	383,867	10,534	570	6	5.529	8.836
# 3	19690000	0.2	2	22.08	563,215	15,456	700	6	5.529	8.836
# 3	28640000	0.14	1	25.94	819,222	22,481	867	6	5.529	8.836
# 3	13200000	0.32	100	18.18	377,574	10,361	570	6	5.529	8.836
# 3	16690000	0.263	3	21.44	477,403	13,101	611	6	5.529	8.836
# 3	28620000	0.14	1	24.58	818,650	22,465	914	6	5.529	8.836
# 4	45384327	0.413	104	19.33	430,589	15,858	820	10	7.978	23.278
# 4	57380000	0.283	1	21.46	544,399	20,049	934	10	7.978	23.278
# 4	57170000	0.345	1	21.45	542,407	19,976	931	10	7.978	23.278
# 4	57550000	0.3	1	21.39	546,012	20,108	940	10	7.978	23.278
# 5	4520000	0.414	90	14.7	289,706	8,954	609	4	4.797	6.765
# 5	6120000	0.362	10	9.22	392,257	12,124	1,315	4	4.797	6.765
# 6	19010000	0.408	100	19.7	292,327	9,767	496	8	6.25	12.37
# 6	47500000	0.111	1	29.6	730,432	24,404	824	8	6.25	12.37
# 6	46980000	0.136	1	24.8	722,436	24,137	973	8	6.25	12.37
# 7	14000000	0.451	100	15.76	370,861	8,076	512	8	6.08	13.806
# 7	20100000	0.361	6	17.22	532,450	11,594	673	8	6.08	13.806
# 7	25840000	0.31	1	19.84	684,503	14,905	751	8	6.08	13.806
# 7	36900000	0.169	1	21.18	977,483	21,285	1,005	8	6.08	13.806
# 8	5250000	0.389	100	12.98	324,664	7,607	586	4	4.676	10.37
# 8	9330000	0.311	1	16.76	577,181	13,524	807	4	4.676	10.37

Table 10 Experimental Data used for the Analysis

Minitab's "Best Subset" function was applied to determine the combination of factors and their relationship that best fits the data. An excerpt from Minitab's output is presented below,

Vars	R-Sq	R-Sq(adj)	Mallows C-p	S	M L	A L	R L	Interface	T P A	P C R
1	62.3	61.1	29.0	0.059758	X					
1	60.6	59.4	31.6	0.061072		X				
2	82.0	80.9	0.2	0.041936		X				X
2	79.4	78.1	4.2	0.044857		X			X	
3	82.3	80.6	1.7	0.042251		X			X	X
3	82.1	80.3	2.0	0.042525	X	X				X
4	82.7	80.3	3.1	0.042527		X			X	X X
4	82.4	79.9	3.6	0.042927	X	X			X	X
5	82.8	79.7	5.0	0.043211	X	X			X	X X
5	82.7	79.6	5.1	0.043276		X	X		X	X X
6	82.8	78.9	7.0	0.044003	X	X	X		X	X X

It is apparent that in the Area Loading and the PCR has a significant influence on the absolute mean μ value. In fact the use of the Area Loading and the PCR can explain 80.9% of the variability of the mean μ. The regression equation is

$$\overline{\mu} = 0.417 - 0.000016AL + 0.00936PCR \qquad (36)$$

Where AL is in ft.lbf/in^2 and PCR is in inches

Note: It has been found in practice that the minimum achievable mean μ value is 0.1, therefore this relationship should be used to estimate the mean μ until the value falls below 0.1 and then it should be held at this value.

This result can be explained physically by remembering that the Area Loading is the energy divided by the total swept area and that it has been shown that the friction at an interface is highly dependent on the surface temperature – thus the Area Loading provides indication of the temperature that the interface reaches. It is not so apparent as to why the PCR also has a significant effect on the mean μ and it may in fact be related to a scaling factor effect. The definitive reason why these factors influence the mean μ has not been established due to the fact that the tests investigated where not designed to determine them but were

qualification tests. However, the regression equation derived does provide a good model by which to predict the mean μ.

Chapter 11

BRAKE DESIGN CASE STUDY

A regional aircraft constructor has designed an aircraft that has a requirement for 4 main wheel brakes. The aircraft constructor has identified 3 conditions for which the brakes have to be designed and the specific requirements are listed in below;

	Service	**Normal**	**RTO**
Kinetic Energy	4.4MJ	6.7MJ	9.7MJ
Brake Application Speed	$47.84ms^{-1}$	$56.07ms^{-1}$	$62.56ms^{-1}$
Deceleration	0.19g	0.35g	0.27g

In addition the following should be noted.

- The heatpack is required to last for 2000 landings before requiring replacement.
- The tyre installed on the main wheels are H34 x 10.0R16.
- Maximum operating pressure is 3000 psi
- Axle and landing gear installation details are shown in figure 85, as well as bearing locations.

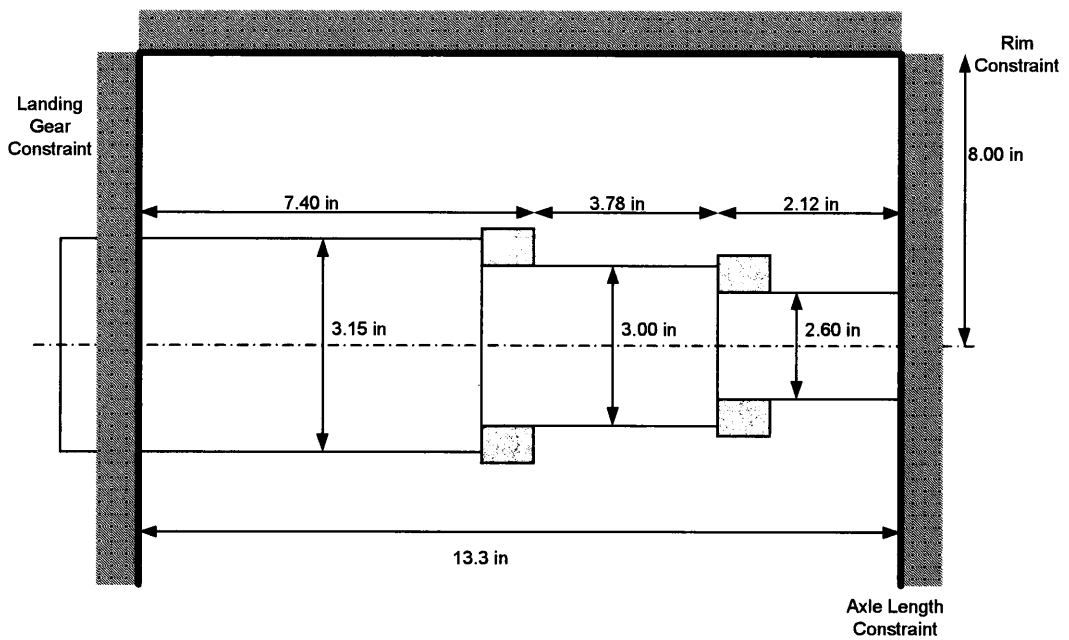

Figure 85 Installation Details

Figure 85 also indicates the rim constraint in addition to the axle and landing gear constraints.

As the aircraft is a civil aircraft the first set of coefficients in Table 4 will be used to estimate disk sizes. Rim Size is already specified through the choice of tyre and in this case is 16 in. Hence,

$$\text{Stator OD} = 0.7091 + (\text{rim size} \times 2.286)\text{in}$$
$$= 0.7091 + (16 \times 2.286)\text{in}$$
$$= 13.6316\text{ in}$$

$$\text{Stator ID} = 0.4170 + (\text{rim size} \times 0.391)\text{in}$$
$$= 0.4170 + (16 \times 0.391)\text{in}$$
$$= 6.637\text{ in}$$

$$\text{No of Stator Drives} = 1.442 - (\text{rim size} \times 11.25)\text{in}$$
$$= 1.442 - (16 \times 11.25)\text{in}$$
$$= 12 \text{ (rounded up to nearest integer)}$$

Similarly for the rotors

$$\text{Rotor OD} = 0.788 + (\text{rim size} \times 2.322)\text{in}$$
$$= 0.788 + (16 \times 2.322)\text{in}$$
$$= 14.93\text{ in}$$

$$\text{Rotor ID} = 0.6645 - (\text{rim size} \times 2.361)\text{in}$$
$$= 0.6645 - (16 \times 2.361)\text{in}$$
$$= 8.271\text{ in}$$

$$\text{No. of Rotor Drives} = 0.350 + (\text{rim size} \times 2.217)\text{in}$$
$$= 0.350 + (16 \times 2.217)\text{in}$$
$$= 8 \text{ (rounded up to nearest integer)}$$

From this the PCR and DSA can be calculated as follows.

$$PCR = \frac{(13.6316/2)+(8.271/2)}{2} = 5.476\,\text{in}$$

$$DSA = \frac{\pi}{4}\left[(13.6316)^2 - (8.271)^2\right] = 92.214\,\text{in}^2$$

It is important to minimise the number of rotors required to achieve brake performance as this maximises overall life. Therefore we will use 2 rotors in the initial design. Hence,

$$A_{TS} = DSA \times 4 \times N_R = 92.214 \times 4 \times 2 = 368.858\,\text{in}^2$$

In order to calculate stator area/face the width and depth of the slot has to be selected. In this case the following values have been chosen.

W_{SD} = 0.615 in and H_{SD} = 0.636 in

$$\begin{aligned}\text{Stator Area/face} &= \frac{\pi}{4}\left[(S_{OD})^2 - (S_{ID})^2\right] - (N_{SD} \times W_{SD} \times H_{SD}) \\ &= \frac{\pi}{4}\left[(13.6316)^2 - (6.673)^2\right] - (12 \times 0.615 \times 0.636) \\ &= 106.276\,\text{in}\end{aligned}$$

For rotors W_{RD} = 1.3 in and H_{RD} = 0.590 in, have been selected.

$$\begin{aligned}\text{Rotor Area/face} &= \frac{\pi}{4}\left[(R_{OD})^2 - (R_{ID})^2\right] - (N_{RD} \times W_{RD} \times H_{RD}) \\ &= \frac{\pi}{4}\left[(14.93)^2 - (8.271)^2\right] - (8 \times 1.3 \times 0.590) \\ &= 115.204\,\text{in}\end{aligned}$$

The stopping distance for each condition is calculated from the following equation

$$v^2 = u^2 + 2(decel)s$$

Now $u^2 = 0$ therefore $s = \frac{v^2}{2(decel)}$ and using equation 19, $t_{stop} = \frac{V_{BAS}}{decel}$, where the deceleration is specified for each stop condition, the following results are calculated.

	Service	**Normal**	**RTO**
Deceleration (specified)	0.19g	0.35g	0.27g
Stopping Distance	2013ft	1501ft	2423ft
Stopping Time	25.65s	16.32s	23.61s

Next step is using the criteria outlined in Table 5 the carbon mass required can be determined.

The calculation is

$$\text{Minimum Mass Required} = \frac{\text{Energy Absorption Required}}{\text{Maximum Loading Criteria}}$$

	Service	**Normal**	**RTO**
Min New Heatsink Material	8.11 lbm	8.23 lbm	7.94 lbm
Min Worn Heatsink Material	6.49 lbm	7.06 lbm	7.15 lbm

Therefore the minimum worn mass required is 7.15 lbm because otherwise the 1,000,000 ft.lbf/lbm maximum mass loading would be exceeded.

It is important to note that unless the minimum worn heatpack carbon mass plus the mass required for wear exceeds the 8.23 lbm additional mass will be required.

Assuming the wear rate of the carbon is 0.00006 in/landing/wear face then the length of the wearable mass required is calculated as follows;

$$\begin{aligned}\text{wear stroke} &= \text{Number of Landings} \times \text{wear rate} \times 4 \times N_R \\ &= 2000 \times 0.00006 \times 4 \times 2 \\ &= 0.96\,\text{in}\end{aligned}$$

The mass of the wearable material, assuming a density of 0.067 lbm/in^3, can be calculated as follows;

$$\begin{aligned}\text{Mass of Wearable} &= \text{Number of Landings} \times \text{wear rate} \times DSA \times N_R \times 4 \times \rho \\ &= 2000 \times 0.00006 \times 92.214 \times 4 \times 2 \times 0.067 \\ &= 5.931 \text{ lbm}\end{aligned}$$

Hence,

$$\begin{aligned}\text{Minimum Mass of Worn Heatsink} &= \text{Minimum Worn Heatsink} + \text{Mass of Wearable} \\ &= 7.15 + 5.931 \text{ lbm} \\ &= 13.081 \text{ lbm}\end{aligned}$$

Now check mass loadings in both worn and new conditions

	Service	**Normal**	**RTO**
Mass Loading New Heatsink	248,089	377,640	546,585
Mass Loading Worn Heatsink	453,889	690,909	1,000,000

The Area Loading is now calculated

$$AL = \frac{Energy}{DSA \times N_R \times 4}$$

	Service	**Normal**	**RTO**
Area Loading (ft.lbf/in^2)	8798	13393	19384

All conditions are below the recommended loadings. Reducing either the DSA or the number of rotors can increase the Area Loading, however this would reduce the mean μ.

To calculate the mean μ equation 36 is used

$$\bar{\mu} = 0.417 - 0.000016AL + 0.00936PCR$$

	Service	Normal	RTO
Predicted mean μ	0.327	0.254	0.158

The next step is to calculate the required torque necessary to achieve the stopping distance already calculated.

$$T = Fr_{tyre} = \frac{0.5mv^2 \times r_{tyre}}{s} = \frac{Energy \times r_{tyre}}{s}$$

Now $r_{tyre} = 0.95 \times (34/2) = 16.15\,\text{in}$

	Service	Normal	RTO
Required Torque (lbf.ft)	2169	4428	3972

Assuming an ineffective pressure of 280psi and selecting a piston diameter of 1.3125in^2 gives the following required pressure.

	Service	Normal	RTO
Required Pressure (lbf/in^2)	848	1776	2436

Now given that the maximum system operating pressure is 3000psi there is enough pressure to provide the required torque.

Rotor disk mass is calculated using equation 24

$$M_R = \frac{(0.5 \times M_{EFFN})}{N_R} = \frac{0.5 \times 13.081}{2} = 3.270\,\text{lbm}$$

The thickness of a rotor is calculated as follows;

$$th_R = \frac{M_R}{\rho \times A_R} = \frac{3.270}{0.067 \times 115.204} = 0.424\,\text{in}$$

Similarly for the stators

$$M_{DS} = \frac{(0.5 \times M_{EFFN})}{N_R} = \frac{0.5 \times 13.081}{2} = 3.270\,\text{lbm}$$

$$th_{DS} = \frac{M_S}{\rho \times A_S} = \frac{3.270}{0.067 \times 115.204} = 0.459\,\text{in}$$

In this case both the pressure and thrust stators are chosen to be half the thickness of the double stator.

$$th_{PS} = th_{DS} = 0.5 \times 0.459 = 0.230\,\text{in}$$

The total new heatpack length is thus

$$\begin{aligned}\text{heatpack length} &= th_{PS} + th_R + th_{DS} + th_R + th_{TS} \\ &= 0.23 + 0.424 + 0.459 + 0.424 + 0.23 \\ &= 1.766\,\text{in}\end{aligned}$$

Now layout the design to ensure that it will fit in the installation envelope. To perform this certain assumptions will be made these are as follows;

- Torque Plate is 2.75 in wide
- Piston running clearance is 0.12 in
- Thrust plate (including cones) is 1.00 in length
- Thrust plate – wheel clearance is 0.40 in
- Inboard hub section thickness is 1.00 in at PCR of cones

Thus the total length of the brake is

$$\begin{aligned}&= \text{Torque Plate} + \text{Clearance} + \text{Heatpack Length} + \text{Thrust Plate} + \text{Clearance} + \text{IB Hub Thickness} \\ &= 2.75 + 0.12 + 1.766 + 1.00 + 0.4 + 1.00 \\ &= 7.036\,\text{in}\end{aligned}$$

Figure 86 shows that the design can achieve the required brake performance within the installation envelope constraints.

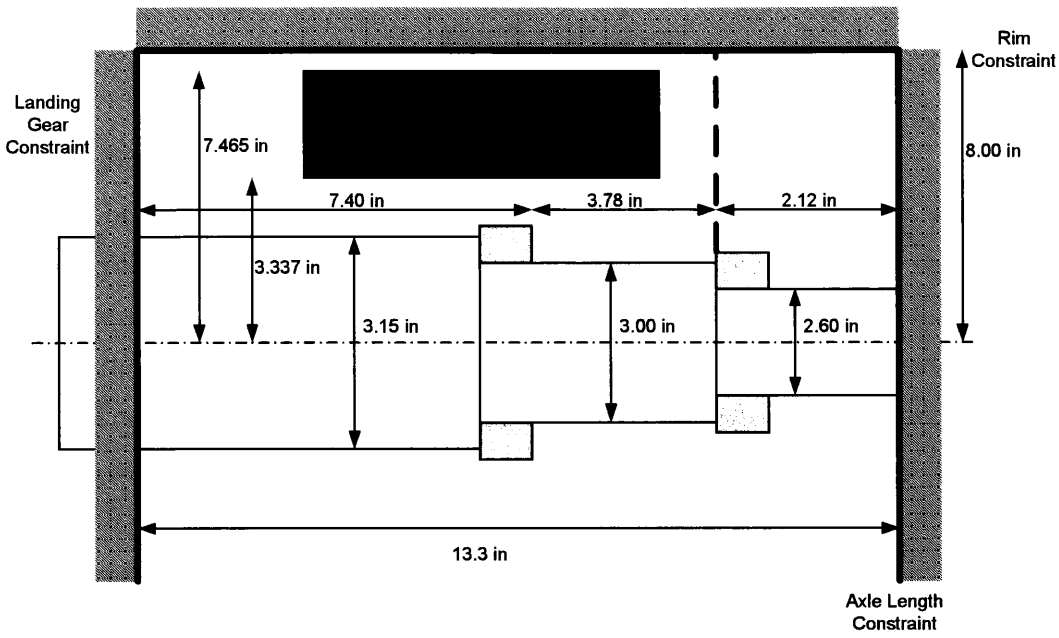

Figure 86 Preliminary Design Concept

Chapter 12

DISCUSSION

System Integration

Aircraft braking is achieved through the pilot controlling brake pressure and hence brake torque. This is realised through the brake control system, which transmits the command to the brake and then the brake generates the torque. This torque is transmitted as drag to the runway through the wheel and tyre combination and to the body of the aircraft through the landing gear structure. The interaction of all the components is a key role in the development of new aircraft. The performance of the brakes is readily apparent to the pilots and passengers especially the vibration performance. It is important to note that the pilot actually controls the aircraft stopping performance through the "seat of his/her pants" i.e. it is the aircraft's deceleration that is being controlled as sensed through his/her centre of gravity. Developments in antiskid have led to systems such as an Autobrake function by which the aircraft's deceleration may be controlled. However, this function is only available during landing and take-off and not during ground manoeuvres.

The multi-disk brake provides a compact method of achieving the brake torque. Up to now brakes have been hydraulic but recently electric brakes have been developed and these will be discussed later. The hydraulic brake has a number of pistons that provide the clamping force on the brake disks. From equation 13 it is clear that the number of pistons required depends on the number of friction interfaces as both have a direct relationship to the torque generated. However, the physical size of the disks and the need to provide evenly spread force also dictates the number. An odd number of pistons tend to be favoured, as it has been found that even numbers may cause a propensity for the brake to whirl.

Brake response time depends heavily on both the size and number of the hydraulic pistons and by the pipe lengths of the brake control systems. In order to minimise delay the pipes must be kept as short as possible and the brake piston area must be as small as is possible. In addition, to keeping the pipes short it is imperative that the pipes be kept the same length and if possible have the same number of bends, fittings etc. This is important because as explained in Chapter 4 carbon-carbon composites undergoes a transition from

having a low friction at temperatures approximately below 180°C to a higher friction value at temperatures higher than this. This may result in the brake that is quickest to generate the brake torque transitioning into this higher friction regime and hence performing more of the work. The distribution of brake torque across all the aircraft's wheel and brakes is a major problem. This can be exacerbated through not knowing the state of the heat sink material. This leads to many aircraft being designed to achieve the required deceleration with "one brake's worth" of torque less than the if all brakes were fully operational. However, this can only be achieved on aircraft with at least 8 wheels otherwise significant weight penalty would be incurred by over-designing the brake. The design of the piston housing and brake chassis also impacts on the volume of fluid displaced and hence effects the brake response time. All effects are taken to reduce the compliance through the use of stiffening ribs on the piston housing and the section thickness of the thrust plate. Care must be taken not to over-stiffen the structure as that would result in a brake that is difficult to control and in particular would give a very poor antiskid response.

An interesting use of the gain change in carbon friction characteristics is the technique of deliberately only using a subset of the total number of aircraft brakes during taxiing with the active subset changed at every landing. By reducing the number of brakes operational during this period forces the active brakes to absorb more energy and thus get hotter than they would if all were operational. This has the effect of causing the active brakes to transition into their low wear regime and hence increase their life. This is only possible if the taxi energy is substantially less than the landing energy and this is typically the case. However, in very large aircraft where there is significant amount of aircraft inertia depending on the total number of brakes this might not be possible. Empirical evidence has shown that this technique can provide up to 30% savings on overall brake life.

The aircraft constructor initially decides the number and the size of tyres required through the flotation needs of the aircraft. This is based on the type of runways the aircraft is intended to operate from and the maximum weight of the aircraft. The analysis in Appendix A has shown that once the rim size is specified the brake's heat sink can be established through the use of the equations derived. The linear equations are presented in Chapter 5 and they provide a very good fit to the data and so this should greatly aid the initial design process.

The length of the heat sink depends on the minimum heat sink mass required to meet the RTO or maximum energy case as well as providing enough wearable material in order to achieve the specified life. From figure 23 it is obvious that the wheel centreline location and the landing gear both heavily influence the size of the envelope. The main drivers for the heat sink length are the brake application speed and the aircraft mass. Note that the velocity of the aircraft has marked effect on the energy absorption requirements due to the square law relationship.

The brake attachment method has significant impact on the piston housing with the lug method providing the best overall design solution. However, it is generally the case that on multi-wheel bogies, e.g. commercial aircraft, the torque pin method is used; on regional aircraft having two wheels per axle the torque lug method is favoured and on two wheel aircraft (both military fighters and business jets) flange mounted brakes are mainly used. It must be remembered that the method of attachment can have a significant effect on the dynamic stability of the brake.

The brake control system has to be designed to meet the Airworthiness Regulations and as with all systems has to achieve the required safety levels. It does this by having to provide an emergency method of applying the brake in the event of loss of one hydraulic source. As discussed this requirement and the many others result in a complex architecture but importantly has a direct impact on the piston housing. To achieve the safety requirements either a shuttle valve or two sets of pistons each operating independently have to be used.

Thermal management requires designing wheel, brake and tyres that can firstly convert the energy into heat, store this heat energy for a given period in the heat sink and then channel this heat into the structural components. Each component does not act in isolation and requires careful design to control the flow of the heat into specific areas. In particular, the tyre must be kept below 325°C or the tyre will ignite. Other important temperature limitations are that the rim and axle must be kept below 200°C or the strength of the material will reduce.

Recently, considerable work has been undertaken on the development of electric brakes suitable for aircraft. In an electric brake, a number of electro-mechanical actuators provide the required heat sink clamping force. The electro-mechanical actuator consists of an

electric motor, a screw mechanism and gearing. There are a number of different design solutions depending on the type of motor chosen, the type of screw i.e. roller or ball and the overall gearing. What is interesting is that the use of electric brakes changes the conventional thinking on the brake control system and brake functional decomposition. In an electric brake system, the electronic controller required for the electro-mechanical actuator replaces the hydraulic valves. This fundamental difference removes the difficulties associated with locating the hydraulic valves and also the saves weight. However, the main advantage in moving to electric brakes is the reduction in maintenance. The hydraulic brake control system has a heavy maintenance burden that arises from having a large number of components.

The electric brake also poses challenges to traditional solutions for aircraft braking vibration problems. In particular, the restrictor fix for brake whirl instability is no longer possible. However, the very fact that the drive train of the electro-mechanical actuator is very stiff compared to the compliance of the hydraulic piston helps to prevent the instigation of the mode.

As discussed in the main text, the brake system architecture must be capable of providing braking under failure and emergency conditions. The hydraulic solution to this is to use two hydraulic systems and an accumulator as a back-up emergency source. In an electric brake the very fact that it is easy to switch electric power sources opens up many more different architectures. However, a major difference is the use of an active-active brake control system, which entails have two systems both controlling a number of electro-mechanical actuators on each brake. This mode of redundancy has been used on hydraulic systems (F16), however it is not common due to the complexity and the added weight.

Antiskid performance of the brake is improved through the increased frequency response of the electro-mechanical actuators. However, more importantly the piston can now be driven off instead of relying on the compliance of the brake to remove the end load.

The brake is designed to meet certain requirements specified by the aircraft constructor. In order to achieve this, an understanding of how the friction couple works and the ability to predict the torque generation capability of the brake is essential. The construction of the carbon-carbon composite has a great effect on the wear rate and the friction generating

capacity of the material. The author discusses the motivation that led to the development of carbon-carbon composites and the specific properties that are important.

The problem of oxidation and its effect on brake life has been examined. Oxidation is due to the oxygen molecules reacting with active sites of the carbon matrix and this occurs at temperatures above approximately 400°C. The rate of oxidation depends on porosity/density, temperature and chemical purity. If a brake is operated for long periods with temperatures exceeding this figure, oxidation will occur. This typically manifests itself as de-lamination of the middle disks of the heat sink starting at the edges of the disk. The reason for the middle of the heat sink being the area affected is due to the fact that this area is exposed to the hottest temperatures. In the past few years there has been an introduction of a new range of environment friendly de-icers and cleaning fluids. Unexpectedly these products have had a significant impact on the life of carbon brakes. This is due to the new fluids being based primarily on potassium, sodium and calcium salts, which are well known to be catalysts for carbon oxidation. Oxidation can cause a severe loss of disk strength and may not be easily detectable by visual inspection. Protection takes the form of two approaches, the first is to restrict the access of oxygen to the carbon and the second is by slowing the rate of oxidation down. The impact of oxidation may mean the refurbishment techniques discussed in Chapter 5 may not be possible due to the condition of the returned disks. This loss of refurbishment may have a great financial impact and render a profitable aircraft programme into loss. If refurbishment is not possible this may also mean that additional manufacturing capacity is required and this would require a large capital expenditure.

The static friction characteristic of carbon-carbon composites dictates that the brake has a certain end load necessary to meet the static drag requirements. As the static μ is lower in value than the dynamic μ this may result in the brake being able to generate a high dynamic torque. This is important because the landing gear has to be designed to be able to react this force. It may be the case that the landing gear has to be increased in size due to this requirement and obviously take a heavy weight penalty. An alternative method would be to limit the brake torque generated and thus prevent this condition. However, in order to limit torque a suitable sensor has to be fitted and a measurement site chosen. There are only two systems known in use, on Concorde and on the Boeing 747, both systems are based on strain gauges attached to the landing gear. The reliability of strain gauges in this

type of application is poor and many alternatives have been suggested but so far they have all stayed in the laboratory.

Brake Performance

The main objective of this research was to provide a scientifically based methodology to improve the predicted performance of the carbon-carbon composite brake. The nature of the research meant that specifically conducted tests would not be possible and so data from previous aircraft development programmes had to be used. The data used covers a fifteen year period and as such much of the data was not store in a form that was readily usable. In addition, due to the nature of the tests, the data was not necessarily derived and so much digging around for data had to be undertaken.

The brake performance investigation work was divided into two main parts, the first to investigate the normals or design landing cases – the situation that the aircraft daily engages in and secondly, that of the higher energy stops which area relatively infrequent and even rare.

The study into the brake performance behaviour during normals found that during the initial stops of the test sequence that the mean μ values were typically much higher. The number of stops required before a stable range of values was reached varied from brake to brake and factors could not be established to predict this number. Work was also conducted to try and establish if this relationship was determined by environmental conditions especially humidity due to the well-known effect of this on the friction performance of carbon-carbon composites. This was only possible for a certain number of brakes and was not through humidity values but had to be derived from the comments associated with the actual time of the test, for instance it was inferred that the first stop of the day may be affected more that later stops due to the absorb water being vaporised off. A major improvement to understanding this phenomenon would be to record the humidity at every stop. In addition, it must be remembered that the 100 normals test is only performed on one brake in an aircraft development programme and while there is enough data across aircraft programmes, within a particular programme the conclusions drawn must be carefully balanced against the statistical significance of the sample size. An important factor that is believed to affect the initial brake performance is that of mechanical tolerances of the disks and the machining finishes. It is recommended in future

that dimensions on all disks be recorded before commencing tests; in particular this is essential for the 100 normals.

The data used in the analysis undertaken to establish the factors that influence the size of the variation within the 100 normals was truncated to avoid the bedding-in effect having a bias that might unduly influence the outcome. In both this analysis and the later analysis of the value of mean μ a larger set of factors were analysed before settling on the set presented. The total list of factors used in the analysis was the following;

- Effective Heat Sink Mass
- Swept Area / Face
- No Of Rotors
- No Of Pistons
- Piston Size
- Total Piston Area
- PCR Of Carbons
- T.W.B. Energy
- Brake Application Speed
- Stop Time
- Mean Deceleration
- Stop Distance
- Mean Torque
- Mean Drag
- Mean Operating Pressure
- Mean Pad Pressure
- Effective Mass Loading – based on actual mass rather can nominal mass
- Area Loading
- Rate Loading

It was decided that a smaller set of data could be used, as many factors were in fact dependent upon others. Another important reason to curtail the number of factors was that brake performance engineers are familiar with the concepts of mass loading, area loading and rate loading and that by using these parameters the methodology had a greater

chance of being used in practice. However, this would only be the case if the relationships established proved to be statistically sound and would provide a better prediction of the mean μ than the method currently employed.

The investigation has shown that as the absorbed energy increases the mean μ decreases. In practice it decreases until it reaches a minimum value of 0.1 and does not (as a mean value) reduce to values below this. The factors chosen were as stated the brake loading parameters and the number of interfaces, the total piston area and the PCR. These last three factors were included due to the belief that these variables have a direct influence into the performance of the brake. The torque is generated at each interface and depends on the μ at that particular interface and hence more interfaces would introduce more variability. The total piston area is linked to the clamping force required to generate the torque and hence it was believed that this has an effect on the frictional force generated. The PCR was included due to a phenomenon widely reported in steel brakes especially in the automotive sector and that is the thermo-elastic effect. This is the interaction of the frictional heat generation, thermal distortion and elastic contact may cause a non-uniform contact pressure on the interfaces. Certain amount of anecdotal evidence indicates that this phenomenon may be happening in carbon brakes. Video footage of certain brake tests clearly show bands of carbon that are visible at a higher temperature than other areas within the swept region. The PCR also provides a scaling factor, as bigger brakes will necessitate a larger PCR.

This research has, through its investigations, established a statistically robust relationship between mean μ and both Area Loading and PCR. This provides a scientifically based approach to predicting brake performance compared to the experience based approach used at present. Interestingly it is seen from the results that the Mass Loading and Rate Loading have very little influence on the mean μ. This is due to the fact that the Mass Loading provides an indication of the bulk temperature, however it is the friction faces surface temperature that has a major influence in the μ developed. It was initially believed that the Rate Loading would have a significant influence but this is not the case. This is due to the fact that the Rate Loading by definition depends on the stop time and this inherently is related to the mean μ achieved. The provision of a relationship to predict the mean μ of an aircraft brake is a significant improvement on the methods and practices currently used.

Case Study

A case study illustrating the use of the design methodology developed and the decisions required to meet an aircraft constructor's specifications has been included into the work. This methodology is important because it not only details the steps and sequences of the design process but it provides guidelines to help the designer in making those choices.

The case study is based on a regional aircraft with the constructor specifying the energy absorption and deceleration required by the brake to achieve. In addition, installation requirements are provided which constrain the design from a space envelope aspect.

The design approach follows the Design flowchart shown in figure 38. An important part of the methodology has been the development of the relationship between Area Loading, PCR and brake effectiveness, μ. In addition, equally important has been the development and codification of the brake designer knowledge into a methodology that is of scientific significance.

The overall design produced is a concept design with more design iterations and manufacturing considerations being necessary to optimise all of the various requirements and constraints.

Chapter 13

CONCLUSIONS

The main objective of this work was to investigate and to provide a scientifically based methodology to improve the prediction of carbon-carbon composite brakes. In addition, another aim of the research was to provide a framework of understanding that would enable better system integration of all the components that together perform the aircraft braking function. These aims and objectives have been met with a methodology to improve the prediction of the mean μ of a carbon-carbon composite brake and a number of recommendations regarding the impact of design features on the overall functionality and performance.

Aircraft brake performance depends on the tribological properties of the friction couple. This behaviour combines both surface and bulk characteristics of the material. In addition, from earlier discussions it is well known that the ability to absorb and dissipate the heat away from the surface is a critical property. The increase in aircraft performance requirements has led to the development of new brake designs and new friction materials. The development of brakes for large commercial aircraft has stabilised to that of a carbon-carbon composite multi-disk brake design.

Carbon-carbon composites are a family of materials and this research has focused on material that is currently manufactured by Dunlop Aerospace Limited. This is a PAN-CVD material that was developed over fifteen years ago. The investigation focused on explaining the variation in stopping performance and more importantly the ability to be able to predict the mean μ value of a stop.

The research initially highlighted the fact that aircraft brakes performed more consistently after a period of bedding-in. This bedding-in period however, could not be linked to any particular factors. This is an area of research that requires considerable more work to understand the nature of this. It is believed that this effect is due to the fact that the wear surfaces have not been condition both thermally and mechanically. This is based upon the visual inspection of disks prior and after the bedding-in period.

A study into the variation of mean μ within the 100 Normals aircraft brake qualification programme was also undertaken. A number of factors were chosen to determine if they influenced this variance. Factors chosen were either related to the how "hard" the friction material was made to work i.e. mass loading, area loading and rate loading and to brake design in particular the number of friction interfaces and the clamping force on them. The work resulted in a linear equation that predicts the variation in mean μ. The level of confidence associated with this relationship is not high. However, it must be remembered that only one brake per aircraft programme undergoes the 100 Normals and therefore the data represents only a small sample. There are still interesting insights to be gained from the analysis as it indicates the relative importance of the variable chosen. In particular, the best-fit variables are mass loading and PCR, followed closely by mass loading and number of interfaces. The established relationship indicates that as the mass loading increases the variance decreases for any given PCR. A more detailed research programme is recommended to specifically investigate the nature of this variance.

The third aspect of brake performance investigated was to determine a relationship that would enable better prediction of brake performance. It was first determined that as the energy absorbed increases, the mean μ of the stop decreases. In order to provide a methodology a more detailed analysis was undertaken with the same factors used in the variance analysis. In this case, the factors chosen were capable of predicting the mean μ very well. The linear equation derived is based on the use of the area loading and the PCR and achieved an adjusted coefficient of determination of 80.9%, which signifies a good fit to the data.

The design of a multi-disk brake is a complex engineering task that requires many specialist engineering disciplines such as structural analysis and dynamic analysis etc. The wider context of aircraft braking is even broader and requires not only mechanical engineering skills but also electronic and software engineering. Importantly it was addressing this aspect of system integration that was also an objective of this research.

The work cohesively presents the influence of individual design features on the overall functionality of the aircraft braking system. A detailed discussion on the interdependencies is presented and improvements to performance by changes or accommodation to the design to benefit the other components in the overall system are suggested.

This study involved understanding the requirements of an aircraft brake friction material and the translation of these material characteristics into a heat sink that can be used was discussed. The generation of torque and how it is transmitted through the tyre is discussed and the relationship to the antiskid system is established and the influence of the tyre choice (bias or radial) on the wheel design is addressed. The method of mounting the brake and its impact on the brake design and on the dynamic stability of the system has been examined and recommendations to improvements that would prevent vibrations as well as some fixes have been made.

The role of the brake control and antiskid system have been discussed. There is little available literature on antiskid and even less on the interaction of the antiskid system on the brake and aircraft braking in general. This work significantly addresses this shortcoming and in great detail establishes the factors that depend on each other. For example, the brake response (and hence antiskid) depends on the time taken to supply fluid to the brake to close the clearance and generate a clamping force. The impact of long and differential pipe lengths on the response was discussed as well as the need to have a stiff brake chassis.

The system integration aspects of aircraft braking are complex and many. This work provides a level of understanding that will hopefully provide engineers working in the field a framework by which to design better systems.

APPENDIX A – BRAKE PARAMETRIC SIZING

Introduction

A study involving up to 14 different aircraft brake designs and including existing aircraft programmes as well as proposed designs.

As discussed in Chapter 5 the main envelope constraints placed on the brake design is firstly the rim size and secondly the axle size. This study investigated the relationship between rim size, stator outer and inner diameter, stator drives, rotor outer and inner diameter, rotor drives and axle size.

For certain variables there was significant differences between Military Aircraft brake designs and Civil Aircraft brake designs. This is expected, as there are usually different design drivers for the different aircraft configurations. Where these differences impact significantly on the statistical confidence of the fitted regression line, a separate parametric model is given for each aircraft category. Note that no attempt was made to separate the categories further e.g. Military Fighter, Military Transport etc.

The statistical software package, Minitab, was used to fit a linear equation to the dependent variable. The software package also provides a confidence interval and a prediction interval for the line.

Military Aircraft

A total of six military aircraft of various types where used to determine the previously mentioned relationships. The fitted equation and plot for the relationship between the stator outer diameter and the rim size is indicated in figure 87.

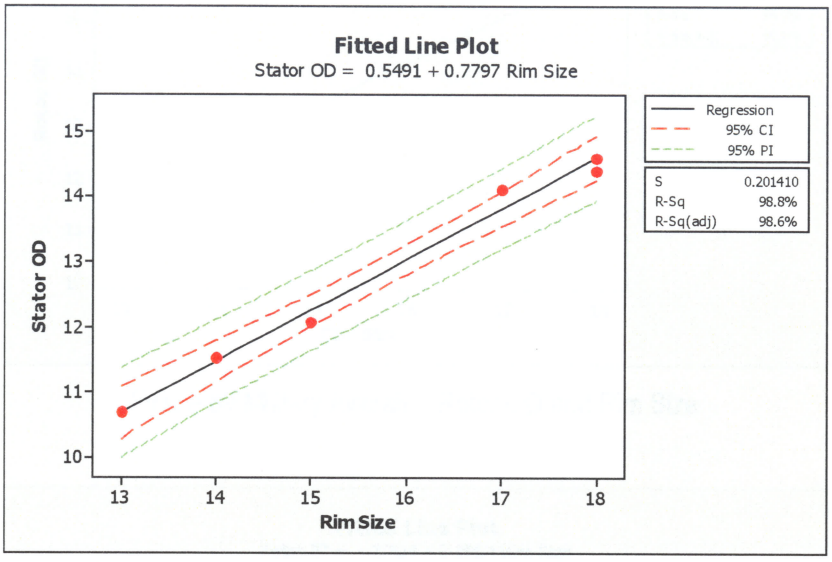

Figure 87 Military Aircraft – Stator OD and Rim Size

The relationship between stator ID and rim size is shown in figure 88.

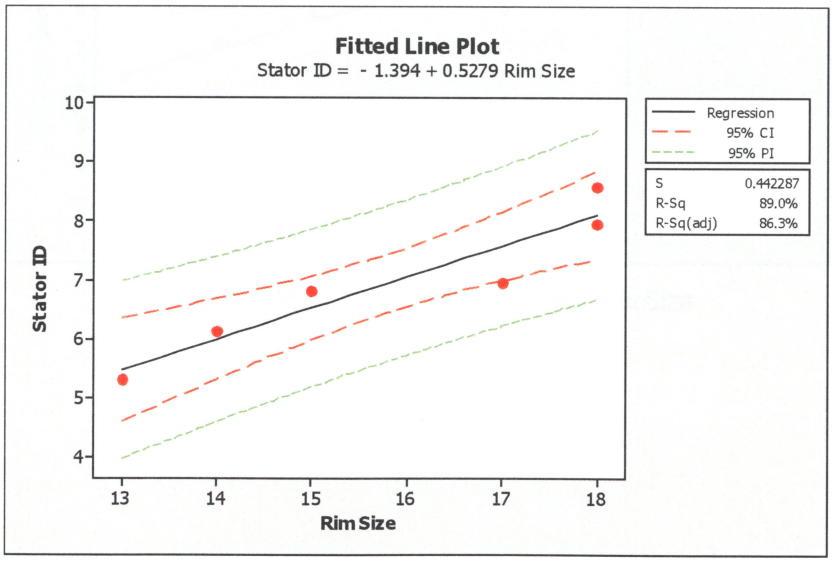

Figure 88 Military Aircraft – Stator ID and Rim Size

The rotor OD and rotor ID fits follow in figures 89 and 90.

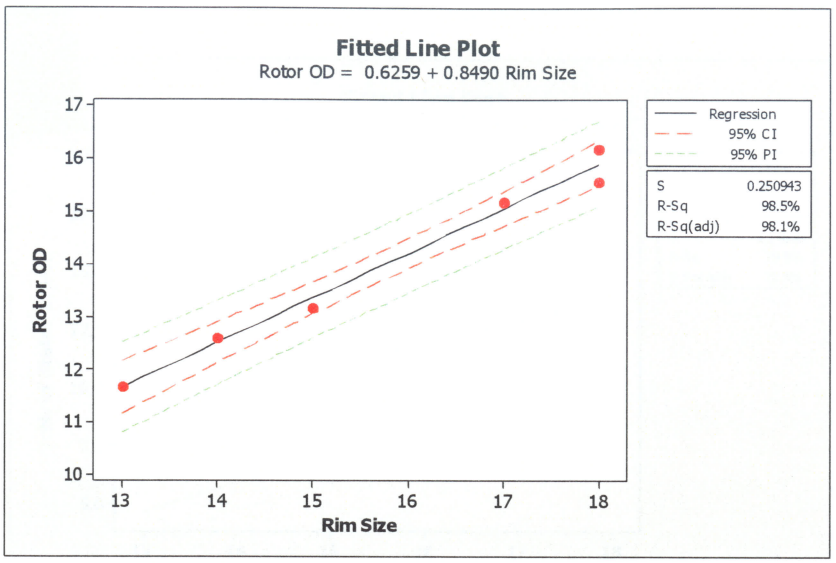

Figure 89 Military Aircraft – Rotor OD and Rim Size

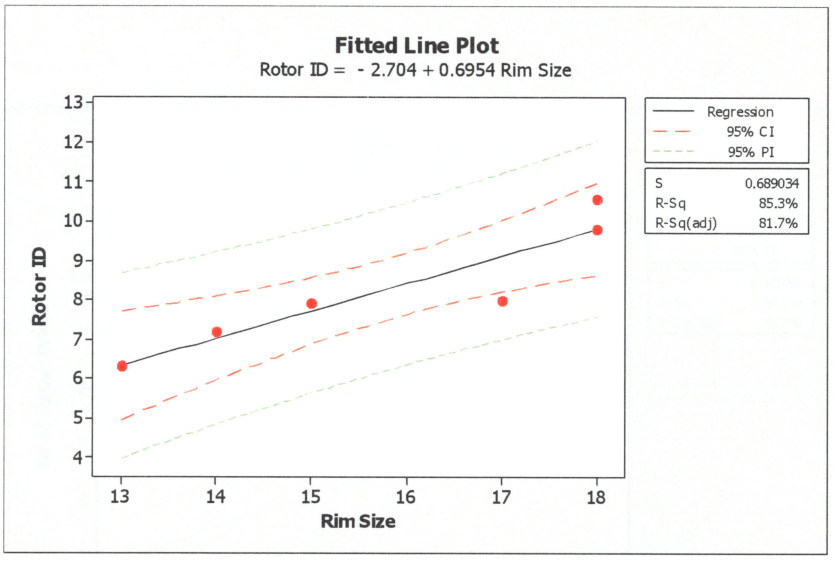

Figure 90 Military Aircraft – Rotor ID and Rim Size

The relationship between the number of stator and rotor drives and the rim size is shown in figures 91 and 92.

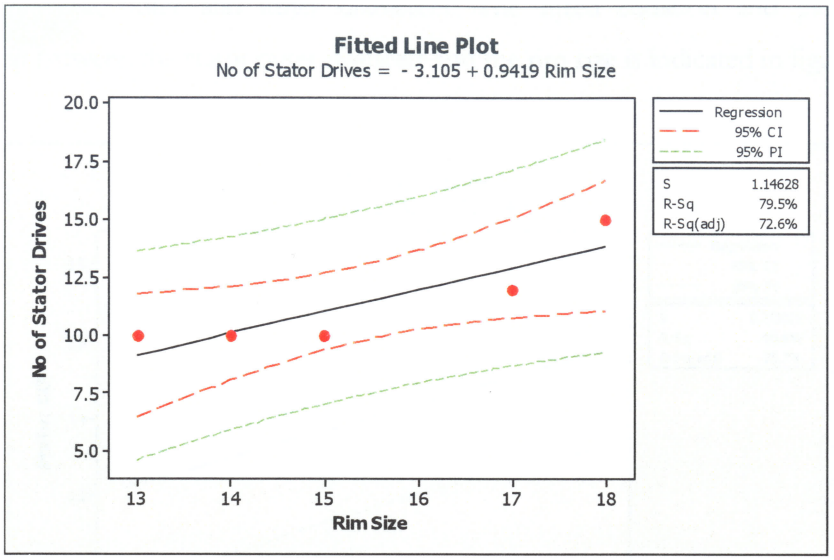

Figure 91 Military Aircraft – Stator Drives and Rim Size

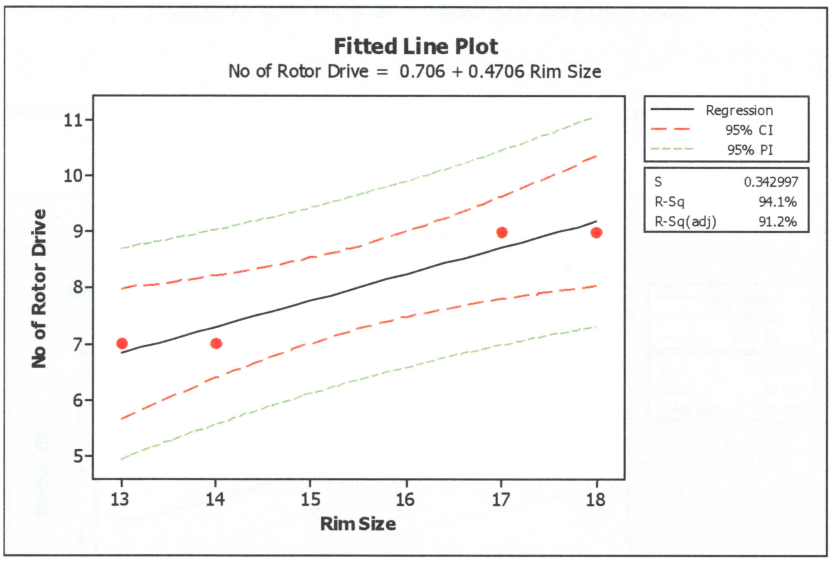

Figure 92 Military Aircraft – Rotor Drives and Rim Size

Civil Aircraft

A total of four civil aircraft of various types where used to investigate the relationships of stator and rotor, outer and inner diameters. The fitted equation and plot for the relationship between the stator outer diameter and the rim size is indicated in figure 93.

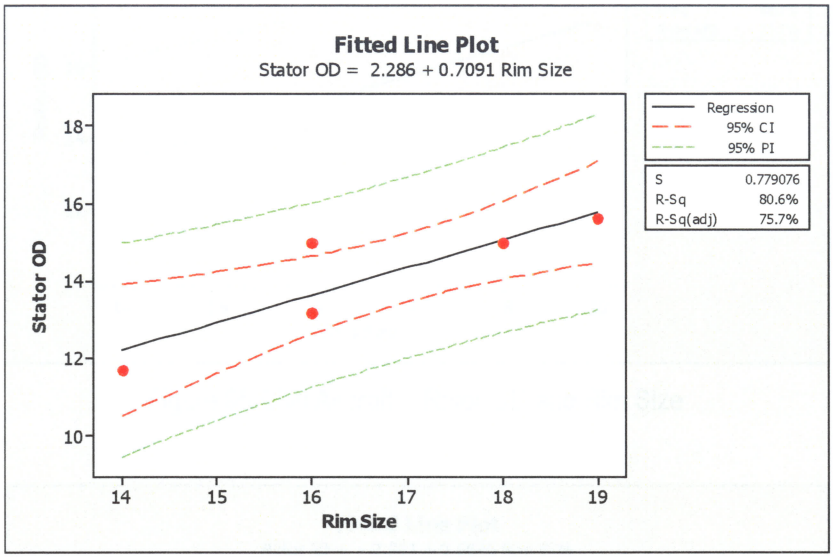

Figure 93 Civil Aircraft – Stator OD and Rim Size

The relationship between stator ID and rim size is shown in figure 94.

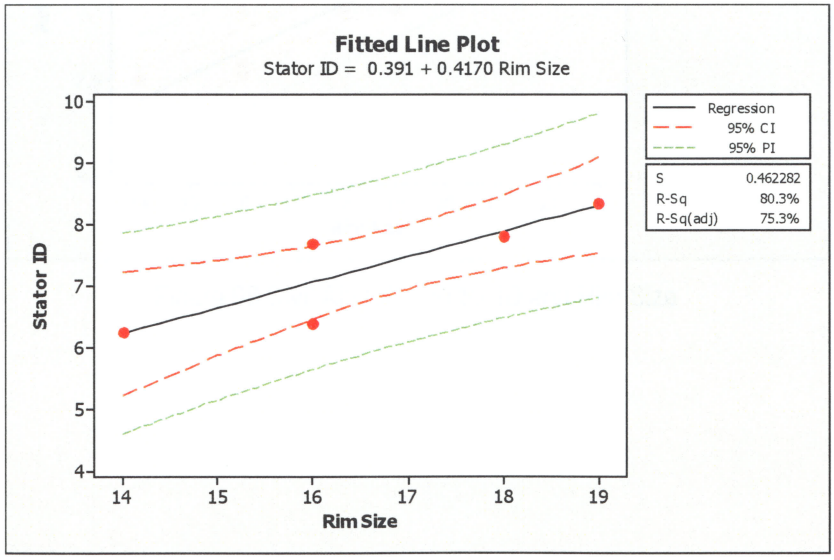

Figure 94 Civil Aircraft – Stator ID and Rim Size

The rotor OD and rotor ID fits follow in figures 95 and 96.

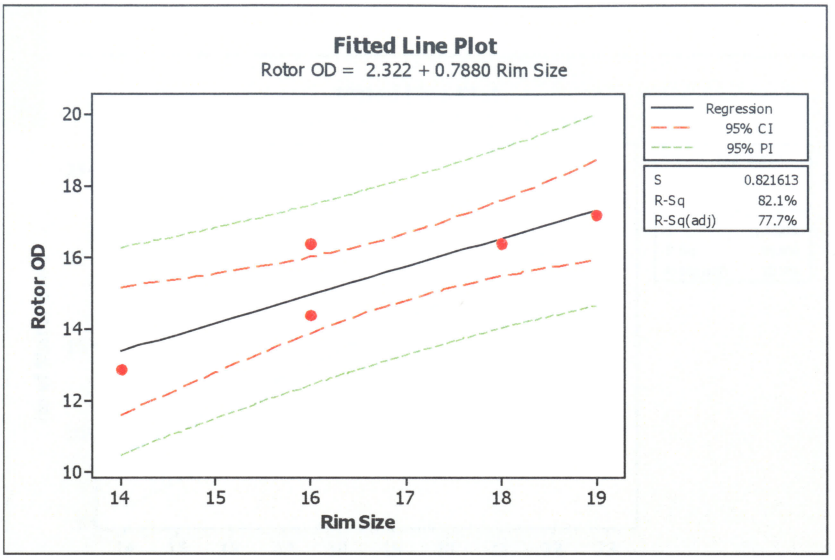

Figure 95 Civil Aircraft – Rotor OD and Rim Size

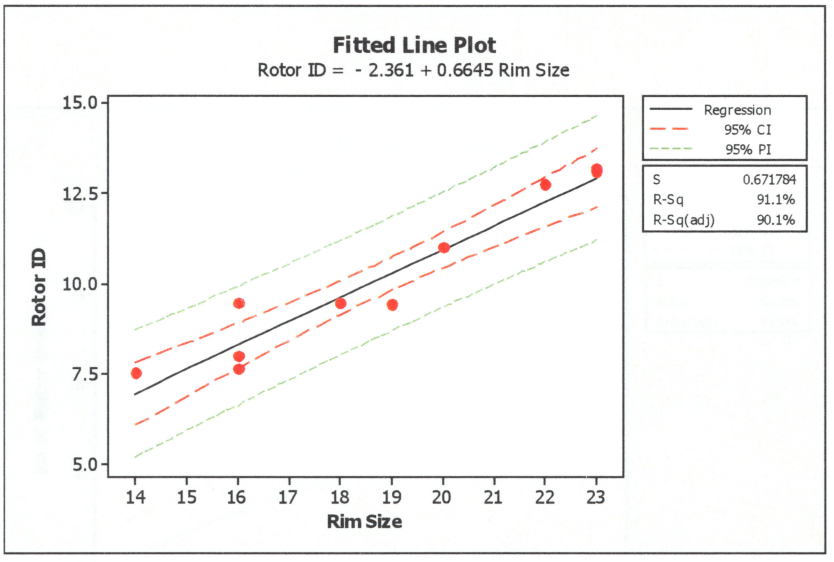

Figure 96 Civil Aircraft – Rotor ID and Rim Size

The relationship between the number of stator and rotor drives and the rim size is shown in figures 97 and 98.

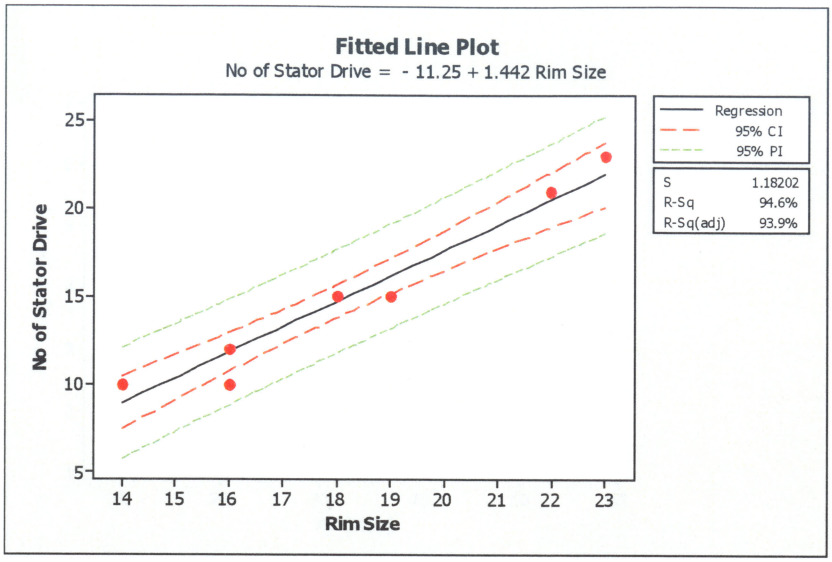

Figure 97 Civil Aircraft – Stator Drives and Rim Size

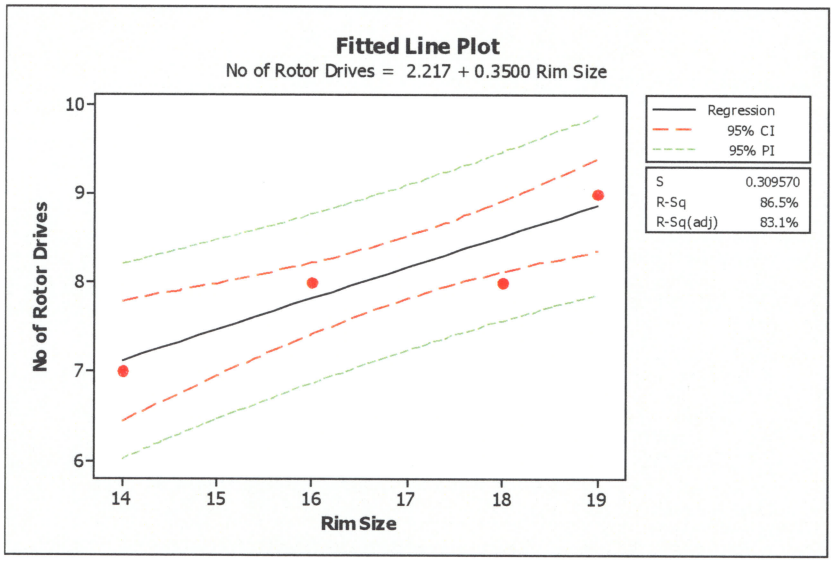

Figure 98 Civil Aircraft – Rotor Drives and Rim Size

Lastly, a relationship between the worn heat sink length and the amount of Kinetic Energy input into the brake is established, see figure 99.

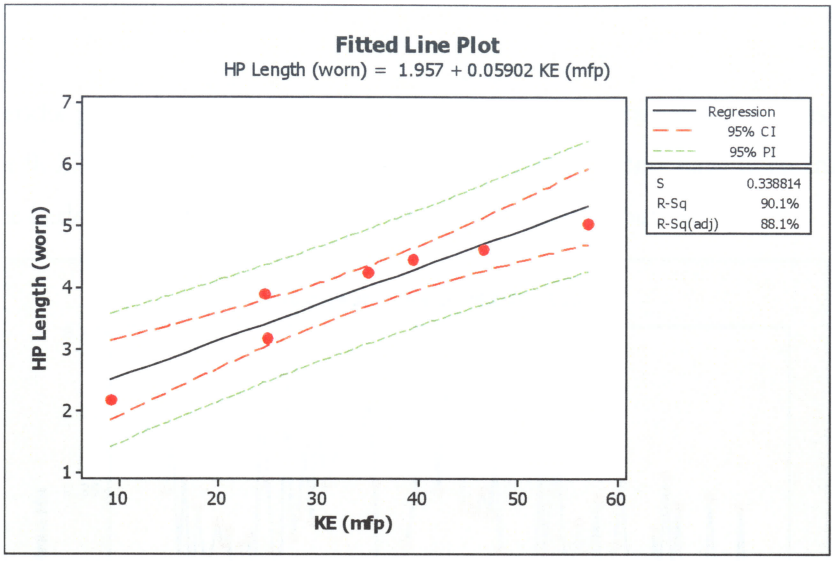

Figure 99 All Aircraft Types – Worn Heat Sink Length vs Kinetic Energy (mfp)

APPENDIX B – BRAKE PERFORMANCE SUPPLEMENTARY DATA

This Appendix presents the remaining data from aircraft programmes 2 to 8 as described in Chapter 9. Note, that as discussed in Chapter 9 some data sets have been truncated to remove the bedding-in effect and hence achieve a normal distribution.

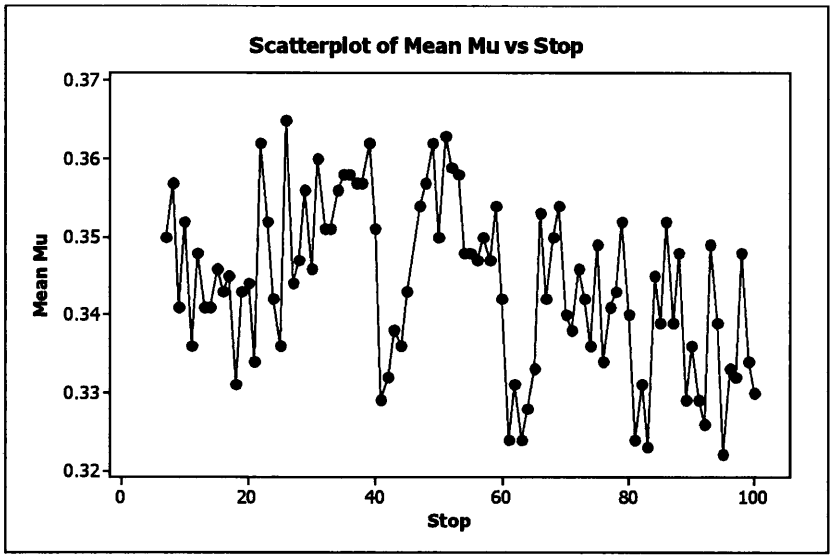

Figure 100 Aircraft Programme #2 Mean μ Variation 100 Normals Data

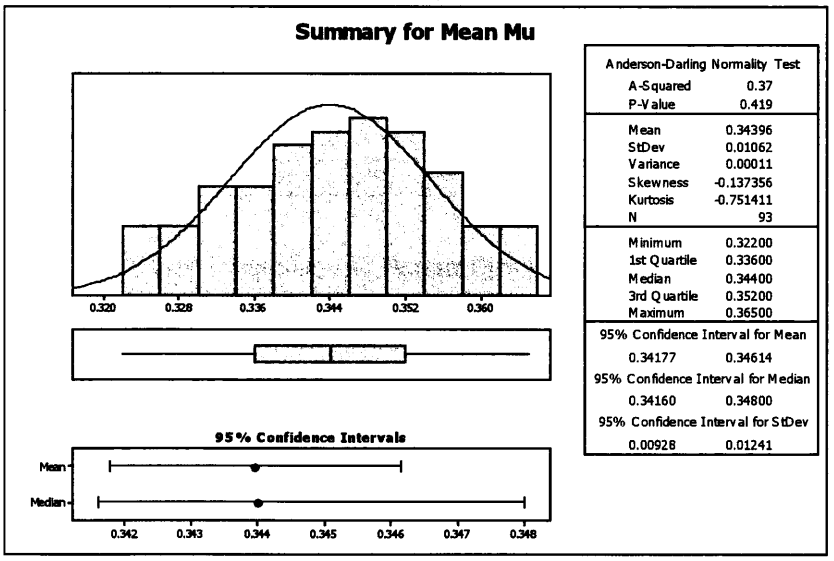

Figure 101 Aircraft Programme #2 Normal Distribution Fit 100 Normals Data

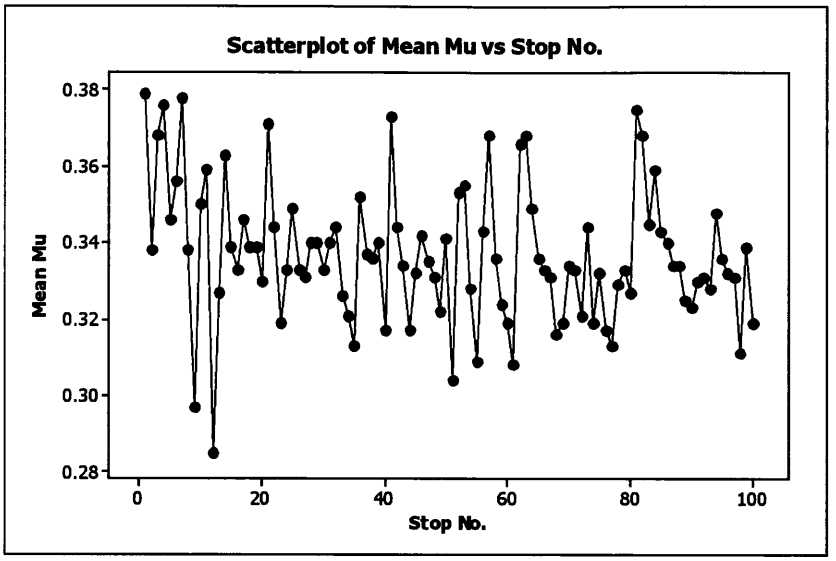

Figure 102 Aircraft Programme #3 Mean μ Variation 100 Normals Data

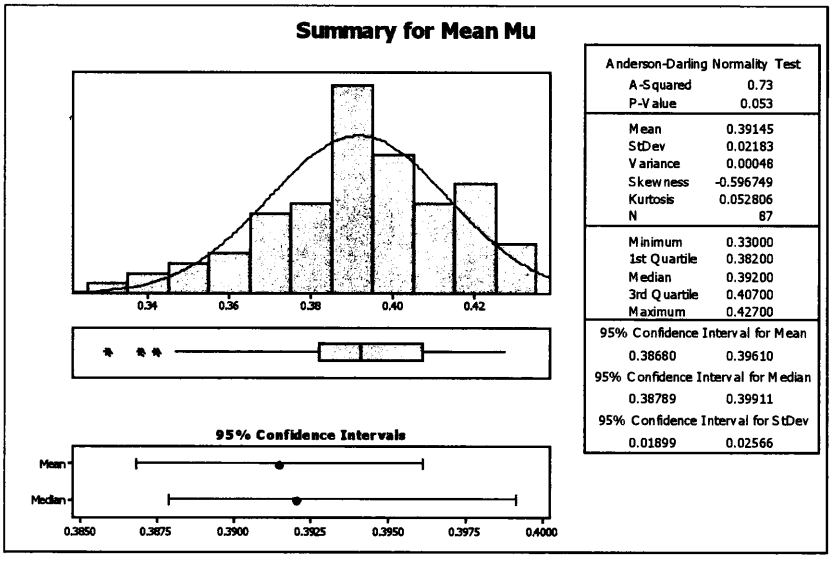

Figure 103 Aircraft Programme #3 Normal Distribution Fit 100 Normals Data

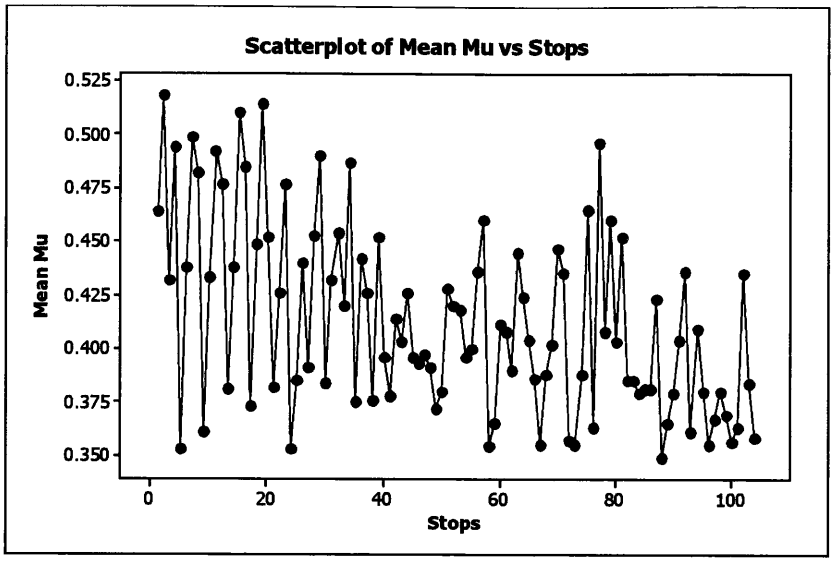

Figure 104 Aircraft Programme #4 Mean μ Variation 100 Normals Data

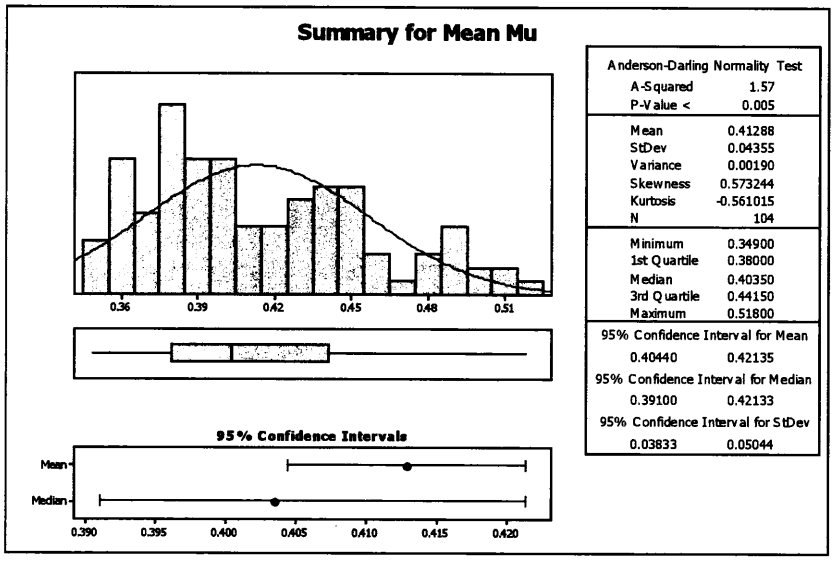

Figure 105 Aircraft Programme #4 Normal Distribution Fit 100 Normals Data

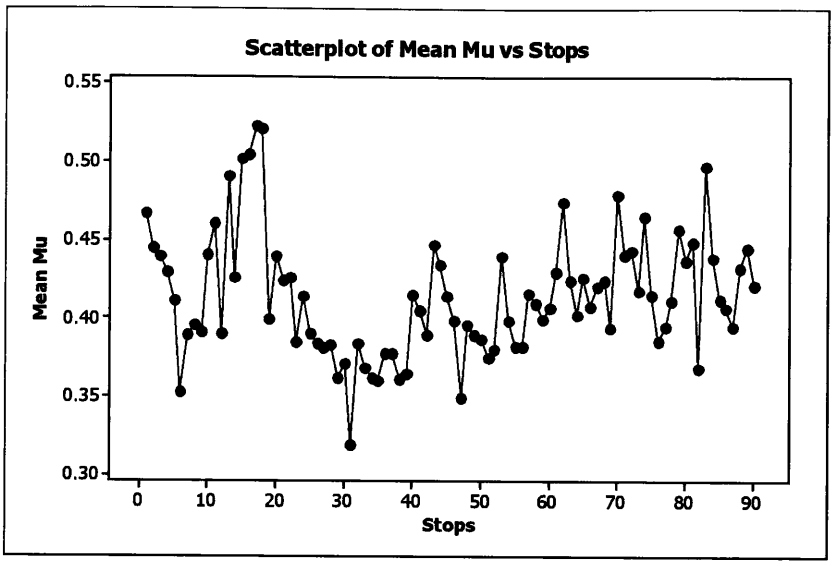

Figure 106 Aircraft Programme #5 Mean μ Variation 100 Normals Data

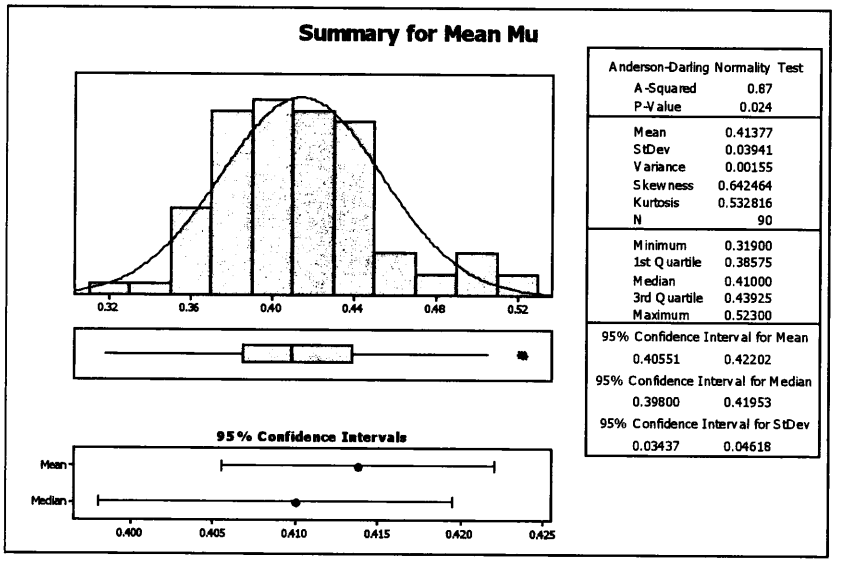

Figure 107 Aircraft Programme #5 Normal Distribution Fit 100 Normals Data

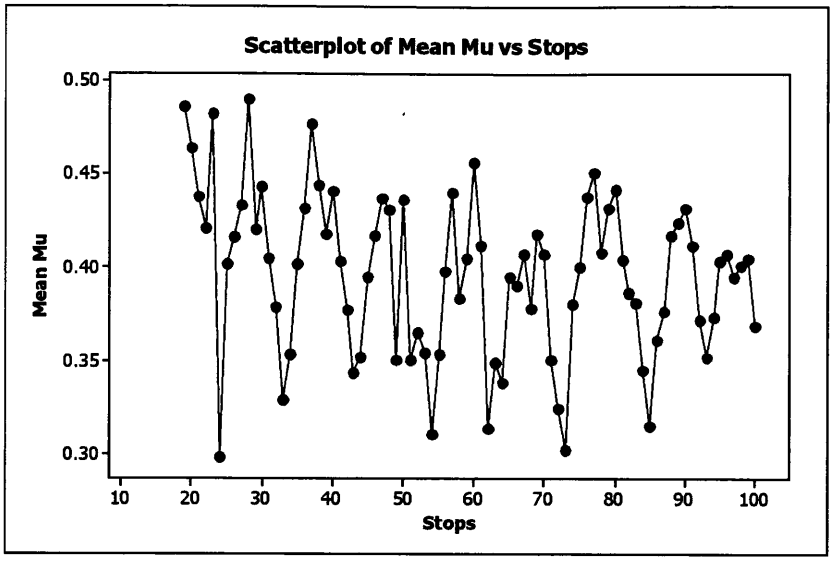

Figure 108 Aircraft Programme #6 Mean μ Variation 100 Normals Data

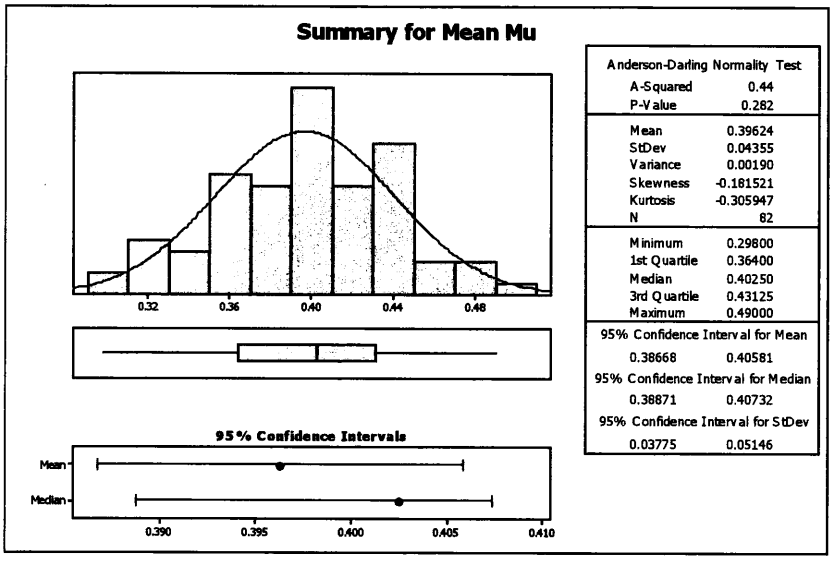

Figure 109 Aircraft Programme #6 Normal Distribution Fit 100 Normals Data

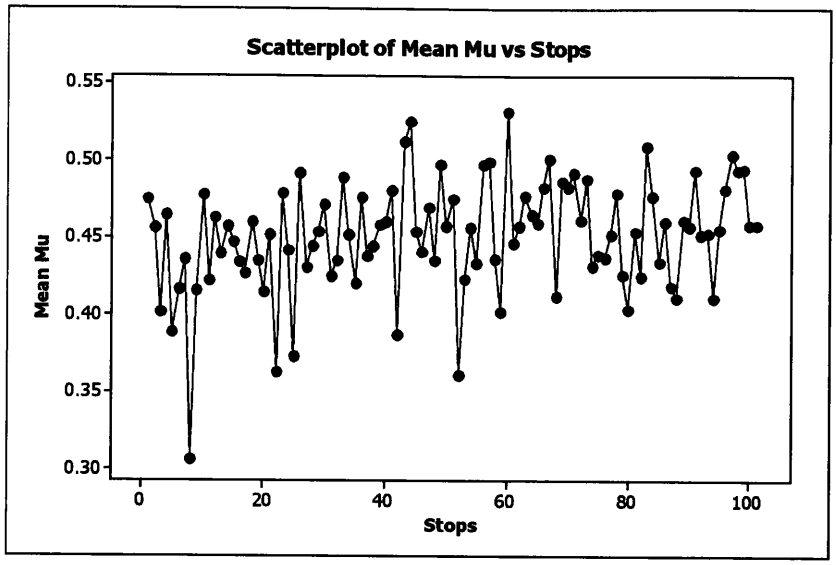

Figure 110 Aircraft Programme #7 Mean μ Variation 100 Normals Data

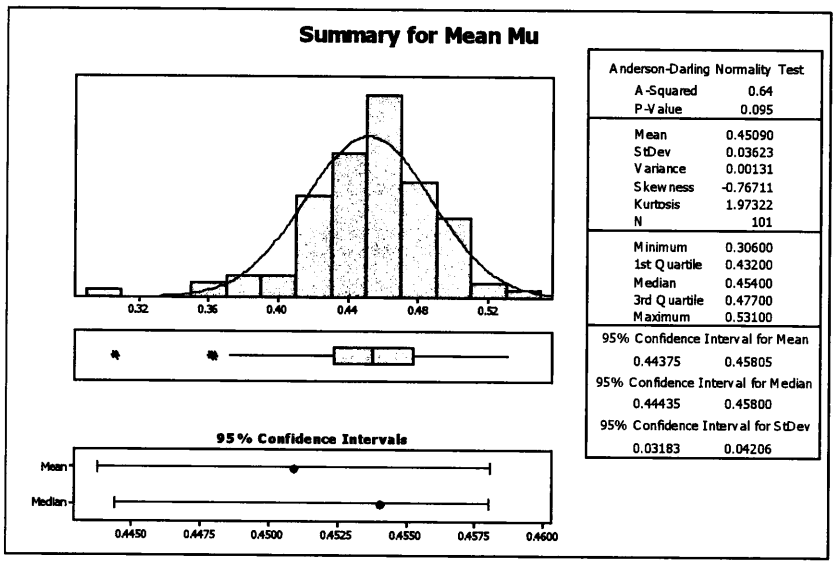

Figure 111 Aircraft Programme #7 Normal Distribution Fit 100 Normals Data

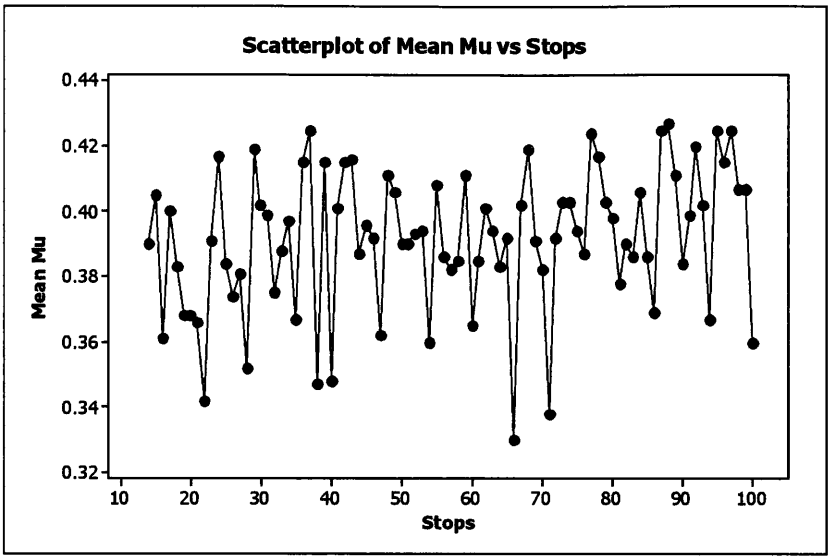

Figure 112 Aircraft Programme #8 Mean μ Variation 100 Normals Data

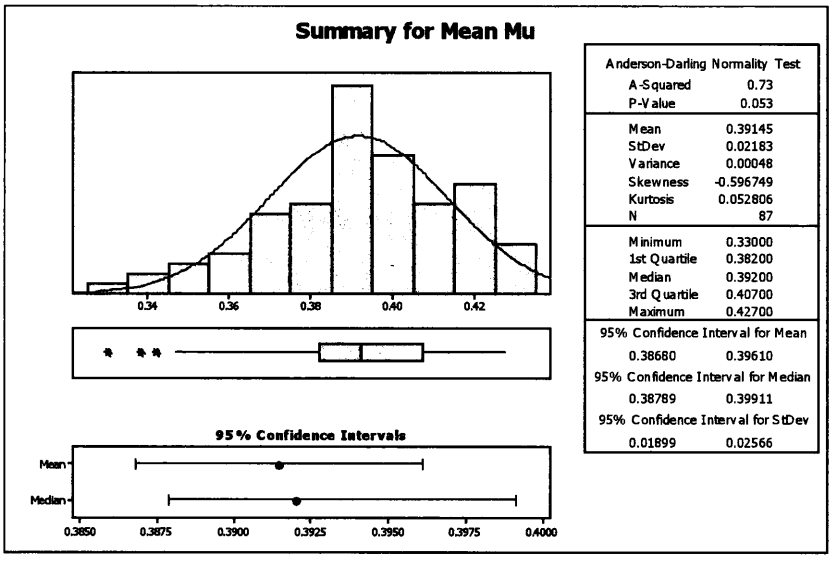

Figure 113 Aircraft Programme #8 Normal Distribution Fit 100 Normals Data

Additional work was conducted to investigate if other distributions were better at describing the data. A Minitab function was used to identify the most appropriate distribution, an excerpt for aircraft programme #8 is shown below.

Descriptive Statistics

N	N*	Mean	StDev	Median	Minimum	Maximum	Skewness	Kurtosis
87	0	0.391448	0.0218253	0.392	0.33	0.427	-0.596749	0.0528063

Box-Cox transformation for Normal distribution: Lambda = 5.00000

Goodness of Fit Test

Distribution	AD	P	LRT P
Normal	0.735	0.053	
Normal (After Transformation)	0.301	0.574	
Lognormal	0.987	0.013	
3-Parameter Lognormal	0.740	*	0.075
Exponential	35.735	<0.003	
2-Parameter Exponential	17.490	<0.010	0.000
Weibull	0.330	>0.250	
3-Parameter Weibull	0.353	0.357	1.000
Smallest Extreme Value	0.395	>0.250	
Largest Extreme Value	2.862	<0.010	
Gamma	0.899	0.023	
3-Parameter Gamma	0.965	*	1.000
Logistic	0.569	0.096	
Loglogistic	0.705	0.039	
3-Parameter Loglogistic	0.570	*	0.159

ML Estimates of Distribution Parameters

Distribution	Location	Shape	Scale	Threshold
Normal*	0.39145		0.02183	
Normal (After Transformation)	0.00947		0.00246	
Lognormal*	-0.93948		0.05688	
3-Parameter Lognormal	3.49410		0.00066	-32.52935
Exponential			0.39145	
2-Parameter Exponential			0.06475	0.32670
Weibull		21.86611	0.40124	
3-Parameter Weibull		37.30771	0.68058	-0.27913
Smallest Extreme Value	0.40168		0.01811	
Largest Extreme Value	0.38004		0.02377	
Gamma		317.15936	0.00123	
3-Parameter Gamma		267.95387	0.00136	0.02749
Logistic	0.39279		0.01232	
Loglogistic	-0.93518		0.03177	
3-Parameter Loglogistic	3.48903		0.00038	-32.36125

* Scale: Adjusted ML estimate

These results indicate that transforming the data through a Box-Cox transformation with lambda = 0.5 then allows a good fit with the normal distribution. The difficulty with this approach was that the most appropriate distribution was different for each data set. This coupled with the fact that there was a low sample size (8 aircraft programmes) a normal distribution was chosen to describe each set of data.

REFERENCES

Adams, H.W. (1943) *Aircraft Hydraulics*, 1st ed. McGraw-Hill, New York

Alsobrook, C.B. (1995) *Wear of F-16 Mainwheel Tires During Constant Slip Braking* SAE Paper 951392, Aerospace Atlantic Conference, Dayton, Ohio, USA, May 23-25

Ashford, N. and Wright, P.H. (1992) *Airport Engineering* 3rd edition, John Wiley & Sons, Inc., New York

Awashi, S. and Wood, J.L. (1988) *Carbon/Carbon Composite Materials for Aircraft Brakes* Ceram. Eng. Sci. Proc., **9** [7-8] pp553-560

Blanco, C., Bermejo, J., Marsh, H. and Menedez, R. (1997) *Chemical and Physical Properties of Carbon as Related to Brake Performance* Wear **213** pp 1-12, Elsevier Ltd.

Bowen, F.P. and Tabor, D. (1964) *The Friction and Lubrication of Solids – Part II* Oxford University Press, Oxford

Carabineiro, S.A., Silva, I.F., Klimkiewicz, M. and Eser, S. (1999) *In-Situ Techniques for Studying Deterioration of C/C Composite Aircraft Brakes by Catalytic Oxidation* Materials and Corrosion, **50**, 689-695, Wiley-VCH GmbH

Chang, H.W. and Rusnak, R.M. (1978) *Contribution of Oxidation to the Wear of Carbon-Carbon Composites* Carbon, Vol. 16, pp 309-312, Pergamon Press Ltd.

Chang, H.W. (1982) *Correlation of Wear with Oxidation of Carbon-Carbon Composites* Wear **80**, pp 7-14, Elsevier Ltd.

Chen, J.D., Chern Lin, J.H. and Ju, C.P. (1996) *Effect of Humidity on the Tribological Behaviour of Carbon-Carbon Composites* Wear **193**, pp 38-47, Elsevier Ltd.

Chichinadze, A.V. (2000) *Evaluation Methods of the Carbon Friction Composite Materials used in Multiple Disc Aviation Brakes – Part I* Tribologia 1-2000 pp 7-21

Chichinadze, A.V. (2000) *Evaluation Methods of the Carbon Friction Composite Materials used in Multiple Disc Aviation Brakes – Part II* Tribologia 2-2000 pp 133-155

Chichinadze, A.V. (2001) *Evaluation Methods of the Carbon Friction Composite Materials used in Multiple Disc Aviation Brakes – Part III* Tribologia 1-2001 pp 23-39

Conway, H.G. (1958) *Landing Gear design* Chapman and Hall, London

Delhaes, P. (2002) *Chemical Vapour Deposition and Infiltration Processes of Carbon Materials* Carbon **40** (2002) 641-657, Pergamon Press Ltd.

Dunlop Limited, *The Dunlop Mk. 5 Anti-Skid System (Electrical)*, (Promotional Material)

Dunlop Limited, *The Dunlop Mk. 6 Anti-Skid System (Electronic)*, (Promotional Material)

ESDU 71025 (1995) *Frictional and Retarding Forces on Aircraft Tyres Part I: Introduction* ESDU Data Item No. 71025, October 1971 (with amendments A to C, March 1988)

Ewers, B., Boerdeneuve-Guibé, J., Garcia, J.P., Piquin, J. (1996), *Expert Supervision of an Antiskid Control System of a Commercial Aircraft*, Proceeding of the 1996 IEEE International Symposium on Intelligent Control, Dearbourn, MI, Sept.15-18

Gouider, M., Berthier, Y., Jacquemard, P., Rousseau, B., Bonnamy, S. and Estrade-Szwarckopf, H. (2004) *Mass Spectrometry during C/C Composite Friction: Carbon Oxidation Associated with High Friction Coefficient and High Wear Rate* Wear **256**, pp 1082-1087, Elsevier Ltd.

Hirzel, E.A. (1972), *Antiskid and Modern Aircraft*, SAE Paper N^0. 720868

Hutton, T.J., M^{c}Enaney, B. and Crelling, J.C. (1999) *Structural Studies of Wear Debris from Carbon-Carbon Composite Aircraft Brakes* Carbon, Vol. 37, pp 907-916, Pergamon Press Ltd.

Jenkins, S.F.N. (1989) *Landing Gear Design and Development* Proc. Instn. Mech. Engrs. Vol 203, pp67-73

Johnson, A. (1996) *The Development of Expertise in a Disciplinary Interstice: Antilock Braking Systems and Electronic Control of a Mechanical Device* Technical Expertise and Public Decisions, IEEE Press

Kragelsky, I.V. (1965) *Friction and Wear* Butterworths, Washington

Olds, R. (1987) *Development of Radial Tires* SAE Paper 871870, Aerospace Technology Conference and Exposition, Long Beach, California, USA, Oct. 5-8

Lay, M.K., Macy, W.W. and Wagner, P.M. (1995) *Initial Identification of Aircraft Tire Wear* SAE Paper 951394, Aerospace Atlantic Conference, Dayton, Ohio, USA, May 23-25

Lester, W.G.S. (July 1973), *Some Factors Influencing the Performance of Aircraft Anti-Skid Systems*, Royal Aircraft Establishment Tech. Memo. EP 550

Liu, S.Y., Gordon, J.T. and Özbek, M.A. (1998) *Nonlinear Model for Aircraft Brake Squeal Analysis: Model Description and Solution Methodology* Journal of Aircraft, Vol.35, No.4, July-August 1998, AIAA

Longyear, D.M. and Hirzel, E.A. (1979) *Advanced Braking Controls for Business Aircraft*, SAE Paper N^0. 790599

Luo, R. (2002) *Friction Performance of Carbon/Carbon Composites prepared using Rapid Directional Diffused Chemical Vapor Infiltration Processes* Carbon, **40** pp 1279-1285, Pergamon Press Ltd.

McCormick, B.W. (1995) *Aerodynamics, Aeronautics and Flight Mechanics* John Wiley & Sons, Inc. New York

Murdie, N., Ju, C.P., Don, J. and Fortunato, F.A. (1991) *Microstructure of Worn Pitch/Resin/CVI C-C Composites* Carbon, Vol. 29, No.3 pp 335-342, , Pergamon Press Ltd.

Nave, R. (2003) *Phonons* [online] Georgia State University, Available from: http://hyperphysics.phy-atr.gsu.edu/hbase/solids/phonon.html#c1 [Accessed 5 October 2004]

Park, H.S., Park, J.H. and Kim, K.S. (1995) *The Effect of Carbon Fiber Heat Treatment on the Frictional Properties of C-C Composites* Extended Abstracts and Program, Carbon '95, San Diego, University of San Diego, USA pp 156-157, Pergamon Press Ltd.

Pierson, H.O and Liebermann, M.L. (1975) *Carbon* **13**, 159, Pergamon Press Ltd.

Plant, N.A. (1994) *Description of Typical Aircraft Braking Systems* IMechE Aerotech Seminar Paper No. C470/24/136

Rand, B. (1993) *Matrix Precursors for Carbon-Carbon Composites* Chapter 3, Essentials of Carbon-Carbon Composites (ed. C.R. Thomas), Royal Society of Chemistry, ISBN 0-85186-804-5

Roberts, J.B. (1981) *Design of Lightweight Braking Systems* Aircraft Dunlop Limited Published Technical Paper

Rudd, R.E. (1999) *Controller and Method of controlling Braking of a Plurality of Wheels* European Patent Application EP 0 936 114 A2

Savage, G. (1993) *Carbon-Carbon Composites* Chapman and Hall, ISBN 0-412-36150-7

Schallamach, A. and Turner, D.M. (1960) *The Wear of Slipping Wheels* Wear Vol. 3, pp 1-25, Elsevier Ltd.

Stanek, P. (1993) *The Effect of Fibre Orientation on Friction and Wear of Carbon-Carbon Composites* Ninth Annual Conference on Materials Technology, Carbon Technology, October 27-27, Southern Illinois University

Stimson, I.L. and Fisher, R . (1980) *Design and Engineering of Carbon Brakes* Phil. Trans. R.Soc. A 294, 583-590

Tunay, I. (1999) *Extremum-Seeking Based Antiskid Control and Functional Principal Components* Doctor of Science Dissertation, Sever Institute of Washington University, Saint Louis, Missouri, USA, UMI Number 9959965

Zierolf, M.L. (1999a) *Brake Control Systems and Methods* European Patent Application EP 0 936 115 A2

Zierolf, M.L. (1999b) *Brake Control Systems and Methods* European Patent Application EP 0 936 116 A2

BIBLIOGRAPHY

Ashley, T.H. and Ochoa, O.O. (1999) *Structural Response of Oxidation-Resistant Carbon/Carbon Composites* Composites Science and Technology **59**, pp 1959-1967, Elsevier Ltd.

Anon, (1968) *Landing Gear Equipment* Aircraft Engineering, January 1968

Dunlop Limited, *The Dunlop Mk. 5 Anti-Skid System (Electrical)*, (Promotional Material)

Dunlop Limited, *The Dunlop Mk. 6 Anti-Skid System (Electronic)*, (Promotional Material)

Chen, J.D. and Ju, C.P. (1995) *Effect of Sliding Speed on the Tribological Behavior of a PAN-Pitch Carbon-Carbon Composite* Materials Chemistry and Physics **39**, pp 174-179, Elsevier Ltd.

Chen, J.D. and Ju, C.P. (1995) *Low Energy Tribological Behavior of Carbon-Carbon Composites* Carbon **33**, No.1, pp 57-62, Pergamon Press Ltd.

Greenbank, S.J. (1991) *Landing Gear – The Aircraft Requirement* Proc Instn Mech Engs. Vol. 205, pp 27-34

Hou, X., Li, H., Shen, J., Wang, C. and Zhu, Z. (2000) *Effects of Microstructure on the Internal Friction of Carbon-Carbon Composites* Materials Science and Engineering **A286,** pp 250-256, Elsevier Ltd.

Ju, C.P., Chern Lin, J.H., Lee, K.J., and Kuo, H.H. (2000) *Multi-Braking Tribological Behavior of PAN-Pitch, PAN-CVI and Pitch-Resin-CVI Carbon-Carbon Composites* Materials Chemistry and Physics **64**, pp 196-214, Elsevier Ltd.

Klett, J.W., Ervin, V.J. and Edie, D.D. (1999) *Finite-Element Modeling of Heat Transfer in Carbon/Carbon Composites* Composites Science and Technology **59**, pp 593-607, Elsevier Ltd.

Lee, K.J., Kuo, H.H. Chern Lin, J.H., and Ju, C.P. (1999) *Effect of Surface Condition on Tribological Behavior of PAN-CVI Based Carbon-Carbon Composites* Materials Chemistry and Physics **57**, pp 244-252, Elsevier Ltd.

Lee, K.J., Chern Lin, J.H. and Ju, C.P. (1996) *Surface Effect on Braking of PAN-Pitch Carbon-Carbon Composite* Wear **199**, pp 228-236, Elsevier Ltd.

Lee, K.J., Chern Lin, J.H. and Ju, C.P. (1997) *Simulated-Stop Tribological Behavior of Pitch-Resin-CVI Carbon-Carbon Composite* Materials Chemistry and Physics **49**, pp 217-224, Elsevier Ltd.

Pink, J. (1990) *Structural Integrity of Landing Gears* SAE Paper 952021

Pritchard, J.I. (1999) *An Overview of Landing Gear Dynamics* NASA/TM-1999-209143, NASA Center for AeroSpace Information (CASI)

Venkataraman, B. and Sundararajan, G. (2002) *The Influence of Sample Geometry on the Friction Behaviour of Carbon-Carbon Composites* Acta Materialia **50**, pp 1153-1163, Elsevier Ltd.

Whittaker, A.J., Taylor, R. and Tawil, H. (1990) *Thermal Transport Properties of Carbon-carbon Fibre Composites* Parts I, II and III Proc. R.Soc. London **430**, pp 167-181, pp 183-197 and pp 199-211 respectively

Young, D.W. (1986) *Aircraft Landing Gears – The Past, Present and Future* IMechE Paper 864752